



Functional analyses of RNA helicases in human ribosome biogenesis

Dissertation

for the award of the degree

“Doctor rerum naturalium” (Dr. rer. nat.)

of the Georg-August-Universität Göttingen

within the doctoral program *Molecular Biology*

of the Georg-August University School of Science (GAUSS)

submitted by

Priyanka Choudhury

from Kolkata, India

Göttingen 2019

Members of the Thesis Committee

Prof. Dr. Markus Bohnsack (1st reviewer)

Department of Molecular Biology, University Medical Center Göttingen

Prof. Dr. Marina Rodnina (2nd reviewer)

Department of Physical Biochemistry, Max Planck Institute for Biophysical Chemistry, Göttingen

Prof. Dr. Jörg Stülke

Institute for Microbiology and Genetics, Georg-August-University Göttingen

Further members of the examination board

Prof. Dr. Ralf Ficner

Department of Molecular Structural Biology; Georg-August-University Göttingen

Prof. Dr. Michael Meinecke

Department of Cellular Biochemistry, University Medical Center Göttingen

Dr. Alexander Stein

Department of Membrane Protein Biochemistry, Max Planck Institute for Biophysical Chemistry, Göttingen

Date of oral examination: 12th July 2019

Affidavit

Herewith I declare that I prepared the PhD dissertation '*Functional analyses of RNA helicases in human ribosome biogenesis*' on my own and with no other sources and aids than quoted.

Göttingen, May 2019

Priyanka Choudhury

Publications associated with the dissertation

Priyanka Choudhury, Philipp Hackert, Indira Memet, Katherine E. Sloan & Markus T. Bohnsack (2019). The human RNA helicase DHX37 is required for release of the U3 snoRNP from pre-ribosomal particles, *RNA Biology*, 16, 54-68.

Table of Contents

Abstract.....	viii
1 Chapter One: Introduction	1
1.1 Overview of ribosome assembly pathway	1
1.1.1 Ribosome biogenesis in yeast and humans	2
1.1.2 pre-rRNA maturation in humans.....	4
1.1.3 Role of ribosomal proteins.....	7
1.1.4 Structural transitions during subunit assembly in humans.....	8
1.1.5 Ribosomopathies.....	11
1.2 RNA helicases.....	12
1.2.1 RNA helicase superfamilies and conserved sequence motifs	12
1.2.2 Mechanism of action of RNA helicases	14
1.2.3 Cellular pathways involving RNA helicases.....	16
1.2.3.1 Role of RNA helicases in pre-mRNA splicing.....	17
1.2.3.2 Role of RNA helicases in translation	17
1.2.3.3 Role of RNA helicases in other cellular pathways	18
1.2.4 Regulation of RNA helicases.....	19
1.2.4.1 Cofactor-dependent regulation of RNA helicases.....	19
1.2.4.2 Cofactor-independent regulation of RNA helicases.....	20
1.3 The roles of RNA helicases in ribosome biogenesis.....	21
1.3.1 RNA helicases regulate snoRNA association with pre-ribosomal particles	22
1.3.2 RNA helicases mediate structural remodelling of pre-ribosomes	23
2 Chapter Two: Scope of the thesis	25
3 Chapter Three: Manuscript I	26
4 Chapter Four: The role of DDX55 in human ribosome biogenesis.....	77
4.1 <i>Introduction</i>	77
4.2 <i>Material and Methods</i>	80
4.2.1 Chemicals.....	80
4.2.2 Plasmids.....	80

4.2.3 Oligonucleotides.....	80
4.2.4 Small Interfering RNAs (siRNAs).....	81
4.2.5 Antibodies.....	81
4.2.6 Molecular Cloning.....	82
4.2.6.1 Amplification of gene of interest	82
4.2.6.2 Restriction digestion and ligation.....	82
4.2.6.3 Transformation of chemically competent <i>E. coli</i>	83
4.2.6.4 Plasmid DNA extraction and sequencing	83
4.2.7 Human cell culture methods.....	83
4.2.7.1 Cell culture conditions	83
4.2.7.2 Generation of stable cell lines	83
4.2.7.3 siRNA transfection.....	84
4.2.7.4 Immunofluorescence	84
4.2.7.5 Analysis of pre-ribosomal complexes by sucrose density centrifugation.....	84
4.2.8 RNA-based methods	85
4.2.8.1 RNA extraction	85
4.2.8.2 Pulse chase metabolic labelling of newly synthesised RNA and northern blotting	85
4.2.8.3 Crosslinking and analysis of cDNA.....	86
4.2.9 <i>In vitro</i> assays	88
4.2.9.1 Recombinant protein expression and purification.....	88
4.2.9.2 Steady-state ATPase assay	89
4.2.10 SDS-PAGE and western blotting.....	89
4.3 <i>Results</i>	91
4.3.1 DDX55 is an ATPase and a mutation in its conserved GKT motif inhibits its ATP hydrolysis capacity	91
4.3.2 The human helicase DDX55 is required for ribosome biogenesis	92
4.3.2.1 DDX55 is localised in the nucleoplasm	92
4.3.2.2 Depletion of DDX55 <i>in vivo</i> impairs ribosome biogenesis	93
4.3.2.3 DDX55 crosslinks to helices 62 and 63 of the 28S rRNA sequence <i>in vivo</i>	94

4.3.3 C-terminal tail of DDX55 is required for its recruitment to pre-ribosomal subunits.....	99
4.4 Discussion.....	103
5 Chapter Five: Discussion.....	106
5.1 Distinct roles of RNA helicase in ribosome biogenesis.....	106
5.2 Division of labour: DEAH-box versus DEAD-box helicases.....	108
5.3 Regulation of RNA helicases.....	111
5.4 Dynamics of RNA helicase association with pre-ribosomes.....	113
6 Bibliography.....	116
List of figures.....	141
List of tables.....	142
Abbreviations.....	143
Acknowledgments.....	146
Curriculum vitae.....	147

Abstract

Eukaryotic ribosomes are essential ribonucleoprotein (RNP) complexes consisting of four ribosomal RNAs (18S, 5S, 5.8S, 28S/25S) and approximately 80 ribosomal proteins, which are required for the process of translating the information encoded in mRNAs into proteins. Ribosome biogenesis requires a dynamic interplay between a multitude of *trans*-acting biogenesis factors such as ATPases, GTPases, snoRNAs, nucleases and RNA helicases, which assist in the maturation of pre-ribosomal subunits. RNA helicases are RNA-dependent NTPases that play key roles in all aspects of RNA metabolism including pre-mRNA splicing, translation, transcription and ribosome biogenesis. The majority of RNA helicases involved in ribosome biogenesis belong to either the DEAD- or DEAH-box family and consist of a structurally conserved helicase core flanked by N- and C-terminal domains that can serve as platforms for protein-protein/protein-RNA interaction. In yeast, 21 RNA helicases are implicated in the process of ribosome biogenesis and likely play key roles in the structural remodelling of pre-ribosomal subunits. Genome-wide screens and proteomic analyses of mammalian nucleoli have suggested the involvement of many orthologues of yeast RNA helicases in the human ribosome assembly pathway as well as highlighting additional helicases that may regulate the process in humans.

Although several RNA helicases are implicated in human ribosome assembly, the precise physiological roles and *in vivo* substrates of these helicases are often not well-characterized. In this study, we aimed to gain insights into the roles of two RNA helicases-DHX37 and DDX55, which are implicated in SSU and LSU biogenesis respectively.

An RNAi-based rescue system indicated that the catalytic activity of DHX37 is required for the effective maturation of 18S rRNA. Using an *in vivo* crosslinking approach, we show that DHX37 crosslinks to the U3 snoRNA and that expression of a catalytically inactive mutant of DHX37 leads to the accumulation the pre-ribosomal accumulation of U3, suggesting a role for DHX37 in release of the U3 snoRNP from pre-ribosomal particles. In addition, we identified UTP14A as a cofactor of DHX37, and our data suggest that UTP14A and DHX37 act in a synergistic manner to promote the dissociation of U3 snoRNA from pre-ribosomal subunits. While our data implied that DHX37 mediated release of U3 snoRNP is conserved in eukaryotes, we also revealed several interesting differences between the yeast and human proteins in terms of recruitment and function of the helicase during late steps of ribosome assembly. Furthermore, our crosslinking data also identified a binding site of DDX55 on the 28S rRNA sequence, consistent with its requirement for LSU maturation. DDX55 was found to predominantly localize in the nucleoplasm suggesting a role in late-stage ribosome biogenesis. We further investigated the function of the lysine-rich C-terminal tail of DDX55 and our results indicate a possible role of the C-terminal tail in the recruitment

of DDX55 to pre-ribosomal complexes. Taken together, our results provide important new insights into the roles of RNA helicases in human ribosome biogenesis.

Chapter One: Introduction

1.1 Overview of ribosome assembly pathway

Translation of the nucleotide sequences of mRNAs into the amino acid sequences of proteins is an essential cellular process that is carried out by large macromolecular complexes called ribosomes. Eukaryotic cytoplasmic 80S ribosomes consist of two ribonucleoprotein (RNP) complexes: the large subunit (LSU; 60S), consisting of three ribosomal RNAs (rRNA; 28S (humans)/25S (yeast), 5.8S, 5S) along with 47 (humans) /46 (yeast) ribosomal proteins (RPs) and the small subunit (SSU; 40S), comprising the 18S rRNA along with 33 proteins (Anger et al., 2013; Ben-Shem et al., 2011). The synthesis of a macromolecular complex of such complexity is one of the most energetically demanding processes in eukaryotic cells and requires the assistance of over 200 ribosome assembly factors in yeast (Woolford and Baserga, 2013).

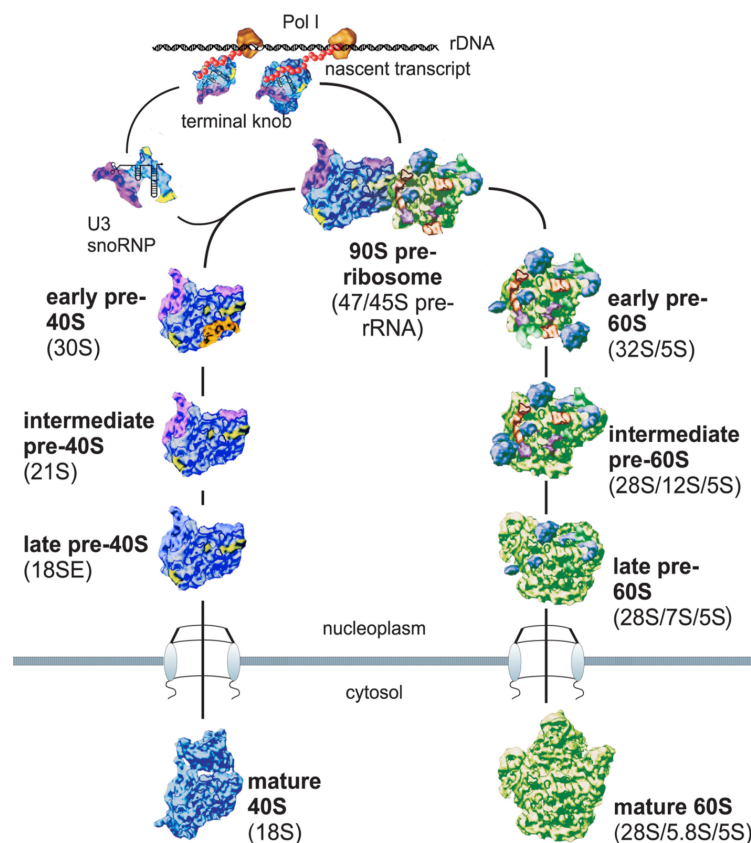


Figure 1.1. Ribosome biogenesis in humans. Ribosome assembly initiates in the nucleolus with the transcription of 47S nascent transcript by RNA polymerase I. The nascent transcript harbours the sequences of mature rRNAs (18S, 5.8S, 28S) along with internal (ITS1 and ITS2) and external (5'ETS and 3'ETS) spacer sequences. Several factors associate co-transcriptionally to generate the 90S pre-ribosome complex. An endonuclease mediated cleavage separates the maturation pathways for the two subunits. The pre-60S and pre-40S undergo independent maturation steps assisted by over 200 *trans*-acting factors before export into the cytoplasm (Panel adapted from Martin, 2014).

The pre-ribosomal subunits undergo extensive nucleolytic processing and structural transitions assisted by a variety of enzymes including AAA-ATPases, helicases, kinases and nucleases (Figure 1.1) (Bohnsack and Bohnsack, 2019; Klinge and Woolford, 2019; Woolford and Baserga, 2013). The pre-ribosomal subunits are exported out of the nucleus to the cytoplasm where the final steps of maturation occur (Sloan et al., 2016). Although ribosome biogenesis is a highly conserved process, best studied in *Saccharomyces cerevisiae* (yeast), there are significant differences in terms of pre-rRNA processing and the functions of ribosomal assembly factors in higher eukaryotes.

1.1.1 Ribosome biogenesis in yeast and humans

In yeast, RNA polymerase I mediated transcription leads to the generation of the 35S pre-rRNA consisting of internal and external spacer sequences (ITS1 and ITS2, and 5' ETS and 3' ETS) along with the sequences of 18S, 5.8S, 25S rRNAs (Long and Dawid, 1980). The 5S rRNA is transcribed in the opposite direction by RNA polymerase III (Figure 1.2) (Sentenac, 1985).

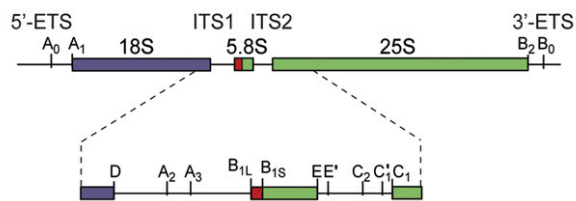


Figure 1.2. Schematic representation of yeast 35S pre-rRNA transcript. The nascent 35S pre-rRNA contains the sequence of mature 5.8S, 25S and 18S rRNA (rectangles) as well as the sequences of external and internal transcribed spacers (adapted from Mullineux and Lafontaine, 2012).

The nascent 35S pre-rRNA transcript undergoes extensive rearrangement mediated by different classes of factors including small nucleolar ribonucleoprotein complexes (snoRNPs), RNA helicases and energy consuming enzymes such as GTPases and AAA-ATPases (Henras et al., 2008; Woolford and Baserga, 2013). A series of highly coordinated, hierarchical processes give rise to the earliest nascent pre-ribosomes known as 90S pre-ribosomes, comprising a large RNP complex, the SSU processome. Although the composition of the 90S and the SSU processome differ slightly, both complexes consist primarily of small subunit proteins and assembly factors (Phipps et al., 2011). Subsequent RNA cleavage events separate the sequences of the mature rRNAs from the spacer segments (Venema and Tollervy, 1995). Cleavage at site A₂, within ITS1 results in the separation of the maturation pathways for the SSU and LSU (Udem and Warner, 1972). Although co-transcriptional cleavage at site A₂ is most prevalent (occurring in 2/3rd of the cases), it is not obligatory. Post-transcriptional processing by the RNase mitochondrial RNA processing (MRP) at the A₃ site also results in the separation of the two pre-ribosomal complexes (Lygerou et al., 1996). UTP24 mediated cleavages at the A₁ and A₂ sites lead to

the generation of 20S and 27SA₂ pre-rRNAs. 20S pre-rRNA is finally processed to 18S rRNA by Nob1 (Pertschy et al., 2009; Wells et al., 2016). Various cryogenic electron microscopy (cryo-EM) structures available for the SSU processome provide molecular snapshots of the earliest stable precursor (Barandun et al., 2017). Interestingly, as the structures obtained by cryo-EM were remarkably similar even when captured under variable physiological conditions, the SSU processome appears to be a very stable intermediate that is formed during the early events of ribosome biogenesis (Barandun et al., 2017; Cheng et al., 2017; Sun et al., 2017). The processing of the LSU precursor 27SA₂ can occur via two alternative pathways, ultimately leading to the generation of 25S rRNA and 6S pre-rRNA. Lastly, after the release of early factors, export adaptors promote the export of pre-60S particles into the cytoplasm wherein further processing of the 6S pre-rRNA sequence occurs to form the mature 5.8S rRNA. Assembly factors also dissociate from pre-60S driven by the action of AAA-ATPase Drg1 leading to the maturation of the large subunit (Lo et al., 2010; Pertschy et al., 2007)

As the sequences of the mature rRNAs and the structure of ribosome is evolutionary conserved, there has been a long-standing assumption that the process of ribosome biogenesis is generally conserved throughout eukaryotes. Moreover, most assembly factors that have been first described in yeast, possess functional homologues in humans (Wild et al., 2010). However, in the recent years, there is compelling evidence suggesting that the process of ribosome biogenesis has acquired greater complexity in humans due to the extension of the primary pre-rRNA transcript (13.3 kb in human vs 6.7 kb in yeast) and emergence of metazoan-specific cleavage sites (Lazdins et al., 1997). Proteomic analysis of the mammalian nucleoli revealed an inventory of 4500 putative (Ahmad et al., 2009) nucleolar proteins in contrast to 150 nucleolar proteins found in budding yeast (Huh et al., 2003). RNAi-mediated screens monitoring pre-rRNA processing defects upon effective depletion identified 286 pre-rRNA processing factors, including 74 lacking yeast homologues (Tafforeau et al., 2013). Furthermore, another genome-wide screen examining nucleolar morphology or number as readouts identified 139 hits consisting of both nucleolar (27.3%) and non-nucleolar proteins (72.7%) revealing the involvement of proteins outside the nucleolus as putative regulators of ribosome biogenesis (Farley-Barnes et al., 2018). Detailed study and characterisation of some of these assembly factors highlight interesting differences between ribosome biogenesis in yeast and humans. For instance, a microscopy-based screen monitoring the localisation of pre-ribosomal subunits highlighted important differences in the assembly pathway of the 60S ribosomal subunit. Similar to yeast, the exportin CRM1 along with adaptor proteins such as NMD3 are implicated in the export of pre-60S subunits in humans (Güttler and Görlich, 2011). Additionally, Exportin 5 (Exp5) is implicated in pre-60S export into the cytoplasm and its depletion leads to

significant defects in LSU maturation (Wild et al., 2010). In contrast, deletion of Msn5 (homologue of Exp5 in yeast) does not affect ribosomal subunit maturation indicating that the pathways for pre-60S export are not conserved between yeast and humans (Stage-Zimmermann et al., 2000). These screens confirm the notion that although many facets of ribosome biogenesis are conserved from yeast to humans, there is a higher degree of complexity in humans as revealed by the involvement of several metazoan-specific assembly factors and the precise roles of many of these factors have still not been elucidated.

1.1.2 pre-rRNA maturation in humans

In humans, nascent 47S pre-rRNA (containing 18S, 5.8S, 28S rRNA sequences) is synthesized by RNA polymerase I from repeats of rDNA sequences situated on chromosomes 13,14,15, 21 and 22. The 5S rRNA is synthesized by RNA polymerase III from multiple genes located on chromosome 1, found in close proximity to the nucleoli (Fedoriw et al., 2012). Within the primary transcript, the sequences of the mature rRNAs are flanked by external and internal transcribed spacer sequences (ITS1 and ITS2, and 5' ETS and 3' ETS), which are excised by the sequential and co-ordinated action of endo- and exo-nucleases (Figure 1.3). In mammalian cells, the 47S pre-rRNA is initially processed at site A' and O2 to generate the 45S pre-rRNA. Interestingly, the A' cleavage site is only found in metazoans (Lazdins et al., 1997). As cleavage at this site did not play a role in downstream processing events (Sloan et al., 2014), the functional relevance of this additional cleavage site still needs to be elucidated. However, as human ribosome biogenesis has a higher degree of complexity compared to yeast, the emergence of an additional cleavage site has been suggested to play a role in quality control during the early stages of ribosomal subunit maturation (Sloan et al., 2014; Wang and Pestov, 2011). Cleavage of the 45S pre-rRNA can either initiate in 5'ETS or within the ITS1 region. The co-existence of alternate pathways for pre-rRNA processing may lead to changes in the ratios of precursors based on cell type or stress conditions (Choismel et al., 2006; Flygare et al., 2006) and suggests a mechanism for fine-tuning the kinetics and pattern of pre-rRNA processing in higher eukaryotes (Henras et al., 2015). In the main pre-rRNA processing pathway, initial cleavage at site 2 within the ITS1 region performed by RNase MRP results in the generation of 30S and 32.5S rRNA precursors. The 5' end of 30S pre-rRNA is processed by co-ordinated cleavages at site A₀ and 1 and the endonuclease hUTP24 is suggested to be required for these events to occur (Tomecki et al., 2015; Wells et al., 2016). The removal of 5' ETS from 30S results in the formation of the 21S pre-rRNA, which gets further processed at the 3' end by the action of RRP6 (Preti et al., 2013; Sloan et al., 2013a; Tafforeau et al., 2013) leading to the generation of the 21S-C pre-rRNA species. A

XRN2 to produce 32.5S pre-rRNA, a short-lived precursor which is rapidly converted to the 32S pre-rRNA, which is an abundant, common LSU precursor arising out of all alternative processing pathways. The 32S pre-rRNA is cleaved within the ITS2 region to form the 12S and 28.5S pre-rRNAs (Schillewaert et al., 2012). 28.5S pre-rRNA is processed by XRN2 to produce the mature 28S rRNA. The 12S pre-rRNA is processed further by numerous 3' - 5' exonucleases to generate the 7S pre-rRNA (Couté et al., 2008; Michot et al., 1999) which subsequently gets processed by the nuclear exosome to form 6S pre-rRNA (Tafforeau et al., 2013), which is exported to the cytoplasm as part of the pre-LSU complex. The final 3' trimming of 6S pre-rRNA by exonuclease ERI1, results in the formation of mature 5.8S rRNA (Ansel et al., 2008).

Along with nuclease-mediated processing of the pre-rRNA transcript, nucleotide modifications of pre-rRNA sequences (Littlefield and Dunn, 1958a, 1958b; Smith et al., 1992) play a significant role in the maturation of pre-rRNAs. Most modifications are well-conserved amongst species and are found to be clustered around functionally important regions of ribosomes (Decatur and Fournier, 2002). The most common rRNA modifications are either methylation of the 2'-hydroxyl group of the sugar residue mostly catalysed by the box C/D snoRNPs or the conversion of uridine residues to pseudouridine mediated by box H/ACA snoRNPs (Decatur and Fournier, 2002). C/D box snoRNPs have also been implicated in the acetylation of cytosine residues in yeast and humans (Sharma et al., 2015). Each snoRNP complex combines a set of proteins, responsible for catalysing the enzymatic reaction along with a specific guide RNA, which base-pairs with the pre-rRNA target region. Apart from these, few modifications are catalysed by specific stand-alone enzymes (Henras et al., 2017; Sloan et al., 2017). As extensive base-pairing with target pre-rRNAs is a prerequisite for snoRNPs to act, most modifications are thought to be installed in the early stages of ribosome biogenesis when the pre-ribosome structure is more open. In human rRNAs, currently 228 modified sites have been identified as opposed to 112 in the yeast rRNAs, and the higher density of rRNA modifications has been attributed to the fact that human ribosome biogenesis is more complex and hence, needs additional regulation via rRNA modifications (Sloan et al., 2017). Although the functional relevance of many of these modified sites remains unknown, it has been suggested that modified nucleotides alter the chemical and topological properties of the basic nucleotides and can therefore, act to structurally stabilize the ribosomal RNAs, thereby influencing translation (King et al., 2003; Yoon, 2006).

Apart from nucleotide modifications, several snoRNAs - including U3 (SNORD3), U14A/B (SNORD14A/B) and the metazoan-specific snoRNAs U8 (SNORD118) and U22 (SNORD22)- play an important role in mediating pre-rRNA folding and cleavage (Watkins and Bohnsack, 2012). Base-pairing between distinct distant regions of pre-rRNAs and the

corresponding snoRNAs results in the interlocking of pre-rRNA, thereby promoting its folding and subsequent processing. For example, long range interactions formed between the U3 snoRNA and the 18S rRNA sequence in the early stages of small subunit biogenesis are important for the efficient maturation of the 18S rRNA. Moreover, the timely release of U3 snoRNA is critical for the maturation of the small subunit (Sardana et al., 2015). Similarly, it was demonstrated in humans that snoRNA guided pre-rRNA folding can influence important cleavage events in the final steps of SSU assembly. For example, the endonuclease NOB1, responsible for the final step of 18S rRNA maturation, initially is recruited away from its cleavage site. However, structural rearrangements during final steps of pre-40S biogenesis bring NOB1 into close proximity to its site of action, triggering the formation of mature 18S rRNA (Ameismeier et al., 2018; Larburu et al., 2016).

1.1.3 Role of ribosomal proteins

Ribosomal proteins (RPs) play crucial roles in the assembly of eukaryotic ribosomes *in vivo* and mutations in genes encoding RPs are associated with a wide range of ribosome-associated diseases, especially bone marrow failures (Liu and Ellis, 2006). The expression of all 80 RPs in humans is precisely regulated and co-ordinated to maintain equal levels in order to ensure appropriate availability for subunit assembly. Hence, most genes encoding RPs share a common promoter sequence. Structural analyses of mature ribosomes have revealed that RPs generally comprise globular domains interspersed by unstructured loops responsible for binding to rRNA, to other RPs or *trans*-acting assembly factors (Melnikov et al., 2012). Upon translation in the cytoplasm, chaperones bind co-translationally to nascent RPs facilitating their import into the nucleus wherein they associate intimately with pre-ribosomal particles (de la Cruz et al., 2015; Pillet et al., 2017). Although precise roles of many RPs during ribosome biogenesis are not known, it is thought that RPs can also act as chaperones during ribosome assembly that assist in processing and proper folding of nascent pre-rRNAs (Robledo et al., 2008). Furthermore, it has been demonstrated that RNAi-mediated depletion of RPs of the SSU impairs maturation of the 18S rRNA (O'Donohue et al., 2010). Depletion of LSU RPs results in the impaired production of 28S and 5.8S rRNA and thus, the decreased production of 60S ribosomal subunit. RPL5 is involved in the processing of pre-5S rRNA and forms the RPL5/5S complex that undergoes nuclear import. In the nucleolus, the RPL5/5S complex associates with RPL11 to form the 5S RNP complex which gets incorporated into the pre-60S subunit (Ciganda and Williams, 2011; Sloan et al., 2013b; Steitz et al., 1988). For the maturation of the SSU, a subset of RPs have been shown to associate with 90S pre-ribosomal complexes and play a role in the early stages of ribosome assembly. The assembly of the first set of RPs helps to attain a critical conformational state before further processing can occur. This is followed by the

assembly of RPs that initiate the folding of the 'head' domain. The second set of RPs, which are incorporated later, are important for efficient processing of ITS1 and structuring the 3' domain of 18S rRNA (O'Donohue et al., 2010). The sequential assembly of RPs leads to an ordered 5' - 3' structuring of the human 40S and was similar to what was observed in yeast (Ferreira-Cerca et al., 2005) and in prokaryotes (Chen and Williamson, 2013) suggesting that this is a highly conserved, critical mechanism for ensuring fidelity of the maturation pathway. Although there is considerable conservation of RPs between yeast and humans, various studies focussing on human ribosome biogenesis have highlighted differences. For example, in humans, knockdown of small subunit proteins, RPS7 and RPS28 impairs processing of 5'ETS and ITS1 (Robledo et al., 2008). In contrast, yeast Rps7 and Rps28 affect the cytoplasmic maturation steps of the 18S rRNA and the pre-40S subunit (Ferreira-Cerca et al., 2005, 2007). Furthermore, depletion of RPS15 in humans, allows efficient export of 18S-E pre-rRNA to the cytoplasm, but final cytoplasmic maturation steps of pre-40S are affected (Robledo et al., 2008). However, in yeast, Rps15 was observed to be crucial for the export of the 20S pre-rRNA (analogous to human 18S-E) from the nucleus (Léger-Silvestre et al., 2004).

In addition to their roles in the assembly pathway of ribosomal subunits, several ribosomal proteins have been implicated in carrying out extra-ribosomal activities. For example, RPs have been shown to play important roles in the innate immune response. Extra-ribosomal RPL13A can act as a translational regulator and can modulate the expression of Interferon- γ (Mukhopadhyay et al., 2009). Additionally, RPL22 and RPL22L1 have been reported to play a key role in the modulation of splicing of distinct pre-mRNAs (Zhang et al., 2017) and RPS13 and RPL10a are implicated in the process of alternative splicing (Malygin et al., 2007; Takei et al., 2016). Another prominent example of an extra-ribosomal function of RPs is the 5S RNP complex (Pelava et al., 2016). The tumour suppressor, p53 is regulated by the levels of the E3 ubiquitin ligase HDM2. HDM2 together with its related protein HDMX binds p53, thereby inhibiting its transcriptional activity and marking the protein, via ubiquitination, for subsequent degradation. In case of defective ribosome assembly, unincorporated, nucleoplasmic 5S RNP complex binds HDM2, blocking its action and leads to the stabilization of p53 (Donati et al., 2013; Sloan et al., 2013b). The 5S-HDM2 pathway has now been shown to act as the sensor responsible for lipid homeostasis (Oie et al., 2014), nutrient stress and oxidative stress (Liu et al., 2016; Pelava et al., 2016).

1.1.4 Structural transitions during subunit assembly in humans

Apart from RPs, formation of mature, functional ribosomal subunits is also assisted by a variety of *trans*-acting ribosome biogenesis factors (RBFs) which co-ordinate proper folding and processing of pre-rRNAs. Unlike RPs, RBFs are not part of the mature ribosome

subunits but engage relatively transiently to ensure directionality, sequential assembly of RPs and productive formation of stable pre-rRNA folding intermediates. Major classes of RBFs involved in ribosome assembly include nucleases responsible for pre-rRNA processing and removal of spacer sequences, modification enzymes that carry out nucleotide modifications, GTPases, which act as important placeholders and molecular switches, ATPases that are essential for mediating conformational rearrangements and nuclear export factors. Importantly, RNA helicases act as crucial remodellers of pre-ribosomal complexes by regulating RNA-RNA or RNA-protein interactions at specific stages of subunit maturation (discussed in detail in section 1.2).

Due to recent advancements in structural biology techniques such as cryo-EM, snapshots of various stages (from middle to late) of human 40S subunit are now available, highlighting the vast range of structural rearrangements that take place resulting in the maturation of the small ribosomal subunit (Ameismeier et al., 2018; Larburu et al., 2016). Assembly of the SSU occurs in sequential, discrete steps involving a large interaction network of RBFs. The maturation of the 40S 'body' domain is completed by the recruitment of several RPs, leading to the recruitment of the nuclease NOB1. At the same time, export adaptor RRP12 binds to the 'head' region of the pre-40S subunit containing the 3' major domain of the 18S rRNA and mediates essential structural rearrangements of the pre-40S complex. The release of RRP12 in cytoplasm is followed by the recruitment of the translational initiation factor, RACK1. Interestingly, in yeast, RACK1 is not present in pre-40S complexes (Larburu et al., 2016) and Rrp12 interacts with nucleoporins to aid the export of pre-40S particles (Oeffinger et al., 2004). In humans, the release of RRP12 has been suggested to ensure the fidelity of the assembly pathway by coupling correct 'head' formation and nuclear export. The biogenesis factors ENP1 and LTV1 are present in the 'beak' region of late pre-40S particles, preventing the folding of rRNAs into their mature conformations and the binding of specific RPs. LTV1 and ENP1 are phosphorylated by the kinase CK1 δ/ϵ , which triggers their dissociation from the pre-40S particles (Ghalei et al., 2015; Zemp et al., 2014) leading to the stable incorporation of RPS3 and the proper arrangement of the rRNA helices that form the mature 'beak' structure. Maturation of the decoding centre, which harbours the A and the P sites within the pre-40S subunit, entails the precise folding between h44 and h28 or h45. The kinase RIOK2, along with the inactive GTPase TSR1 and LTV1, bind and stabilize h44 maintaining the helices in immature conformational states and blocking proper folding of this region (Ameismeier et al., 2018; Larburu et al., 2016). Along with these RBFs, the RNA-binding protein PNO1 stabilizes h28 and h45 in an immature state and also helps spatially retain NOB1 distant from its target cleavage site. Release of PNO1 results in a large structural rearrangement, promoting the rearrangement of the 3' end of 18S rRNA into the catalytic pocket of NOB1, leading to its cleavage. In yeast, Dim1 is responsible for

methylation of two adenosine residues (A1781/A1782) in the 18S rRNA in the cytoplasm (Lafontaine et al., 1998). Interestingly, in humans, DIMT1L carries out the equivalent methylations in the 18S rRNA sequence in the nucleus and is not exported out into the cytoplasm along with the pre-40S subunit (Zorbas et al., 2015). Although the purpose of this difference in spatial compartmentalization is not yet understood, it has been suggested that the methylation status of the 18S rRNA can serve as an important quality-control checkpoint and commit the pre-40S subunits for nuclear export (Zorbas et al., 2015). Export of pre-40S particles into the cytoplasm is mediated by the exportin CRM1 in association with adaptor proteins such as RIOK2 and PDCD2L (Landry-Voyer et al., 2016). The nuclear transport factors Mex67-Mtr2 play crucial roles in the export of pre-40S and pre-60S subunits in yeast (Faza et al., 2012), however, their human homologues were not found to be required for pre-40S export (Wild et al., 2010), suggesting that this function of these proteins might not be conserved in higher eukaryotes.

While in yeast structural information on several pre-60S particles is already available, less is currently known about the structural rearrangements that occur during 60S biogenesis in humans. In yeast, the AAA-ATPase Rea1 plays a key role in triggering the release of ribosomal proteins during the maturation of 60S particles. The orthologue of Rea1 in humans, MDN1, has been suggested to play a similar role (Raman et al., 2016). One aspect of pre-60S maturation that has been well-studied in humans is the release of pre-60S factor eIF6 (Tif6 in yeast). Tif6 associates with pre-60S subunits in yeast and acts as an anti-association factor by inhibiting the association of pre-60S and (pre-) 40S subunits in the cytoplasm and is released by action of the GTPase, Efl1 (Senger et al., 2001). In humans, eIF6 is reported to bind to ribosomal proteins RPL3, RPL14 and RPL24 and prevents the joining of subunits by inhibiting inter-subunit bridge formation (Gartmann et al., 2010). This event seems to be conserved as recruitment of the GTPase EFL1 leads to the release of eIF6 (Gartmann et al., 2010; Klinge et al., 2011).

1.1.5 Ribosomopathies

Ribosomopathies constitute a growing class of diseases caused by mutations in genes encoding RPs and RBFs. These abnormalities can alter the quantity of ribosomes by preventing the production of translation efficient subunits or affect the quality by altering the protein composition or modification pattern (Danilova and Gazda, 2015; Mills and Green, 2017; Narla and Ebert, 2010). Ribosomopathies are often associated with developmental abnormalities and increased risk of cancer. Diamond-Blackfan anemia (DBA) is the most well-understood of all the ribosomopathies with its link to ribosome biogenesis clearly established. DBA is relatively rare with 5-7 cases per million live births. Mutation in 19 RP genes have now been associated with DBA, which is characterized by bone marrow failure leading to severe anaemia (Da Costa et al., 2018). Mutations in the RP genes resulting in DBA include missense, nonsense or frameshift mutations resulting in impaired mRNA synthesis or stability leading to decreased RP production (Boria et al., 2010). Several other congenital disorders resulting in haematopoietic dysregulation are also associated with mutations in genes encoding RBFs, including Shwachman-Diamond syndrome (Shwachman et al., 1964), 5q- syndrome (Trainor et al., 2009) and Dyskeratosis congenita (Knight et al., 2001). Additionally, both Treacher-Colins syndrome (Vincent et al., 2016) and Bowen-Conradi syndrome (Armistead et al., 2009), which result in craniofacial defects, are caused by mutations in RBFs. Affecting ribosome biogenesis, thus often leads to overlapping phenotypic characteristics; therefore, understanding the tissue-specific defects that manifest as a result of impaired ribosome synthesis still remains a challenge. Several models have been suggested in order to explain the molecular basis of ribosomopathies. The number of ribosomes is tightly controlled in cells, a phenomenon known as ribosome homeostasis. Ribosome deficiency in cells, as a result of mutations in genes encoding RPs and assembly factors, might lead to changes in ribosome homeostasis. As the number and concentration of ribosomes can vary depending on cell type and cell-cycle phase, alterations in the number of functional ribosomes can adversely impact the synthesis of specific proliferation regulators. This leads to the tissue-specific pathologies as observed in ribosomopathies. In the case of DBA, genes involved in erythroid differentiation are observed to be most sensitive to the reduced number of ribosomes (Khajuria et al., 2018; Ludwig et al., 2014). Additionally, new techniques that enable detailed investigations into the stoichiometry of rRNA modifications and the protein composition of ribosomes, suggest that ribosomes can have varied modifications and may differ in their protein compositions. These differences imply the presence of heterogeneous populations of ribosomes (Bortoluzzi et al., 2001; Simsek et al., 2017). Hence specialized ribosomes might be important for the translation of specific mRNAs that are involved in development and proliferation. Therefore, alterations in ribosome composition due to mutation in genes

encoding RPs or RBFs might affect tissue specific pathways. Moreover, impaired ribosome biogenesis can also lead to the accumulation of the 5S RNP complex that can bind to the HDM2 ubiquitin ligase and sequester it, resulting in the stabilization of p53 leading to cell cycle arrest and apoptosis (Donati et al., 2013; Sloan et al., 2013b). Many of the developmental defects in ribosomopathies can be attributed to the activation of p53. Moreover, prolonged stimulation of p53 also leads to loss of sensitivity resulting in higher susceptibility to cancer as observed in many ribosomopathies.

1.2 RNA helicases

RNA helicases are ubiquitously expressed and highly conserved enzymes that participate in nearly all aspects of RNA metabolism. These proteins bind and remodel RNA or RNPs in a nucleoside triphosphate (NTP) dependent manner (Tanner et al., 2001). RNA helicases comprise a structurally conserved core, often flanked by N- and C-terminal domains that contribute to their specificity. Although RNA helicases were originally defined as enzymes that play a key role in unwinding RNA duplexes, they are now known to be involved in a wide range of molecular remodelling functions such as strand annealing, displacement of protein from RNA and acting as RNA clamps (Bourgeois et al., 2016).

1.2.1 RNA helicase superfamilies and conserved sequence motifs

DNA and RNA helicases can either form, or not form, toroidal, hexameric rings (Singleton et al., 2007). Based on structural and functional analyses, all helicases are categorised into six major superfamilies (SFs) (Gorbalenya and Koonin, 1993). SF1 and SF2 include non-ring forming helicases whereas the helicases that form ring-like structures are classified into SFs 3-6. SF1 and SF2 consist of characteristic helicase families that have high sequence conservation and all RNA helicases cluster within these families. A hallmark of RNA helicases belonging to SF1 and SF2 is the presence of a structurally conserved helicase core comprising two related domains arranged in tandem (Figure 1.4). These domains are similar to the fold of the bacterial recombination protein RecA (Singleton et al., 2007). Within the two RecA-like domains (D1 and D2), up to 12 highly conserved sequence motifs have been identified that have been found to play key roles in RNA substrate-binding, and NTP-binding and hydrolysis (Fairman-Williams et al., 2010). Motifs I (Walker A), II (Walker B) and VI are highly conserved and co-ordinate NTP-binding and hydrolysis. Motif I, classically defined as GxxxxGKT (Walker et al., 1982), requires the active participation of the three terminal residues (GKT). The side chain of the lysine interacts with β -phosphate of ATP and mutations in this motif lead to compromised NTP hydrolysis by the helicase (Pause and Sonenberg, 1992). Motif II consists of conserved amino acid stretches, aspartate-glutamate-alanine-glutamate (DEAD) or aspartate-glutamate-alanine-histidine (DEAH).

The glutamic acid residue is reported to act as a catalytic base during ATP hydrolysis whereas the carboxyl group of the aspartate is involved in the co-ordination of Mg^{2+} ion. Motif VI comprises two highly conserved arginine residues, involved in the stabilization of transition states during catalysis (Caruthers and McKay, 2002). The relatively recently identified Q motif has been suggested to play a role in regulation of ATP-binding and hydrolysis and is absent in DEAD box helicases, which can potentially interact with other NTPs (Tanner et al., 2003). Additional conserved motifs include motifs III, which is involved in coupling NTP- and nucleic acid-binding, and motifs which primarily contact the RNA substrate (Ia, Ib, Ic, IV, IVa, V). These motifs have been also shown to play roles in bridging interactions between the RNA substrate and the NTP-binding site (Banroques et al., 2008).

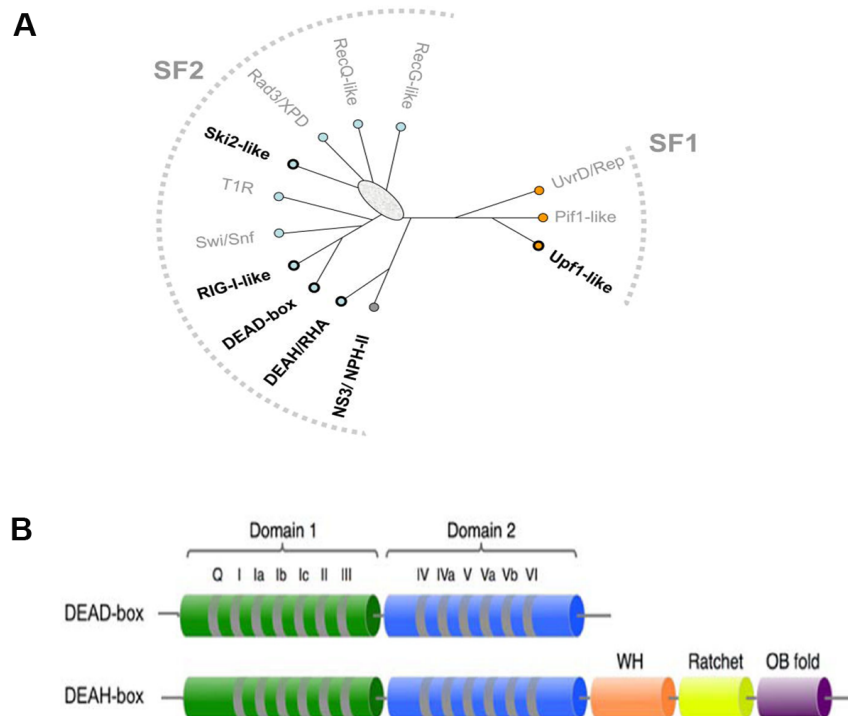


Figure 1.4. SF1 and SF2 superfamily of helicases. (A) RNA helicases cluster within 6 sub-families (Ski2, RIG-I-like, DEAD-box, DEAH/RHA, NS3/NPH-II, Upf1-like) of SF1 (right) and SF2 (left) superfamily of helicases (in bold) (Jankowsky, 2011) **(B)** Domain architecture of DEAD-box and DEAH-box members of RNA helicases represents the conserved helicase core formed by two RecA-like domains (Domain 1 and Domain 2). The helicase core constitutes of sequence motifs essential for NTP binding and hydrolysis. DEAD-box helicases don't possess conserved N- or C-terminal extensions, however, C-terminal domain of DEAH-box helicases share conserved domains such as winged-helix (WH), ratchet domain or the OB-fold (panel adapted from Gilman et al., 2017).

Along with the conserved helicase core, RNA helicases frequently contain N- and C-terminal domains that are often larger than the helicase core in size and are highly variable within and across the helicase families (Fairman-Williams et al., 2010). As the core is highly

conserved across all helicases, these terminal domains are suggested to play important roles in conferring substrate specificity. Additionally, they can assist in increasing the substrate repertoire of multi-functional helicases and can also serve as platforms for cofactor interactions (Karginov et al., 2005; Lattmann et al., 2010). The auxiliary domains can adopt distinct folds to confer additional functions such as nuclease activity, or serve as RNA-binding domains or protein-interaction domains (e.g. CARD domains) (Yoneyama and Fujita, 2008). The majority of the DEAD-box proteins have variable C- and N-terminal domains typically including RNA recognition motifs (RRM) or zinc fingers (Linder, 2006). Interestingly, DEAD-box proteins can also exist with the minimal helicase core, lacking the terminal accessory domains (Rudolph and Klostermeier, 2015). In contrast, DEAH-box proteins all contain a highly conserved C-termini, which is organized into specific domain known as the OB-fold (oligonucleotide-binding), winged-helix domain and the ratchet domain. The winged-helix domain and the ratchet domain associate, and form stacking interactions with the nucleic acid base moieties (Walbott et al., 2010). The OB-fold includes five β -strands that form a β -barrel structure (Murzin, 1993) and can interact with nucleic acids or *trans*-acting protein cofactors (Arcus, 2002; Theobald et al., 2003)

1.2.2 Mechanism of action of RNA helicases

Although the three-dimensional structure of the core domains is similar between the DEAD- and DEAH-box family proteins, detailed structural studies have revealed that the mechanism of substrate binding and unwinding vary considerably between the two families (Gilman et al., 2017; Hamann et al., 2019; He et al., 2010; Tauchert et al., 2017).

DEAD-box proteins constitute the largest sub-group of the SF2 family with 37 members in humans and 26 in yeast (Fairman-Williams et al., 2010; Linder and Jankowsky, 2011). They are characterized by two flexible RecA-like domains interrupted by a linker and consist of a variable N- and C-terminal tail region. Pioneering studies with the DEAD-box helicase eIF4A, have demonstrated that DEAD-box helicases can interact directly with dsRNA and successfully unwind helices up to 15 bp, however, the efficiency of unwinding decreases with substrate length (Rogers et al., 1999). Hence, they are thought to act as local 'unwindase' with low processivity. Structural characterization of yeast DEAD-box Mss116, which is involved in RNA splicing of group I and II introns, has further revealed the detailed mechanism of action of this family of helicases (Figure 1.5A).

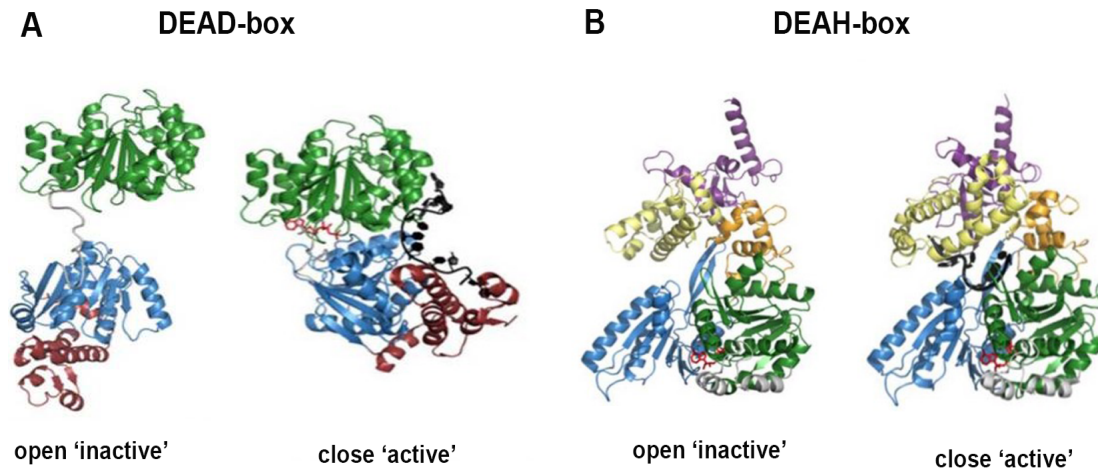


Figure 1.5. Structural characterization of DEAD-box and DEAH-box helicases. (A) Structure of DEAD-box helicase Mss116 in the 'open' conformation (left) based on small-X-ray scattering data and the 'close' conformation (right) derived from crystal structure (PDB: 315X). The structure of the 'closed' conformation was obtained in the presence of bound nucleotide (in red) and the ssRNA substrate (in black). Additional C-terminal domains present in Mss116 but not conserved amongst all DEAD-box proteins is represented in magenta (B) Structure of DEAH-box helicase Prp43 in the 'open' (left) and 'close' (right) conformation obtained from crystal structures (PDB: 5LTK and PDB: 5LTA, respectively). The bound nucleotide and ssRNA shown in red and black, respectively. All domains are coloured as in figure 3 (Panel adapted from Gilman et al., 2017).

In the absence of ligands, the two RecA-like domains of DEAD-box helicases are spatially separated and adopt an 'open' inactive conformation (Mallam et al., 2011, 2012).

Co-operative binding of ATP to D1 and the dsRNA substrate to D2 promotes structural rearrangement, resulting in the formation of a 'closed' active state, characterized by the intimate inter-domain contacts between the conserved sequence motifs. The closed conformation distorts the bound dsRNA by introducing a kink in one strand leading to duplex unwinding and release of the other strand by the complex. ATP hydrolysis and release of inorganic phosphate (P_i) then facilitates the dissociation of the enzyme complex and release of the bound RNA strand (Hilbert et al., 2009; Yang et al., 2007). DEAD-box helicases, due to their low processivity, can unwind only short stretches of RNA by stochastic dissociation of double stranded helices around the sequence tightly bound by the helicase. Notably, a single round of ATP hydrolysis is only required for the recycling of the helicase but not for strand unwinding (Chen et al., 2008; Liu et al., 2008). In order to unwind longer RNA structures, DEAD-box helicases (for example, Mss16 or DDX43) can sometimes employ the assistance of their auxiliary domains. The basic C-terminal domain of Mss16 or the N-terminal domain of human DEAD-box protein, DDX43, have been shown to anchor the helicase close to their target sites, allowing multiple rounds of unwinding (Mohr et al., 2008; Talwar et al., 2017).

In contrast, DEAH-box helicases are highly processive, and are able to translocate along and unwind long RNA duplexes (Jarmoskaite and Russell, 2014; Pyle, 2008). Similar to DEAD-box proteins, they comprise conserved RecA-like domains, however, DEAH-box helicases contain different sequences within the conserved motifs (Figure 1.5B). In addition, the conserved C-terminal domains of DEAH-box proteins have been shown to physically associate with the core domains, resulting in the formation of a relatively rigid structure in comparison to DEAD-box helicases (Pyle, 2008). Furthermore, NTP binding can lead to extensive structural rearrangement in the C-terminal extension. This results in the opening of an RNA-binding tunnel located between the C-terminal and D2, facilitating substrate loading (Tauchert et al., 2017). In contrast to DEAD-box proteins, DEAH-box helicases require 3' single-stranded regions to serve as 'launch pads' for the effective loading of the helicase (Tanaka and Schwer, 2005) and they can utilize all four NTPs for efficient translocation (Fairman-Williams et al., 2010). Translocation along a substrate RNA duplex requires a diverse range of dynamic interactions between conserved motifs within the helicase. Upon binding to NTPs, DEAH-box helicases can advance in the 3'→5' direction as the conserved domains bind the substrate RNA in a defined order. D1 preferentially associates with 3' end of the RNA substrate whereas D2 interacts towards the 5' end, trapping the bound RNA. (He et al., 2017; Pyle, 2008; Tauchert et al., 2017) A β -hairpin structure from D2 stimulates unwinding by positioning itself between the last unpaired base and the first base-pair of the substrate duplex (Büttner et al., 2007). Hence, directional translocation occurs as the RNA duplex, locked in a defined geometry, is unwound as the helicase moves in steps, encompassing a new base from the 5' end while releasing one base from the 3' side (He et al., 2017). *In vivo*, RNA duplexes are often found in combination with bound proteins, forming large ribonucleoprotein particles. In order to gain access to dsRNA substrates, a 'winching' mechanism has been suggested for DEAH-box proteins. This involves loading of the helicase on an accessible single-stranded RNA region but upon encountering a physical block during translocation, continued pulling on the RNA strand, which ultimately results in the disruption of downstream base-pairing (Gilman et al., 2017; Semlow and Staley, 2012)

1.2.3 Cellular pathways involving RNA helicases

Traditionally, RNA helicases were considered to be an essential family of proteins catalysing the task of strand unwinding. Detailed biochemical and structural studies have revealed unexpected modes by which these proteins are able to carry out a diverse range of functions, and have now emerged as key players co-ordinating various aspects of RNA metabolism (Jarmoskaite and Russell, 2014; Linder and Jankowsky, 2011; Putnam and Jankowsky, 2013). Although the helicase-core domain does not inherently endow substrate

specificity, in combination with various *cis*- and *trans*-acting factors, they can be involved in specific RNA-related processes such as translation, pre-mRNA splicing, ribosome biogenesis, RNA decay and pre-mRNA nuclear export (Bourgeois et al., 2016). While some RNA helicases are only implicated in one cellular process, many other RNA helicases appear to participate in a diverse range of processes (Jarmoskaite and Russell, 2014). Although, detailed mechanistic studies have revealed the precise functions of an increasing number of helicases, lack of identified target RNAs, coupled with uncharacterized binding partners, prove to be challenging obstacles for elucidating the physiological roles of RNA helicases.

1.2.3.1 Role of RNA helicases in pre-mRNA splicing

Pre-mRNA splicing is an essential nuclear event in eukaryotes leading to the removal of introns from the nascent transcript resulting in mature, translatable mRNAs. The removal of introns and the subsequent ligation of adjacent or distant exons (in case of alternative splicing) requires the involvement of over 100 proteins that facilitate the formation of the spliceosome (Fica and Nagai, 2017). The nascent pre-mRNA transcript, during RNA polymerase II-mediated synthesis, associates with RNA-binding proteins, triggering the recognition of splice sites (Bourgeois et al., 2016; Fu and Ares, 2014; Witten and Ule, 2011). Various RNA helicases mediate pre-mRNA splicing by either interacting directly with the core spliceosome machinery or are involved in the process of dynamic regulation. Eight helicases (DDX39B, DDX46, DDX23, Brr2, DHX16, DHX15, DHX8, DHX38) have so far been shown to associate with the spliceosome and assist in the formation of mature mRNAs by facilitating protein displacement, structural rearrangement, reaction intermediate stabilization, and ensuring the fidelity and directionality of this complex process (Cordin and Beggs, 2013; Fica and Nagai, 2017).

Apart from these proteins that modulate spliceosome assembly and function, a number of additional RNA helicases play important roles in regulating the mechanism of pre-mRNA splicing. For example, the DEAD box helicases, DDX5 and DDX17, control splicing events of a large number of exons (Dardenne et al., 2014). Likewise, DDX48 (eIF4AIII) is a major constituent of the exon junction complex (EJC) and can regulate alternative splicing (Michelle et al., 2012; Wang et al., 2014). Another DEAD-box helicase, DDX41 was shown to be an important moderator of alternate splicing; and mutations in DDX41 resulted in impaired splicing events (Polprasert et al., 2015).

1.2.3.2 Role of RNA helicases in translation

Eukaryotic cap-dependent translation initiation requires the disruption of secondary structures present in the 5' UTRs of mRNAs that can impede efficient scanning by the pre-

initiation complex (PIC) (Aitken and Lorsch, 2012). Several RNA helicases have been implicated in resolving and restructuring 5'UTR regions, thereby promoting PIC loading and subsequent scanning. The DEAD-box helicase eIF4A, assisted by other translation factors including eIF4G (Rogers et al., 2001), facilitates association of the PIC with the mRNA by unwinding secondary structures in its vicinity (Aitken and Lorsch, 2012; Svitkin et al., 2001). Moreover, in yeast, efficient scanning by the initiation complex in cap-dependent initiation is also aided by the RNA helicase Ded1, which has been shown to stimulate (by promoting loading and scanning) or inhibit translational initiation (Hilliker et al., 2011). Apart from resolving 5'UTR structures, the DEAH-box helicase DHX29 can associate with the 40S ribosomal subunit near the mRNA entry channel and promotes the entry of mRNA by unwinding highly ordered structures (Abaeva et al., 2011). Furthermore, RNA helicases have also been shown to function at late stages of translation. The DEAH-box helicase DHX9 can modulate the translational process by anchoring to distinct secondary structures within mRNA and thereby promoting 40S scanning and mRNA circularization (Halaby et al., 2015; Manojlovic and Stefanovic, 2012). In addition, DDX33 and DDX19B are also key players in later steps of translation; DDX33 facilitates assembly of the 80S ribosomal complex (Zhang et al., 2015), and DDX19B is suggested to be involved in the recruitment of the eukaryotic release factor eRF3 (Gross et al., 2007).

1.2.3.3 Role of RNA helicases in other cellular pathways

In addition to their roles in translation and splicing, RNA helicases are central players in a variety of other cellular pathways. For example, nuclear export of mRNPs necessitates the formation of EJCs, which serve as binding platforms for factors essential for efficient export of mRNA into the cytoplasm and the formation of EJCs is facilitated by the action of DDX48 (eIF4AIII) (Wang et al., 2014). A subset of mRNAs require specialized export adaptor proteins such as Aly/REF (ALYREF), which are recruited by the DEAD-box helicase DDX39B (Luo et al., 2001). Following successful transition through the nuclear pore complex (NPCs), mRNPs can undergo extensive structural and conformational rearrangements mediated by DDX19B (Tieg and Krebber, 2013). Apart from facilitating mRNP export, RNA helicases have been shown to be important for processes such as cytoplasmic mRNA decay and microRNA (miRNA)-induced gene silencing. mRNA decay in the cytoplasm is promoted by DDX6, which stimulates the de-capping process and facilitates mRNA degradation by the 5' - 3' exonuclease, XRN1 (Fischer and Weis, 2002; Tieg and Krebber, 2013). Nonsense-mediated decay requires the action of the SF1 helicase, UPF1 (Lykke-Andersen and Jensen, 2015). Cytoplasmic mRNA storage has evolved to be an alternate fate for mRNAs not undergoing translation or decay and the DEAD-box helicases DDX6 and DDX3X can enhance the formation of RNA storage

granules in response to cellular stress (Hooper and Hilliker, 2013). Furthermore, miRNA biogenesis entails the processing of a primary miRNA (pri-miRNA) to form a precursor miRNA (pre-miRNA), which undergoes further processing to form the mature miRNA, involved in gene silencing. Helicases such as DDX5 and DDX17 (Moy et al., 2014) are involved in the processing of pri-miRNAs, demonstrating that RNA helicases also play important roles in the biogenesis of miRNAs. Additionally, ribosome biogenesis employs a vast network of RNA helicases that are necessary for the formation of mature, translation-competent ribosomes (discussed in detail in section 1.3)

1.2.4 Regulation of RNA helicases

Although RNA helicases inherently lack substrate specificity and demonstrate very low rates of catalysis, they are known to be multi-functional and co-ordinate various cellular events (Bourgeois et al., 2016; Jarmoskaite and Russell, 2014). These features necessitate the involvement of *trans*-acting proteins that can regulate the activity of RNA helicases and can endow tight spatial and temporal control in the complex cellular milieu. Helicase regulation can be also achieved *in cis* via the N- and C-terminal domains of RNA helicases or by post-translational modifications, which can result in the activation or inhibition of the helicase (Ozgun et al., 2015). Under the influence of these regulators, RNA helicases are able to associate with specific target RNA substrates, exhibit an increased rate of catalysis, and can be efficiently anchored to their sites of action (Sloan and Bohnsack, 2018).

1.2.4.1 Cofactor-dependent regulation of RNA helicases

A growing number of helicases have been shown to associate with proteins termed 'cofactors', which play important roles in modulating their functions *in vivo*. These cofactors can either be a heterogeneous group of proteins (stand-alone cofactors) that can regulate the activity of RNA helicases or may share a common domain via which they interact with the helicase. For example, the MIF4G family of proteins and the G-patch proteins act as cofactors for DEAD-box and DEAH-box helicases, respectively (Ozgun et al., 2015; Robert-Paganin et al., 2015; Sloan and Bohnsack, 2018). DEAD-box proteins such as eIF4A-like helicases are known to interact with cofactors containing evolutionarily-conserved MIF4G domains (Ponting, 2000). Structural studies have revealed that MIF4G domain-containing proteins, such as eIF4G, can interact with the helicase-core region of eIF4A1 and its paralogue eIF4AII, stabilizing the 'half-open' conformation promoting RNA-binding and increasing the rate of catalysis during cap-dependent translation (Andreou and Klostermeier, 2014; Hilbert et al., 2011; Schütz et al., 2008). Interestingly, in addition to such stimulatory roles, MIF4G domain proteins such as CWC22 can also inhibit the activity of helicases. CWC22 binding to eIF4AIII results in the reorientation of the helicase-core

domains creating a distance between the ATP- and the RNA-binding sites, leading to the stabilization of an inactive conformation of the helicase (Alexandrov et al., 2012; Steckelberg et al., 2012). Therefore, MIF4G domain-containing proteins are able to interact with their specific cognate helicase and can induce opposing outcomes despite possessing high sequence and structural conservations. As a result, this family of proteins plays an important role in intricately balancing the activity of multi-functional enzymes such as eIF4AIII. On the other hand, the C-termini of DEAH-box proteins consist of conserved sequence folds such as the OB-fold, which can serve as binding platforms for proteins (Arcus, 2002; Theobald et al., 2003). A family of effector proteins known as 'G-patch proteins' have been shown to interact with the OB-folds of specific DEAH-box helicases and regulate their activity (Robert-Paganin et al., 2015). G-patch proteins possess glycine rich stretches of 45-50 amino acid residues and are defined by the consensus sequence-HHX₃GAX₂GXGHGX₄G (H - hydrophobic, A - aromatic, X - non-conserved amino acid, G – conserved glycine) (Aravind and Koonin, 1999). In yeast, five G-patch proteins (Pfa1, Gno1, Spp382, Cmg1 and Spp2) have been shown to positively regulate the ATPase and unwinding activity of their cognate helicases (Boon et al., 2006; Chen et al., 2014a; Heininger et al., 2016; Lebaron et al., 2009; Tanaka et al., 2007; Warkocki et al., 2015). The mechanistic details of helicase activation via G-patch domain-containing proteins are not fully understood. However, the binding of G-patch domains to OB-folds is thought to induce conformational changes that can influence the catalytic activity of the helicase (Christian et al., 2014; Heininger et al., 2016; Tanaka et al., 2007). Although these proteins were found to be conserved in higher eukaryotes, detailed studies have demonstrated that there are additional G-patch proteins found in higher eukaryotes (Chen et al., 2014b; Wen et al., 2008; Zang et al., 2014). This suggests that mammalian gene expression requires additional layers of RNA helicase regulation owing to a higher degree of complexity. MIF4G domain and presumably G-patch containing cofactors influence the activity of the helicase by triggering conformational changes in their tertiary structure. In contrast, several protein cofactors can modulate the activity of helicases without inducing structural rearrangements. As RNA helicases are RNA-dependent ATPases, these proteins can either inhibit (negative regulators) or promote (positive regulators) RNA binding to the cognate helicases (Napetschnig et al., 2009).

1.2.4.2 Cofactor-independent regulation of RNA helicases

In addition to functioning as binding platforms for cofactors, the N- and C-terminal domains flanking the helicase core can also contribute to helicase autoregulation by intrinsically stabilizing the core domains in an active/inactive conformation. In humans, the N-terminal region of the DEAD-box helicase DDX19 interacts with the two RecA-like domains, thus

stabilizing the inactive conformation. The N-terminal domain is displaced upon RNA binding, which promotes the active state of the helicase (Collins et al., 2009). Apart from intramolecular regulation via auxiliary domains, some RNA helicases can also distinguish and preferentially associate with distinct RNA sequences. For example, the RNA recognition motif present in the C-terminal tail of the bacterial DEAD-box protein DbpA, is responsible for its specific recruitment to the 23S rRNA (Diges and Uhlenbeck, 2001). Additionally, the basic C-terminal tail of the DEAD-box helicase, Mss116 is crucial for its recruitment to the target RNA substrate (Mallam et al., 2012). The regulation of RNA helicases can also occur by post-translational modifications, which can either directly impact the catalytic activity or might influence protein-protein interactions (Sloan and Bohnsack, 2018). For example, acetylation of DDX21 has been shown to inhibit its unwinding activity and deacetylation can reinstate the helicase in its active form (Song et al., 2017). Recent data reveal that long non-coding RNAs (lncRNA) can also function as modulators of RNA helicase activity thereby, providing an additional layer of regulation necessary to regulate the dynamic functions of RNA helicases. For example, in dendritic cells, BC1 lncRNA modulates the activity of eIF4A1 during translation. BC1 has been reported to specifically inhibit the duplex unwinding activity of eIF4A1 while stimulating its ATP hydrolysis (Lin et al., 2008). Additionally, the lncRNA BC200 has been reported to serve as a cofactor for DEAD-box helicase DHX36, and regulates the unwinding of quadruplex containing RNA substrates (Booy et al., 2016).

1.3 The roles of RNA helicases in ribosome biogenesis

The process of ribosome biogenesis involves a dynamic interplay of a vast majority of factors including RNA helicases that play a key role in the remodelling of ribosomal subunits. In bacteria, four out of the five reported DEAD-box helicases have been implicated in ribosome biogenesis (Martin et al., 2013). In eukaryotes, the assembly of ribosomal subunits engages a large number of RNA helicases. These play a crucial role in mediating pre-rRNA folding and processing, and regulating the association of snoRNAs with pre-ribosomal subunits and thereby remodelling protein-RNA and RNA-RNA interactions. Although several RNA helicases have been implicated in the process of ribosome biogenesis, the physiological roles of only a few, especially in higher eukaryotes, have been characterized in detail. As the process of ribosome biogenesis is largely conserved in eukaryotes, RNA helicases that have been well-characterized in yeast, are assumed to play similar roles in humans. Although this is true for a subset of RNA helicases, genome-wide screens and detailed characterization of specific helicases have highlighted that they might have additional or different roles in higher eukaryotes.

1.3.1 RNA helicases regulate snoRNA association with pre-ribosomal particles

snoRNAs associate with pre-ribosomal subunits by forming base-pairing interactions with the pre-rRNA. These interactions either direct pre-rRNA modification or facilitate structural rearrangements of pre-ribosomal particles by mediating long-range interactions (Watkins and Bohnsack, 2012). So far, 72 of the 75 snoRNAs identified in yeast belonging to the box C/D or H/ACA families, guide nucleotide modification and are non-essential. However, three snoRNAs, namely, U3, U14 and snR30, are essential and mediate pre-rRNA folding and cleavage (Rodríguez-Galán et al., 2013; Watkins and Bohnsack, 2012). snoRNA-guided restructuring and modification usually occurs early in the biogenesis pathway. The snoRNA-pre-rRNA interaction preserves the pre-rRNA in a stable, accessible conformation, to be acted upon by various *trans*-acting factors. Following snoRNA association and function, dissociation and subsequent removal from pre-ribosomal complexes is imperative for the formation of mature ribosomal subunits. Furthermore, snoRNA-mediated modifications often occur in clusters within distinct regions of the rRNA sequence. This implies that snoRNAs must dissociate in order to grant access to subsequent snoRNAs. In yeast, several of the 21 RNA helicases that associate with pre-ribosomal subunits have been implicated in promoting either binding or dissociation of specific snoRNAs from pre-ribosomal complexes (Martin et al., 2013). U3 snoRNA is a central part of the SSU processome and forms long-range interactions with 18S rRNA sequences and with 5'ETS, close to the A' (humans) or A₀ (yeast) sites. These interactions play an important role in regulating the timing of formation of the central pseudoknot, a key structural element found in mature 40S ribosomal subunits, and also for co-ordinating cleavage events within the 5' ETS and ITS1 region (Dutca et al., 2011; Sharma and Tollervey, 1999). In yeast, Dhr1 promotes the unwinding and displacement of the U3 snoRNA from the pre-ribosomal particles, allowing the downstream pre-40S maturation events to occur (Sardana et al., 2015; Zhu et al., 2016). The DEAD-box helicase Has1 has been shown to play a prominent role in the displacement of the box C/D snoRNA U14, which is implicated in directing 18S pre-rRNA processing and modification (Brüning et al., 2018; Enright et al., 1996; Li et al., 1990). The box H/ACA snoRNA snR30 is important for cell viability and co-ordinates early pre-rRNA cleavage events at sites A₀, A₁ and A₂ (Beltrame and Tollervey, 1995; Hughes and Ares, 1991; Li et al., 1990). The DEAD-box helicase, Rok1 was found to be required for its efficient release, promoting subunit maturation (Bohnsack et al., 2008). One of the best characterized helicases in the context of yeast ribosome biogenesis is Prp43, a multi-functional DEAH-box protein involved in various steps of ribosome assembly. It is required for the dissociation of a subset of box C/D snoRNAs, which direct the methylation of nucleotides in helices 32 to 35 in 25S rRNA (snR39, snR39b, snR50, snR59, snR60 and snR72) from pre-ribosomal subunits (Bohnsack et al., 2009). *In vivo* crosslinking data

indicates that Prp43 directly interacts with the snoRNAs guiding methylation and also crosslinks to the snoRNA base-pairing sites in the pre-rRNA. This overlap suggests a direct role of Prp43 in the displacement of these snoRNPs from the pre-rRNA sequence (Bohnsack et al., 2009). Moreover, Prp43 is required for the binding of snoRNAs snR64 and snR67 to the pre-ribosomal subunit and snR67 mediated methylation of the 25S rRNA sequence (Bohnsack et al., 2009; Leeds et al., 2006).

In humans, the mechanistic details of snoRNA distribution on pre-ribosomal subunits is not yet well-studied. The DEAD-box helicase DDX51 associates with early pre-ribosomal particles and is implicated in the release of the box C/D snoRNA U8. The timely binding of U8 to the nascent the 47S pre-rRNA is important for the proper folding of the pre-rRNA transcript and the subsequent displacement of U8 is required for the efficient processing of the 3' end of the 28S rRNA sequence (Peculis and Steitz, 1993; Srivastava et al., 2010). Although, the functions and regulation of certain snoRNAs, for example U3 snoRNA, seem to be conserved in higher eukaryotes (Choudhury et al., 2019; Sardana et al., 2015), recent studies have highlighted the presence of additional snoRNAs lacking yeast counterparts. For example, The DEAD-box helicase DDX21 plays a prominent role in facilitating the pre-ribosomal association of the late-acting box C/D snoRNAs SNORD56 and SNORD68, which are required for guiding methylation at specific sites within the 18S rRNA sequence. Although, the molecular details leading to the binding of these snoRNAs is not known, it has been suggested that DDX21 might be involved in the structural rearrangement of pre-rRNA transcript or in the removal of certain ribosome associated factors from the binding site of these snoRNAs. Notably, DDX21 as well as the rRNA modifications installed by SNORD56 and SNORD68 are not present in yeast, suggesting that specific RNA helicases might have co-evolved with their RNA targets (Sloan et al., 2015). Genome-wide screens have revealed the requirement of additional RNA helicases such as DDX10, DDX56 for efficient assembly of ribosomal subunits in human cells, however, the precise roles of these proteins in the context of ribosome biogenesis is yet to be established (Tafforeau et al., 2013; Turner et al., 2012; Wild et al., 2010).

1.3.2 RNA helicases mediate structural remodelling of pre-ribosomes

Apart from modulating the association of snoRNAs with pre-ribosomal particles, RNA helicases likely participate in structural rearrangement of pre-rRNA, promoting efficient cleavage or remodelling events during subunit maturation. The remodelling events induced by helicases could facilitate the stable incorporation of RPs, the release or binding of *trans*-acting RBFs, or promote the folding of pre-rRNA into mature secondary structures. For instance, in addition to its role in snoRNA release, Prp43 is implicated in the maturation of 18S rRNA in yeast. During the final maturation steps in the cytoplasm, Prp43 likely induces

structural remodelling of pre-ribosomal particles resulting in cleavage of the 3' end of 18S pre-rRNA by the endonuclease Nob1 (Bohnsack et al., 2009; Pertschy et al., 2009). Although, the process of 18S cleavage by Nob1 in the cytoplasm is conserved in higher eukaryotes (Preti et al., 2013; Sloan et al., 2013a), DHX15 (human homologue of Prp43) was not found to be required for the efficient processing of 18S rRNA (Sloan et al., 2019) but is instead required for efficient cleavage at the A' site within the 5' ETS (Memet et al., 2017). In yeast, deletion of the DEAD-box protein Dbp3 leads to pre-rRNA processing defects mirroring the defects observed upon knockdown of RNase MRP, which mediates cleavage at site A₃ in the ITS1 region (Weaver et al., 1997). It was therefore suggested that Dbp3 is involved in promoting structural rearrangement in the vicinity of site A₃, facilitating the recruitment of the RNase MRP (Kressler et al., 1999). Furthermore, Dbp6, together with Dbp7 and Dbp9, can promote the incorporation of the yeast large subunit ribosomal protein Rpl3 by extensive remodelling of the pre-60S ribosomal sub-complex (Daugeron and Linder, 2001; Rosado et al., 2007). In recent findings, the DEAD box helicase Spb4 has been implicated in the recruitment of pre-60S export adaptor protein, Arx1 (Brüning et al., 2018) and biogenesis factor Nog1 (Talkish et al., 2012), likely through structural rearrangement of the 25S pre-rRNA. As Nog1 functions as a placeholder for Nmd3, which is another pre-60S export adaptor protein (Matsuo et al., 2014; Sloan et al., 2016), Spb4 has been suggested to play a role in the efficient export of pre-60S subunits (Brüning et al., 2018). Mak5 binding to pre-60S particles has also been shown to be required for the incorporation of Rpl10 in the cytoplasm (Brüning et al., 2018), highlighting the importance of structural remodelling events carried out by RNA helicases in the maturation of ribosomal subunits.

Chapter Two: Scope of the thesis

Eukaryotic ribosome biogenesis is one of the most energy-consuming and complex processes in the cell, involving more than 200 *trans*-acting factors including AAA-ATPases, GTPases, nucleases, snoRNPs and RNA helicases. These ribosome biogenesis factors play key roles in promoting pre-rRNA cleavage, folding and modification, as well as the structural remodelling of RNA-RNA and RNA-protein interactions within pre-ribosomal complexes. The pathway of ribosome biogenesis is largely conserved amongst eukaryotes and hence, most ribosome biogenesis factors characterised in yeast are expected to fulfil similar roles in higher eukaryotes. Although, this notion has been experimentally verified for a subset of assembly factors, RNAi-based genome-wide screens for human ribosome biogenesis factors and detailed characterization of some of the identified proteins imply that some proteins may have additional or different roles in comparison to their yeast counterparts. Despite the growing list of RNA helicases implicated in the process of human ribosome biogenesis, detailed functional characterization of many of these proteins is still lacking.

Hence, this study aimed to gain insight into the roles of the DEAH-box helicase DHX37 and the DEAD-box helicase DDX55 in the context of ribosome biogenesis.

The primary objectives of the study were to:

- Demonstrate the catalytic activity of DHX37 and DDX55 *in vitro* and characterize mutants.
- Determine the sub-cellular localisation of the candidate helicases.
- Analyse the requirement for DHX37 and DDX55 for pre-rRNA processing.
- Identify the binding sites of DHX37 and DDX55 on pre-ribosomal complexes or target RNAs *in vivo*.
- Understand the functional roles of DHX37 and DDX55 in maturation of the SSU and LSU, respectively.
- Explore potential modes of regulation of DHX37 and DDX55, including identification of cofactors proteins that influence their catalytic activity and/or determining the contribution of protein sequences beyond the conserved helicase core in regulating recruitment to target RNAs.

Chapter Three: Manuscript I

Priyanka Choudhury, Philipp Hackert, Indira Memet, Katherine E. Sloan & Markus T. Bohnsack (2019). The human RNA helicase DHX37 is required for release of the U3 snoRNP from pre-ribosomal particles, *RNA Biology*, 16, 54-68

Author contributions:

- Figure 1:** Immunofluorescence analysis of DHX37 localisation (PC); RNAi-mediated depletion analysis of DHX37 followed by western blotting (PC); sucrose density gradient centrifugation upon DHX37 depletion (PC); pulse-chase labelling assays for pre-rRNA detection (IM).
- Figure 2:** Northern blot analysis for pre-rRNA detection (PC); RNAi-mediated depletion of DHX37 and XRN2 (PC).
- Figure 3:** Recombinant expression and purification of DHX37 and DHX37_{T282A} (PC); *in vitro* ATP hydrolysis assay (PC); generation of cell line expressing DHX37-Flag and DHX37_{T282A}-Flag (PC); RNAi-based rescue system and northern blot analysis of pre-rRNA levels (PC).
- Figure 4:** PAR-CRAC experiments for DHX37 (PH); native RNA-Immunoprecipitation and northern blotting for snoRNAs-U3 and U8 (PC).
- Figure 5:** Western blot analysis upon expressing DHX37-Flag and DHX37_{T282A}-Flag expression (PC); sucrose density gradient centrifugation and northern blotting for U3 snoRNA (PC).
- Figure 6:** Immunoprecipitation assays with Flag-tag and DHX37-Flag followed by western blotting for UTP14A, WBSCR22, tubulin (PC); recombinant expression and purification of UTP14A (PC); *In vitro* binding assay with DHX37 and UTP14A (PC); *in vitro* ATP hydrolysis assay (PC); RNAi-mediated depletion of UTP14A followed by western blotting (PC); northern blot analysis for pre-rRNA detection upon DHX37 and UTP14A depletion (PC); sucrose density gradient centrifugation and northern blotting for U3 snoRNA (PC).

Figure S1: RNAi-mediated depletion of DIMT1L, TSR1, DHX37 followed by western blotting and northern blot analysis (PC).

Figure S2: Sucrose density gradient centrifugation and western blotting for DHX37 (PC).

Figure S3: Sequence alignment of DHX37 and Dhr1 (PC).

Figure S4: Immunoprecipitation assays with Flag-tag and DHX37-Flag followed by western blotting for DIMT1L, TSR1 and tubulin (PC).

Figure S5: *in vitro* ATP hydrolysis assay (PC).

Non-experiment contribution: Markus Bohnsack and Katherine Sloan conceived this project. Katherine Sloan, Markus Bohnsack and Priyanka Choudhury wrote the manuscript and organised the figures. Markus Bohnsack and Katherine Sloan supervised the study. All listed authors contributed to data analysis and preparation of the manuscript.

Digital Object Identifier: 10.1080/15476286.2018.1556149

The human RNA helicase DHX37 is required for release of the U3 snoRNP from pre-ribosomal particles

Priyanka Choudhury¹, Philipp Hackert¹, Indira Memet¹, Katherine E. Sloan^{1*} and Markus T. Bohnsack^{1,2*}

¹ Department of Molecular Biology, University Medical Centre Göttingen, Humboldtallee 23, 37073 Göttingen, Germany

² Göttingen Center for Molecular Biosciences, Georg-August University, Göttingen, Justus-von-Liebig-Weg 11, 37077 Germany

* Please address correspondence to:

Markus T. Bohnsack

Address: Department of Molecular Biology, University Medical Centre Göttingen, Humboldtallee 23, 37073 Göttingen, Germany

Phone: +49-551-395968; Fax: +49-551-395960

E-mail: markus.bohnsack@med.uni-goettingen.de

Katherine E. Sloan

Address: Department of Molecular Biology, University Medical Centre Göttingen, Humboldtallee 23, 37073 Göttingen, Germany

Phone: +49-551-395978; Fax: +49-551-395960

E-mail: katherine.sloan@med.uni-goettingen.de

Key words: RNA helicase, ribosome, ribosome biogenesis, snoRNA, protein cofactor, RNA processing

Abstract

Ribosome synthesis is an essential cellular process, and perturbation of human ribosome production is linked to cancer and genetic diseases termed ribosomopathies. During their assembly, pre-ribosomal particles undergo numerous structural rearrangements, which establish the architecture present in mature complexes and serve as key checkpoints, ensuring the fidelity of ribosome biogenesis. RNA helicases are essential mediators of such remodelling events and here, we demonstrate that the DEAH-box RNA helicase DHX37 is required for maturation of the small ribosomal subunit in human cells. Our data reveal that the presence of DHX37 in early pre-ribosomal particles is monitored by a quality control pathway and that failure to recruit DHX37 leads to pre-rRNA degradation. Using an *in vivo* crosslinking approach, we show that DHX37 binds directly to the U3 small nucleolar RNA (snoRNA) and demonstrate that the catalytic activity of the helicase is required for dissociation of the U3 snoRNA from pre-ribosomal complexes. This is an important event during ribosome assembly as it enables formation of the central pseudoknot structure of the small ribosomal subunit. We identify UTP14A as a direct interaction partner of DHX37 and our data suggest that UTP14A can act as a cofactor that stimulates the activity of the helicase in the context of U3 snoRNA release.

Introduction

The production of eukaryotic ribosomes, which are responsible for the translation of mRNAs into proteins, is a highly complex, dynamic and energy-consuming cellular process involving the maturation of four ribosomal RNAs (rRNAs) and their assembly with approximately 80 ribosomal proteins (RPs).¹ Numerous ribosome biogenesis factors (RBFs), which associate transiently with pre-ribosomal particles, are responsible for mediating key maturation events and in the yeast *Saccharomyces cerevisiae*, approximately 200 such factors have been identified (see for example reference 2). Due to the larger size of human (pre-) ribosomal complexes and the evolution of regulatory networks that coordinate ribosome production with other cellular processes, the inventory of human ribosome biogenesis factors is likely to be much larger than that of yeast. Proteomic analyses of human nucleoli,^{3,4} together with several recent genome-wide RNAi-based screens⁵⁻⁸ have uncovered a plethora of factors without yeast homologues that are required for human ribosome assembly. Furthermore, detailed analyses of the human pre-rRNA processing pathway (see for example references 9-11) and functional characterisation of various individual human RBFs have revealed that many human RBFs have different or additional functions compared to their yeast counterparts. A portfolio of genetic diseases, termed ribosomopathies, that are caused by mutations in genes encoding RPs and/or RBFs (reviewed in reference 12), as well as an increasing body of evidence linking ribosome assembly to cancer (reviewed in reference 13), emphasise the importance of a detailed knowledge of the human ribosome assembly pathway.

In human cells, ribosome assembly is initiated in the nucleolus by synthesis of a 47S pre-rRNA transcript containing the sequences of three of the four rRNAs (18S, 5.8S and 28S), separated by internal transcribed spacers (ITS) and flanked by external transcribed spacers (ETS). Maturation of the pre-rRNAs involves processing of this transcript by endo- and exonucleases and extensive modification of the mature rRNA sequences by small nucleolar RNPs (snoRNPs) and stand-alone modification enzymes.¹⁴⁻¹⁶ A subset of RPs and RBFs are recruited to the nascent pre-rRNA transcript giving rise to an early pre-ribosomal complex termed the small subunit (SSU) processome. The SSU processome is composed of numerous sub-complexes, including the UTP-A, UTP-B and UTP-C complexes, as well as various enzymes that mediate important steps in SSU biogenesis, such as the endonuclease UTP24, the PIN domain protein UTP23, the rRNA methyltransferase EMG1 and the GTPase BMS1.^{6,17-19} A core component of the SSU processome is the U3 snoRNP, which in contrast to most other snoRNPs, does not guide rRNA modification, but instead bridges key interactions within early pre-ribosomes.²⁰ This is achieved by base-pairing

interactions between the U3 snoRNA 3' hinge region and the 5' ETS, and the U3 5' region (GAC box, box A and box A') and the 18S rRNA sequence that forms the central pseudoknot in mature SSU complexes.^{21–23} Recent structural analyses of *S. cerevisiae* SSU processomes^{24,25} have revealed that the base-pairing interactions formed between the U3 snoRNA and the pre-rRNA tether the SSU processome in a conformation that allows essential pre-rRNA processing events to be co-ordinated. Release of the U3 snoRNP, which in yeast requires the RNA helicase Dhr1²⁶, is an essential step in SSU biogenesis as it licences downstream maturation events and allows folding of the 18S rRNA sequence into its mature conformation. A pre-rRNA cleavage step in ITS1 separates the SSU (40S) and LSU (60S) precursor particles, which undergo separate maturation pathways in the nucleolus and nucleoplasm involving further pre-rRNA processing steps, the recruitment and release of various RBFs and significant structural rearrangements. Such remodelling events serve as important checkpoints during the assembly pathway and are often a pre-requisite for establishing export competence. The pre-40S and pre-60S subunits are independently exported to the cytoplasm²⁷ where final maturation and quality control steps take place before the mature subunits re-join during translation.

RNA helicases, which are typified by a helicase core domain composed of tandem RecA-like domains containing conserved sequence motifs involved in NTP/substrate binding, NTP hydrolysis and its coordination with unwinding activity, are proposed to be important regulators of pre-ribosome remodelling events.^{28,29} Structural rearrangements, such as the release of snoRNPs from pre-ribosome, recruitment or dissociation of RPs and/or RBFs, and altering pre-rRNA base-pairing/folding, are proposed functions of RNA helicases during the maturation of pre-ribosomal subunits.^{26,30–35} In human cells, the DEAD-box helicases DDX51 and DDX27 are implicated in release of the metazoan-specific snoRNA U8 from its base-pairing sites with the 28S rRNA and ITS2 sequences, and maturation of the 3' end of the 28S rRNA respectively.^{36,37} Interestingly, the catalytic activity of the DEAH-box RNA helicase DHX15, which is the human homologue of yeast Prp43, is required for a metazoan-specific cleavage event (A') in the 5' ETS.³⁸ However, unlike Prp43, DHX15 does not appear to be required for the final steps of 18S rRNA maturation, implying that the functions of this helicase are different in yeast and humans. Furthermore, human ribosome assembly involves RNA helicases not present in yeast; for example, it was recently shown that the action of the metazoan-specific DEAD-box protein DDX21 is required for rDNA transcription and that this enzyme also facilitates the access of late-acting snoRNPs to pre-40S complexes.^{39,40} Recent cryo-EM structures of late pre-40S complexes^{41,42} provide the first snap-shots of structural rearrangements that take place during the final steps of SSU

maturation but the roles of many human RNA helicases during ribosome assembly remain uncharacterised.

Here, we show that the putative RNA helicase DHX37 is an RNA-dependent ATPase that is required for biogenesis of the SSU. Our data show that lack of DHX37 triggers a surveillance pathway that leads to degradation of pre-ribosomal particles. Depletion of DHX37 inhibits the conversion of the 21S pre-rRNA to 18SE and expression of catalytically inactive DHX37 also impairs a pre-rRNA cleavage step in the 5' ETS. Using *in vivo* protein-RNA crosslinking, we demonstrate that DHX37 binds close to the 3' hinge region of the U3 snoRNA, which base-pairs with the 5' ETS in proximity of the A' cleavage site, and we show that expression of catalytically inactive DHX37 causes accumulation of the U3 snoRNA on pre-ribosomes. Together, our data imply that dissociation of the U3 snoRNA, which requires DHX37, is an important early pre-ribosome remodelling event that licences downstream steps in human ribosome assembly.

Results

The human RNA helicase DHX37 is required for biogenesis of the small ribosomal subunit. Although many components of the ribosome assembly machinery are conserved throughout eukaryotes, the precise functions of many RBFs, especially RNA helicases, differ in yeast and humans. Based on its homology to yeast Dhr1, the putative RNA helicase DHX37 is anticipated to play a role in human ribosome biogenesis, however, a detailed functional characterisation of this protein is lacking. To first ascertain the localisation of DHX37 in human cells, we performed immunofluorescence in HeLa cells using antibodies against DHX37 and, as a nucleolar marker, the rRNA methyltransferase NSUN5. This revealed that DHX37 predominantly localises to nucleoli (Figure 1A), which is consistent with a role during the early stages of ribosome assembly. Next, to enable the effects of depletion of DHX37 on ribosome assembly to be analysed, RNAi against DHX37 was established using two alternative siRNAs. HeLa cells were left untreated (wild-type), or were transfected with control siRNAs or siRNAs targeting DHX37, then the levels of the DHX37 protein were examined using western blotting. This demonstrated that the amount of DHX37 in cells treated with either of the two siRNAs against DHX37 was markedly reduced (Figure 1B), thereby confirming the effectiveness of both siRNAs. To determine the effect of depletion of DHX37 on ribosomal subunit production, whole cell extracts prepared from cells treated with either non-target siRNAs (siNT) or those targeting DHX37 (siDHX37_1) were separated by sucrose density gradient centrifugation and the relative amounts of small subunits (40S), large subunits (60S) and monosomes (80S) were determined by monitoring the absorbance of each fraction at 260 nm. The obtained profile shows that depletion of DHX37 does not affect production of 60S subunits but leads to a significant decrease in the abundance of 40S particles as well as a decrease in the amount of 80S monosomes (Figure 1C), indicating a role for DHX37 in production of the small ribosomal subunit. Consistent with this, pulse-chase labelling of newly synthesised RNAs in siRNA-treated cells as described above confirmed the requirement for DHX37 for production of the 18S rRNA, but not the 28S rRNA (Figure 1D and E). To determine at what stage of SSU production DHX37 is required, northern blotting was used to examine the levels of different pre-rRNA species in cells depleted of DHX37. Compared to RNA from wild-type cells or cells treated with non-target siRNAs, depletion of DHX37 caused accumulation of the 21S pre-rRNA and a concomitant decrease in the levels of the 18SE pre-rRNA (Figures 1D and F), which is largely produced by exonucleolytic processing of the 21S pre-rRNA following site 2 cleavage.^{10,11} Interestingly, several aberrant pre-rRNAs were also detected when DHX37 was depleted; in particular, prominent species that migrated below the 41S and 18SE pre-rRNAs were observed.

The detection of these aberrant pre-rRNA species upon depletion of DHX37 raised the question of how they are produced. The pre-rRNA regions present in each of the prominent intermediates were therefore determined by northern blotting using a series of probes hybridising within the 5' ETS and ITS1 (Figure 2A). The 16S* species was detected with probes hybridising to ITS1 upstream, but not downstream, of site 2 (Figure 2B), implying that the 3' end of this pre-rRNA is generated by site 2 cleavage. The finding that a probe hybridising within the 5' ETS, immediately upstream of site 1 was not able to detect 16S*, together with the estimated size of this intermediate, indicates that its 5' end lies within the mature 18S rRNA sequence. While the 38S* intermediate could be visualised using probes spanning ITS1, it was not detected with probes hybridising in the 5' ETS (Figure 2A and B), implying that, similarly, the 5' end of this species lies within the mature 18S rRNA sequence. A series of northern blot probes spanning the 18S rRNA sequence (Figure 2A) were therefore utilised to map the 5' end of the 38S* intermediate. While 38S* was readily observed using probes 18S-1285, 18S-1377 and 18S-1670, it was only very weakly detected by probe 18S-1230 and was not visualised using probes 18S-1 or 18S-1004 (Figure 2C). This suggests that the 5' end of the 38S*, and by analogy, the 16S* species, is somewhat heterogeneous but primarily lies between nucleotides 1253 and 1285 (helix 32) of the 18S rRNA (Supplementary Figure S1A). The finding that the 38S* and 16S* intermediates are not part of the normal pre-rRNA processing pathway, but instead represent turnover intermediates derived from the 41S and 30S/21S pre-rRNAs respectively, suggests the existence of a surveillance pathway that targets pre-ribosomal complexes lacking DHX37 for degradation. Relatively little is known about how incorrectly assembled pre-ribosomes are turned over in human cells, however, an enzyme that has been implicated in the degradation of aberrant pre-rRNAs is the 5'-3' exonuclease XRN2.⁴³ To determine if the 5' ends of the 38S* and 16S* intermediates are generated by the stalling of XRN2 during exonucleolytic processing, pre-rRNA intermediates were examined in HeLa cells depleted of DHX37, XRN2 or both DHX37 and XRN2. As previously reported, depletion of XRN2 impaired A' cleavage, leading to accumulation of the 30SL5' intermediate^{10,43} and the previously observed defect in conversion of the 21S pre-rRNA to 18SE was detectable when the levels of DHX37 were reduced both in the absence and presence of XRN2 (Figure 2C). Upon co-depletion of DHX37 and XRN2, the 38S* and 16S* fragments were clearly observed, implying that this surveillance pathway does not rely on XRN2 and that other endo-/exonuclease(s) mediate the degradation of pre-rRNAs within aberrant pre-ribosomes lacking DHX37.

Interestingly, the 38S* and 16S* pre-rRNA intermediates are also detected upon depletion of the rRNA methyltransferase DIMT1L, which installs two evolutionarily conserved N^6 - N^6 -

dimethylations at positions A1850 and A1851 of the 18S rRNA sequence that forms the decoding centre in the mature SSU, and TSR1, which acts during the late stages of SSU biogenesis where it is proposed to prevent premature association of the small and large ribosomal subunits (Supplementary Figure S1B,C).^{6,44–46} This suggests that the presence of DHX37, DIMT1L and TSR1 in early pre-ribosomal complexes may all be monitored by a common surveillance pathway.

DHX37 is an RNA-dependent ATPase and its catalytic activity is required for the conversion of the 21S pre-rRNA to the 18SE pre-rRNA.

Several enzymes involved in ribosome biogenesis have been shown to have both catalytic and non-catalytic functions in the pathway (see for example references 47–49). Given the extensive pre-rRNA processing defects detected upon depletion of DHX37 and the fact that DHX37 is a putative DEAH-box RNA helicase, we next aimed to demonstrate that DHX37 is a catalytically active enzyme and determine if this activity is required for its function(s) in biogenesis of the small ribosomal subunit. A characteristic feature of RNA helicases is their capability to hydrolyse nucleotide triphosphates (NTPs) in an RNA-dependent manner^{29,50} and we therefore expressed recombinant His₆-tagged DHX37 in *Escherichia coli* and purified the protein for use in *in vitro* ATPase assays (Figure 3A). To confirm the specificity of any ATPase activity detected, DHX37 carrying a threonine to alanine substitution (T282A) in the evolutionarily conserved “GKT” sequence of motif I that is implicated in NTP binding,^{26,50} was also expressed and purified (Figure 3A). NADH-coupled ATPase assays were performed using DHX37 or DHX37_{T282A} in the absence and presence of RNA. Compared to a control reaction containing neither protein nor RNA, DHX37 showed mild ATPase activity in the absence of RNA and the addition of RNA stimulated ATP hydrolysis by DHX37 almost four-fold (Figure 3B), demonstrating that DHX37 is an RNA-dependent ATPase. While DHX37_{T282A} also weakly hydrolysed ATP in the absence of RNA, the effect of RNA addition on the activity of DHX37_{T282A} was minimal, indicating that this amino acid substitution within the GKT motif impairs the catalytic activity of the helicase. To enable the requirement for the catalytic activity of DHX37 for small subunit biogenesis to be examined in human cells, HEK293 cell lines were generated in which endogenous DHX37 could be depleted using an established siRNA (Figure 1B) and a C-terminally His₆-PreScission protease-2x Flag (Flag) tagged version of DHX37 or DHX37_{T282A} could be expressed from a genomic locus via a tetracycline regulatable promoter. HEK293 cells were transfected with non-target siRNAs (siNT) or siRNAs targeting DHX37 (siDHX37_1) and expression of the Flag tag, DHX37-Flag or DHX37_{T282A}-Flag was induced (Figure 3C). Western blot analysis confirmed specific expression of the Flag-tagged proteins, albeit at slightly higher than endogenous levels. Examination of pre-rRNA levels in these cells by northern blotting

using a probe hybridising to the 5' end of ITS1 demonstrated that depletion of DHX37 from HEK293 cells leads to pre-rRNA processing defects similar to those observed in HeLa cells (Figure 1F) and that expression of wild-type DHX37 from a transgene can rescue these defects (Figure 3D). Interestingly, the aberrant 38S* and 16S* pre-rRNA fragments did not accumulate upon expression of DHX37_{T282A} (Figure 3D), implying the presence of the protein rather than its ATPase activity is sensed by the quality control pathway that monitors DHX37 recruitment to pre-ribosomal complexes. In contrast, the accumulation of the 21S pre-rRNA and reduced level of the 18SE pre-rRNA observed upon depletion of DHX37 were also detected in cells expressing DHX37_{T282A} (Figure 3D; left panel), demonstrating that lack of the catalytic activity of DHX37 is responsible for these defects. Expression of DHX37_{T282A} also lead to accumulation of a pre-rRNA longer than 30S that was not detected in cells lacking DHX37. Northern blotting with a probe hybridising close to the 5' end of the 47S pre-rRNA transcript confirmed this species to be the 5' extended version of 30S, 30SL5' (Figure 3D; right panel), which accumulates when A' processing is impaired. These data suggest that while cleavage at the A' site in the 5' ETS can take place when DHX37 is lacking, the presence of inactive DHX37 in pre-ribosomal particles reduces the efficiency of this cleavage event or promotes bypassing of this step.

DHX37 associates directly with the U3 snoRNA *in vivo*.

Elucidating the precise functions of RNA helicases in ribosome biogenesis necessitates identification of the precise targets of their remodelling activity. To gain insight into the *in vivo* RNA substrates of DHX37, the crosslinking and analysis of cDNA (CRAC) approach was applied.^{51,52} HEK293 cells expressing either the Flag tag or Flag-tagged DHX37 were grown in the presence of 4-thiouridine before *in vivo* crosslinking using light at 365 nm. Cell extracts were used for tandem affinity purification under native and denaturing conditions, and a partial RNase digestion was performed to ensure that only RNA sequences directly contacted by DHX37 were recovered. RNA fragments co-purified with DHX37-Flag or the Flag tag were ligated to sequencing adaptors and labelled with [³²P]. RNA-protein complexes were separated by denaturing polyacrylamide gel electrophoresis (PAGE), transferred to a nitrocellulose membrane and then visualised by autoradiography (Figure 4A). A signal migrating at the molecular weight of DHX37 was detected in the sample derived from cells expressing DHX37-Flag but not the Flag tag, confirming the direct interaction of DHX37 with RNA *in vivo*. This area of the membrane, and a corresponding region for the control sample (Figure 4A), were excised and RNA fragments were isolated. After reverse transcription, the cDNA library was amplified by PCR and subjected to Illumina sequencing. The obtained sequence reads were mapped to the human genome using a filter to allow only mapping of reads containing a specific T-C mutation introduced during

the reverse transcription step at positions where an amino acid remained crosslinked to a 4-thiouridine. Relatively few sequence reads mapped to the rDNA and no specific crosslinking site(s) could be identified. This suggests that, similar to yeast Dhr1²⁶, DHX37 interacts only transiently or unstably with pre-rRNA/pre-ribosomal complexes. Consistent with this, sucrose density gradient analysis of the distribution of DHX37 between pre-ribosomal and non-ribosomal complexes showed that under normal conditions, only a small proportion of the helicase co-migrates with pre-ribosomal particles (Supplementary Figure 2). A higher proportion of sequence reads mapping to snoRNA genes was, however, observed in the DHX37-Flag CRAC dataset compared to the control, suggesting the association of DHX37 with snoRNA(s) (Figure 4B). Analysis of the relative distribution of sequence reads mapping to snoRNA genes in the two datasets highlighted an enrichment of reads corresponding to the U3 snoRNA (Figure 4C; Supplementary Table 1). To confirm the association of DHX37 with the U3 snoRNA, extracts from cells expressing Flag-DHX37 or the Flag tag were used in immunoprecipitation experiments and the amounts of the U3, and as a control the U8, snoRNAs present in the inputs and eluates were examined by northern blotting. While the U8 snoRNA was not retrieved in either eluate, the U3 snoRNA was specifically co-purified with Flag-DHX37 but not the Flag tag, further supporting the interaction of DHX37 with the U3 snoRNA *in vivo* (Figure 4D). We next examined the distribution of CRAC sequencing reads mapping to each nucleotide of the U3 snoRNA sequence. Almost no sequence reads were observed to be derived from the very 5' end of the snoRNA containing the U3-specific GAC and A/A' boxes, which basepairs with an 18S rRNA sequence that forms part of the central pseudoknot in the mature SSU particle. Instead, the majority of sequence reads in the DHX37-Flag dataset were mapped towards the 3' end of the snoRNA containing the box C/D elements and close to the 3' hinge region of the U3 snoRNA that basepairs with pre-rRNA sequences present in the 5' ETS proximal to the A' cleavage site (Figure 4E; upper panel). The binding of DHX37 to these sequences is supported by the detection of T-C mutations in the sequencing reads as these are specifically introduced at nucleotides crosslinked to amino acids (Figure 4E; lower panel).

The U3 snoRNA accumulates on pre-ribosomes when the catalytic activity of DHX37 is impaired.

The direct interaction of DHX37 with the U3 snoRNA suggests that, like its yeast counterpart Dhr1, DHX37 may regulate the interactions of this snoRNA with pre-ribosomal complexes. The amounts of U3 present on pre-ribosomal complexes in cells expressing either wild-type DHX37 or catalytically inactive DHX37_{T282A} was examined. Endogenous DHX37 was depleted and expression of DHX37-Flag or DHX37_{T282}-Flag was induced to equal levels (Figure 5A). Extracts from these cells were then subjected to sucrose density gradient

centrifugation followed by northern blotting for the U3 snoRNA (Figure 5B). In cells expressing wild-type DHX37, the U3 snoRNA was present in fractions containing non-ribosomal complexes as well as those containing larger pre-ribosomal complexes. Expression of DHX37_{T282A} lead to a notable increase in the proportion of the U3 snoRNA associated with pre-ribosomal complexes (Figure 5B), implying that the catalytic activity of DHX37 is required for release of this snoRNA from pre-ribosomal particles.

DHX37 interacts directly with the SSU biogenesis factor UTP14A.

The finding that the catalytic activity of DHX37 is required for release of the U3 snoRNA from pre-ribosomal particles raises the question of how this activity is regulated in the cellular environment. The promiscuity of many RNA helicases is limited by their inherently low catalytic activity, which is stimulated by dedicated cofactors upon binding to their cognate RNA substrates. Furthermore, protein cofactors can bestow specificity to RNA helicases by directing their recruitment to particular target RNAs *in vivo* (reviewed in 53). In yeast, Dhr1 physically interacts with the 18S rRNA m⁷G methyltransferase Bud23 and the SSU biogenesis factor Utp14 to facilitate its access to pre-ribosomal particles, and it has been suggested that the unwinding activity of Dhr1 is stimulated by a direct interaction with Utp14.^{26,54,55} To determine if DHX37 interacts with the human orthologues of Bud23 (WBSCR22) and/or Utp14 (UTP14A) immunoprecipitation assays were performed. Extracts from cells expressing DHX37-Flag or the Flag tag were treated with RNase A or left untreated to determine if any interactions detected are bridged by RNA, and inputs (1%) and eluates were analysed by western blotting. This revealed that neither tubulin nor WBSCR22 were recovered with DHX37-Flag in the presence or absence of RNase treatment (Figure 6A). In yeast, Bud23 interacts with amino acids in the N-terminal region of Dhr1^{55,56} and the lack of a direct interaction between DHX37 and WBSCR22 likely reflects the poor sequence conservation of this region of the helicase between yeast and humans (Supplementary Figure 3). Furthermore, in contrast to yeast Bud23, which is recruited to early pre-ribosomal complexes, WBSCR22 is reported to be recruited to late pre-40S complexes,⁵⁷ consistent with the lack of an interaction with DHX37, which is likely to only be present in early complexes. UTP14A was, however, efficiently co-precipitated with DHX37-Flag, but not the Flag tag alone, implying the existence of pre-ribosomal complexes containing both these proteins (Figure 6A). The observed interaction between DHX37-Flag and UTP14A was not affected by RNase treatment, suggesting that this interaction is mediated by protein-protein contacts (Figure 6A). As depletion of DIMT1L or TSR1 appears to trigger the same quality control pathway as depletion of DHX37 (indicated by the accumulation of the aberrant 38S* and 16S* pre-rRNA species; Supplementary Figure 1), we speculated that these proteins might interact in human cells. Analysis of the IP inputs

and eluates revealed that while both DIMT1L and TSR1 could be co-precipitated with DHX37-Flag from cell extracts, these interactions were dependent on RNA (Supplementary Figure 4A and B), implying that DHX37, DIMT1L and TSR1 are present in common pre-ribosomal complexes but that they do not form direct interactions.

To test the hypothesis that UTP14A represents a direct interaction partner of DHX37, an *in vitro* binding assay was performed using recombinant ZZ-UTP14A-His₁₀ and DHX37-His₆. DHX37-His₆ was incubated with either IgG sepharose or IgG sepharose on which ZZ-UTP14A-His₁₀ had been immobilised. After thorough washing steps, bound proteins were eluted and analysed by western blotting alongside input samples. DHX37-His₆ was co-precipitated with the ZZ-UTP14A-His₁₀-bound beads, but not with the empty IgG sepharose (Figure 6B), confirming that these proteins can interact directly. We next explored the influence of UTP14A on the catalytic activity of DHX37 using *in vitro* ATPase assays performed in the presence and absence of UTP14A. As previously shown (Figure 3B), DHX37 displayed RNA-dependent ATPase activity (Figure 6C) whereas the amount of ATP hydrolysed by UTP14A in the presence or absence of RNA was minimal. However, addition of UTP14A stimulated the RNA-dependent ATPase activity of DHX37 more than two-fold. To verify the specificity of UTP14A in stimulating the ATPase activity of DHX37, we also examined the influence of UTP14A on the ATPase activity of another DEAH-box RNA helicase, DHX15. While recombinant MBP-DHX15-His₁₀ displayed RNA-dependent ATPase activity, the rate of ATP hydrolysis was not stimulated by the addition of UTP14A (Supplementary Figure 5). To determine if UTP14A acts as a cofactor of DHX37 during SSU biogenesis, we first established RNAi against UTP14A (Figure 6D) and compared the pre-rRNA processing defects observed upon depletion of the helicase and its cofactor. Depletion of UTP14A caused accumulation of the 30S pre-rRNA and a corresponding decrease in the levels of the 21S and 18SE pre-rRNAs (Figure 6E). The aberrant 38S* and 16S* pre-rRNA fragments observed upon depletion of DHX37 did not accumulate when the level of UTP14A was reduced, suggesting that the presence of the helicase in pre-ribosomal particles, but not its cofactor, is monitored. The finding that depletion of UTP14A impedes a pre-rRNA processing step (conversion of 30S to 21S) upstream of the processing event for which the catalytic activity of DHX37 is required (conversion of 21S to 18SE) could suggest that UTP14A has an additional role in SSU biogenesis that is not linked to its stimulation of DHX37. To investigate if, like DHX37, UTP14A is required for the release of the U3 snoRNA from pre-ribosomes, extracts from cells treated with control siRNAs (siNT) or siRNAs targeting UTP14A were separated by sucrose density gradient centrifugation and the amounts of U3 co-migrating with non-ribosomal and (pre-)ribosomal complexes were determined by northern blotting. Similar to expression of catalytically inactive DHX37 (Figure 5B), depletion of UTP14A lead to increased amounts of the U3 snoRNA present in

fractions containing pre-ribosomal complexes (Figure 6F), suggesting that stimulation of DHX37 by UTP14A may be linked to the requirement for the helicase for the release of U3 from pre-ribosomes.

Discussion

Here, we have analysed the putative RNA helicase DHX37, which is the homologue of the yeast DEAH-box protein Dhr1. In yeast, Dhr1 is required during the early steps of SSU maturation where it is proposed to trigger dissociation of the U3 snoRNA from its pre-rRNA base-pairing site(s) allowing formation of the central pseudoknot, a key structural feature of the 18S rRNA within the small ribosomal subunit.²⁶ Our data demonstrate that in human cells, DHX37 is also required for pre-40S maturation and that lack of DHX37 impairs various steps in the maturation of the 18S rRNA leading to reduced levels of both the mature 18S rRNA and 40S subunits. We further show that DHX37 crosslinks to the U3 snoRNA and that expression of catalytically inactive DHX37 leads to increased levels of U3 on pre-ribosomal complexes, suggesting that the function of this helicase in facilitating U3 snoRNA release may be conserved from yeast to humans. In yeast, changes in the solvent accessibility of a residue within the 18S sequence that basepairs with the 5' region of the U3 snoRNA have been observed upon Dhr1 depletion, and Dhr1 has been reported to crosslink to the 5' region of the U3 sequence containing the GAC and A/A' boxes.²⁶ However, *in vitro* Dhr1 has also been shown to unwind a duplex formed between the U3 3' hinge region and the corresponding 5' ETS sequence.²⁶ It therefore remains unclear whether the remodelling activity of Dhr1 is directed at both of these U3-pre-rRNA duplexes or if disruption of one interaction is sufficient to trigger spontaneous dissociation of the U3 snoRNA from the other site leading to release of the snoRNA from early pre-ribosomal complexes. This open question is likely best addressed by structural analyses of Dhr1-containing pre-ribosomal complexes; however, Dhr1 is not present in any of the currently available high resolution structures of SSU processomes, as these particles still contain the U3 snoRNA and evidence suggests that Dhr1 does not interact stably with pre-ribosomes.²⁴⁻²⁶ Interestingly, *in vivo* crosslinking in human cells revealed direct interactions between DHX37 and U3 sequences that lie close to the 3' hinge region, which is predicted to basepair with the 5' ETS, implying that DHX37 may influence U3-5' ETS interactions. Consistent with this, we observed that expression of catalytically inactive DHX37 impairs processing at the A' cleavage site in the 5' ETS, a pre-rRNA cleavage event that has previously been shown to be sensitive to depletion of the U3-associated protein U3-55K (RRP9).⁵⁸ Our complementation assays show that the catalytic activity of DHX37 is required for the conversion of the 21S pre-rRNA to 18SE, indicating that removal of the 5' ETS and site 2 cleavage in ITS1 can take place but that subsequent processing of ITS1 is inhibited. The finding that removal of the 5' ETS and site 2 processing can take place although A' is impaired is consistent with previous data showing that A' cleavage can be bypassed.⁹ The pre-rRNA processing defects observed upon depletion of DHX37 could suggest that failure

to release the U3 snoRNA during earlier stages of pre-40S maturation may not inhibit pre-rRNA processing until later. However, it is not yet known at precisely which stage of ribosome biogenesis the U3 snoRNA is released from human pre-ribosomes. Although production of the 21S pre-rRNA involves cleavages in 5' ETS, which would be anticipated to remove U3 base-pairing sites, it remains to be determined how U3 release is co-ordinated with pre-rRNA processing events. An alternative possibility is that the requirement for DHX37 for the conversion of 21S to 18SE represents an additional function for the helicase in SSU biogenesis, beyond its proposed role in facilitating U3 dissociation.

Similar to yeast Dhr1, DHX37 does not appear to associate stably with pre-ribosomal complexes in sucrose density gradient experiments. Nevertheless, the binding of DHX37 to the U3 snoRNA observed by immunoprecipitation and CRAC is anticipated to take place in the context of pre-ribosomal particles. Consistent with this, our complementation assays suggest that the presence of DHX37 in early pre-ribosomal complexes is monitored and that in the absence of the helicase, pre-ribosomes are targeted for degradation. Relatively little is known about the quality control pathways that are responsible for turnover of aberrant pre-ribosomes, especially in human cells, but it has been suggested that exonucleases involved in pre-rRNA processing steps could be utilised as degradation machines if particular ribosome biogenesis steps have not taken place correctly. Mapping of the aberrant 38S* and 16S* pre-rRNAs detected upon depletion of DHX37 demonstrates that they are 5' truncated derivatives of the 41S and 21S pre-rRNA, but depletion of the 5'-3' exonuclease XRN2 did not influence production of these species. This implies that other nucleases are involved in the turnover of pre-ribosomes lacking DHX37. Stalling of exonucleases at highly structured pre-rRNA sequences, or pre-rRNA-bound ribosome biogenesis factors or ribosomal proteins may lead to formation of discrete pre-rRNA intermediates, and the diffuse nature of the 16S* intermediate, which often appears as two bands, suggests that this species may be heterogenous as would be expected if it is produced by exonucleolytic trimming. It is possible however, that during surveillance, the 18S rRNA sequence is first targeted by an endonuclease, as was recently reported in yeast.⁵⁸ In yeast, Utp24 cleaves the 18S rRNA sequence at nucleotide 618 (Q1 site) between helices 19 and 20, whereas the 5' end of 38S* maps to helix 32 of the human 18S rRNA. While both these rRNA sequences lie in close proximity to the Utp24 binding site identified in yeast, as UTP24 is a core component of the SSU processome, expression of a catalytically inactive form of UTP24 would be required to investigate its potential role in pre-ribosome quality control in human cells.

The finding that pre-ribosomes lacking DHX37 are targeted for degradation further highlights the importance of this protein for ribosome assembly. Interestingly, the surveillance pathway also appears to be triggered when the pre-40S biogenesis factors

DIMT1L or TSR1 are lacking. While our data indicate that DHX37, DIMT1L and TSR1 can be present in the same pre-ribosomal particles, their association *in vivo* is dependent on RNA, implying that they do not form a discrete complex whose presence is monitored by this surveillance system. It is possible that the quality control pathway instead monitors maturation or folding of the central domain of the 18S rRNA as human TSR1 and yeast Dim1 have been demonstrated to bind this region, and DHX37 is implicated, either directly or indirectly, in regulating assembly of the central pseudoknot structure via U3 release. Alternatively, as the evolutionarily conserved rRNA modifications installed by DIMT1L are implicated in maintaining the fidelity of translation, and TSR1 plays an important role in preventing premature subunit joining, the requirement for a quality control pathway to confirm the pre-ribosomal recruitment of these three factors may reflect the critical roles they individually play during ribosome assembly.

In yeast, Dhr1 interacts with the rRNA methyltransferase Bud23 and with the pre-40S biogenesis factor Utp14.⁵⁴⁻⁵⁶ While Dhr1 has been shown to be required for the recruitment of Bud23 to pre-ribosomes, Bud23 and Utp14 are also necessary for the association of Dhr1.^{55,56} As these proteins also form direct interactions, it has been proposed that they are recruited to pre-ribosomes as a complex. Our data reveal that although the interaction between Dhr1/DHX37 and Utp14/UTP14A is conserved between yeast and humans, DHX37 does not co-precipitate the Bud23 orthologue WBSR22 from human cells. On a molecular level this difference can readily be explained as structural analysis of the Dhr1-Bud23-Trm112 complex revealed that amino acids in the N-terminal region of Dhr1 contact Bud23⁵⁵ and this region of the protein is largely absent from human DHX37. In yeast, Bud23 is recruited to early pre-ribosomal complexes but is reported to install the 18S-m⁷G1575 modification at a later stage.^{55,59} In contrast, and consistent with the lack of interaction with DHX37, WBSR22 is only present in later pre-40S complexes,^{38,57} implying that pre-ribosomal recruitment of these two proteins is independent in human cells. However, as in yeast, we discovered a direct, RNA-independent interaction between DHX37 and UTP14A in human cells. The interaction surface between yeast Dhr1 and Utp14 has been identified and amino acid substitutions within this region have been shown to impair the association of these proteins.⁵⁶ Surprisingly, introduction of the equivalent amino acid substitutions in DHX37 did not block its interaction with UTP14A (data not shown), suggesting that the precise contacts between these proteins are different in humans than yeast. Yeast Utp14 has been reported to stimulate the unwinding, but not ATPase, activity of the Dhr1 *in vitro* and is proposed to act as a cofactor for the helicase.²⁶ The precise mechanism by which Utp14 regulates Dhr1 therefore remains unclear. We observe a mild increase in the rate of ATP hydrolysis by DHX37 in the presence of UTP14A compared to the helicase alone, suggesting that human UTP14A can also function as a helicase cofactor. Depletion of either

yeast Utp14⁵⁶ or human UTP14A causes accumulation of the U3 snoRNA on pre-ribosomes. As lack of UTP14A causes defects in early pre-rRNA processing steps, we cannot rule out the possibility that the observed accumulation of U3 on pre-ribosomes is an indirect effect caused by impaired ribosome assembly. However, taken together with the stimulation of DHX37 by UTP14A and data from a yeast complementation system showing that disruption of the interaction between these proteins causes a similar phenotype, it is likely that, on a cellular level, UTP14A acts together with DHX37 to promote U3 release. Taken together, while our analysis of DHX37 suggests that the requirement for this helicase for efficient dissociation of the U3 snoRNP from pre-ribosomes is conserved in eukaryotes, we also highlight differences in the precise RNA and protein interactions formed by this helicase in yeast and human cells. To gain further mechanistic insights into Dhr1/DHX37 regulation by Utp14/UTP14A and to understand precisely how Dhr1/DHX37 contributes to U3 release, structural analyses of the helicase alone and within the context of pre-ribosomes will likely be required.

Materials and methods

Molecular cloning

The coding sequence of DHX37 (NM_032656.3) was cloned into a pcDNA5-based vector for the expression of proteins with a C-terminal His₆-PreScission protease cleavage site-2xFlag (Flag) tag from a defined genomic locus via a tetracycline-regulatable promoter in human cells. To express RNAi-resistant DHX37, site-directed mutagenesis was used to introduce 5 silent mutations within the binding site of siDHX37_1 (Supplementary Table 2). The coding sequences of DHX37 and UTP14A (NM_006649.3) were also cloned into pQE80-derivatived vectors (A42 and A15) for expression of proteins with a C-terminal His₆ tag or an N-terminal ZZ tag and C-terminal His₁₀ tag from IPTG-regulatable promoters in *E. coli*. Site-directed mutagenesis was performed on both the DHX37 constructs to introduce point mutations that lead to a threonine 282 to alanine substitution (T282A) in the expressed protein.

Human cell culture, generation of cell lines and RNAi

Hela CCL2 and HEK293 cells were cultured according to standard protocols at 37 °C with 5% CO₂ in 1x Dulbecco's Modified Eagle Medium (DMEM) supplemented with 10% foetal calf serum. To generate cell lines for expression of RNAi-resistant, wild-type or mutant DHX37, or the Flag tag, HEK293 Flp-In-T-Rex (Thermo Scientific) cells were transfected with the appropriate pcDNA5 constructs according to the manufacturer's instructions. Selection of stably transfected cells was achieved using hygromycin and blasticidin. Protein expression was induced by addition of 0.5-1000 ng/mL tetracycline for 24 h before harvesting. For RNAi, cells were transfected with 20-50 nmol of siRNA (Supplementary Table 2) using lipofectamine RNAiMAX (Thermo Scientific) according to the manufacturer's instructions. Cells were harvested 72 h after transfection unless otherwise stated.

Immunofluorescence

Immunofluorescence was essentially performed as previously described in ¹⁹. HeLa cells were grown on coverslips before fixing using 4% paraformaldehyde in PBS for 10 min at room temperature. Cells were first permeabilised using 0.1% Triton-X-100 in PBS for 20 min then blocked with 10% FCS and 0.1% Triton-X-100 in PBS for 1 h at room temperature. Cells were incubated with anti-DHX37 and anti-NSUN5 antibodies (Supplementary Table 3) diluted in 10% FCS in PBS for 2 h at room temperature. Coverslips were washed and cells were incubated with Alexa Fluor 488-conjugated and Alexa Fluor 657-conjugated secondary antibodies for 1 h at room temperature. Coverslips were washed again and then

mounted using Vectashield (Vector Laboratories) containing DAPI. Cells were analysed by confocal microscopy using a ConfoCor2 microscope (Carl Zeiss).

RNA extraction, northern blotting and pulse-chase metabolic labelling

Total RNA was extracted from human cells using TRI reagent (Sigma Aldrich) according to the manufacturer's instructions. Detection of pre-rRNAs by northern blotting was performed as previously described in ⁹. In brief, 5 µg of total RNA were separated on a 1.2% agarose-glyoxal gel and transferred to a nylon membrane by vacuum blotting or alternatively, RNAs were separated on a 10% denaturing (7 M urea) polyacrylamide gel and transferred to nylon membrane by wet electroblotting. Membranes were pre-hybridised in SES1 (0.25 M sodium phosphate pH 7.0, 7 % SDS (w/v), 1 mM EDTA) buffer before incubation with 5' [³²P]-labelled DNA oligonucleotides (Supplementary Table 4) in SES1 buffer at 37°C overnight. After washing, signals were visualised using a Typhoon FLA9500 phosphorimager. Pulse-chase labelling of nascent RNAs was essentially performed as previously described in ¹⁰. siRNA-treated cells were grown in phosphate-free DMEM for 1 h before exchanging the media for phosphate-free DMEM supplemented with 15 µCi/mL [³²P]-labelled orthophosphate and growth for a further 1 h. The labelled media was then removed, cells were washed and grown in unlabelled DMEM for an additional 3 h before harvesting. Total RNA was extracted, separated by denaturing agarose gel electrophoresis, transferred to a nylon membrane by capillary blotting and abundant, labelled RNA species were visualised using a phosphorimager.

Immunoprecipitation of complexes from human cells

Expression of DHX37-Flag or the Flag tag was induced in HEK293 cells for 24 h and cells were harvested. Cells were lysed by sonication in a buffer containing 50 mM Tris- HCl pH 7.8, 150 mM NaCl, 0.5 mM ethylenediaminetetraacetic acid (EDTA), 5 mM β-mercaptoethanol and extracts were centrifuged at 20,000 x g for 10 min to remove insoluble material. The cleared lysate was supplemented with 1.5 mM MgCl₂ and was either treated with RNase A (2.5 U) or was left untreated. The extracts were then incubated with anti-Flag magnetic beads (Sigma Aldrich) for 2 h at 4 °C, and bound proteins and RNAs were eluted with 250 µg/mL Flag peptide. Proteins were precipitated with 20% trichloroacetic acid (TCA) and analysed by western blotting using antibodies listed in Supplementary Table 3. Alternatively, RNAs were extracted using phenol:chloroform:isoamylalcohol (PCI; 25:24:1), ethanol precipitated and analysed by northern blotting using probes listed in Supplementary Table 4.

Sucrose density gradient centrifugation

HeLa cells, or HEK293 cell lines expressing DHX37-Flag or DHX37_{T282}-Flag were lysed by sonication in a buffer containing 50mM Tris pH 7.5, 100mM NaCl, 5mM MgCl₂ and 1mM DTT before centrifugation at 20,000 x g for 10 min at 4°C to remove insoluble material. The cleared extracts were separated on 10-45% sucrose density gradients in an SW-40Ti rotor for 16 h at 23,500 rpm. 530 µL fractions were collected and the absorbance of each fraction at 260 nm was determined using a nanodrop (Pqclab). The proteins present in each fraction were precipitated using 20% TCA, separated by SDS-PAGE and analysed by western blotting using antibodies listed in Supplementary Table 3. RNAs present in each fraction were extracted using PCI, ethanol precipitated and analysed by northern blotting using probes listed in Supplementary Table 4.

Crosslinking and analysis of cDNA (CRAC)

CRAC was performed as previously described in references 38,40,51,52. Briefly, expression of DHX37-Flag or the Flag tag was induced in HEK293 cell lines for 24 h before growth in media supplemented with 100 µM 4-thiouridine for 6 h. *In vivo* crosslinking was then performed using 2 cycles of 180 mJ/cm² light at 365 nm in a Stratalinker (Agilent Technologies). Cells were harvested and RNA-protein complexes were enriched by tandem affinity purification on anti-Flag M2 magnetic beads and NiNTA. After a limited RNase digestion, co-precipitated RNAs were 5' end labelled with [³²P] and sequencing adaptors were ligated. RNA-protein complexes were separated by denaturing PAGE, transferred to a nitrocellulose membrane and labelled RNAs were visualised by autoradiography. Regions of the membrane were excised and RNAs were eluted by Proteinase K digestion then extracted using PCI. RNA fragments were reverse transcribed, amplified by PCR and the resulting library was subjected to Illumina sequencing. The obtained sequence reads were mapped to the human genome (GRCh37.p13).

Purification of recombinant proteins, and in vitro binding and ATPase assays

Expression of DHX37-His₆ or ZZ-UTP14A-His₁₀ was induced in BL21 codon plus cells by addition of 1 mM IPTG for 16 h at 18°C. Cells were pelleted, resuspended in Lysis buffer (50 mM Tris-HCl pH 7.0, 500 mM NaCl, 1 mM MgCl₂, 10% glycerol and 5 mM imidazole) and disrupted by sonication. The cell lysate was cleared by centrifugation at 50,000 x g for 30 min and the soluble fraction was incubated with cComplete His-tag purification resin (Roche) for 2 h at 4°C. After thorough washing steps with low and high salt buffers (50 mM Tris-HCl pH 7.0, 500 mM/1000 mM NaCl, 1 mM MgCl₂, 10% glycerol and 25 mM imidazole), bound proteins were eluted with lysis buffer supplemented with 500 mM imidazole. The

eluate was dialysed against a buffer containing 50 mM Tris-HCl pH 7.0, 150 mM NaCl and 20% glycerol. MBP-DHX15-His₁₀ was prepared as previously described in reference 38.

For *in vitro* binding assays, 200 pmol of recombinant ZZ-UTP14A-His₁₀ was immobilised on IgG sepharose (GE Healthcare) that had been pre-equilibrated in 50 mM Tris-HCl pH 7.4, 100 mM NaCl, 1.5 mM MgCl₂, 0.2 % Triton X-100 and 1 mM DTT. After washing steps to remove unbound protein, IgG sepharose and ZZ-UTP14A-His₁₀-IgG sepharose was incubated with 200 pmol DHX37-His₆ for 1 h rotating at 4 °C. The beads were then washed and elution was performed by treatment with 2 µM TEV protease overnight at 4 °C in 50 mM Tris-HCl pH 7.4, 100 mM NaCl, 1.5 mM MgCl₂, 0.2 % Triton X-100 and 1 mM DTT. Inputs and eluates were separated by SDS-PAGE then analysed by western blotting using antibodies listed in Supplementary Table 3.

Hydrolysis of ATP was monitored in an NADH-coupled assay.⁶⁰ Reactions were set up containing 45 mM Tris-HCl pH 7.4, 25 mM NaCl, 2 mM MgCl₂, 1 mM phosphoenolpyruvate, 300 µM NADH, 20 U/ml pyruvate kinase and 4 mM ATP and were supplemented with 500 nM recombinant DHX37/DHX37_{T282}/DHX15, 500 nM recombinant UTP14A and/or 1.5 µM RNA (5'-GUAAUGUAAGUGAACGUAAAACAAAACAAAAC-3') as indicated. The decrease in absorbance at 340 nm was monitored using a BioTEK Synergy plate reader and this was used to calculate the rate of ATP hydrolysis.

ACKNOWLEDGEMENTS

We would like to thank Jens Kretschmer for help with bioinformatics analyses and cloning, and Claudia Schneider for helpful discussions. This work was funded by the Deutsche Forschungsgemeinschaft (SFB1190 and BO3442/1-2) and the University Medical Centre Göttingen.

DISCLOSURE OF INTEREST

The authors declare no conflict of interest.

REFERENCES

1. Anger AM, Armache J-P, Berninghausen O, Habeck M, Subklewe M, Wilson DN, Beckmann R. Structures of the human and Drosophila 80S ribosome. *Nature* 2013; 497:80–5.
2. Woolford JLJ, Baserga SJ. Ribosome biogenesis in the yeast *Saccharomyces cerevisiae*. *Genetics* 2013; 195:643–81.
3. Andersen JS, Lyon CE, Fox AH, Leung AKL, Lam YW, Steen H, Mann M, Lamond AI. Directed proteomic analysis of the human nucleolus. *Curr Biol* 2002; 12:1–11.
4. Scherl A, Coute Y, Deon C, Calle A, Kindbeiter K, Sanchez J-C, Greco A, Hochstrasser D, Diaz J-J. Functional proteomic analysis of human nucleolus. *Mol Biol Cell* 2002; 13:4100–9.
5. Wild T, Horvath P, Wyler E, Widmann B, Badertscher L, Zemp I, Kozak K, Csucs G, Lund E, Kutay U. A protein inventory of human ribosome biogenesis reveals an essential function of exportin 5 in 60S subunit export. *PLoS Biol* 2010; 8:e1000522.
6. Tafforeau L, Zorbas C, Langhendries J-L, Mullineux S-T, Stamatopoulou V, Mullier R, Wacheul L, Lafontaine DLJ. The complexity of human ribosome biogenesis revealed by systematic nucleolar screening of Pre-rRNA processing factors. *Mol Cell* 2013; 51:539–51.
7. Badertscher L, Wild T, Montellese C, Alexander LT, Bammert L, Sarazova M, Stebler M, Csucs G, Mayer TU, Zamboni N, et al. Genome-wide RNAi Screening Identifies Protein Modules Required for 40S Subunit Synthesis in Human Cells. *Cell Rep* 2015; 13:2879–91.
8. Farley-Barnes KI, McCann KL, Ogawa LM, Merkel J, Surovtseva Y V, Baserga SJ. Diverse Regulators of Human Ribosome Biogenesis Discovered by Changes in Nucleolar Number. *Cell Rep* 2018; 22:1923–34.
9. Sloan KE, Bohnsack MT, Schneider C, Watkins NJ. The roles of SSU processome components and surveillance factors in the initial processing of human ribosomal RNA. *RNA* 2014; 20:540–50.

10. Sloan KE, Mattijssen S, Lebaron S, Tollervey D, Pruijn GJM, Watkins NJ. Both endonucleolytic and exonucleolytic cleavage mediate ITS1 removal during human ribosomal RNA processing. *J Cell Biol* 2013; 200:577–88.
11. Preti M, O'Donohue M-F, Montel-Lehry N, Bortolin-Cavaille M-L, Choesmel V, Gleizes P-E. Gradual processing of the ITS1 from the nucleolus to the cytoplasm during synthesis of the human 18S rRNA. *Nucleic Acids Res* 2013; 41:4709–23.
12. Mills EW, Green R. Ribosomopathies: There's strength in numbers. *Science* 2017; 358.
13. Pelletier J, Thomas G, Volarevic S. Ribosome biogenesis in cancer: new players and therapeutic avenues. *Nat Rev Cancer* 2018; 18:51–63.
14. Henras AK, Plisson-Chastang C, O'Donohue M-F, Chakraborty A, Gleizes P-E. An overview of pre-ribosomal RNA processing in eukaryotes. *Wiley Interdiscip Rev RNA* 2015; 6:225–42.
15. Watkins NJ, Bohnsack MT. The box C/D and H/ACA snoRNPs: key players in the modification, processing and the dynamic folding of ribosomal RNA. *Wiley Interdiscip Rev RNA* 2012; 3:397–414.
16. Sloan KE, Warda AS, Sharma S, Entian K-D, Lafontaine DLJ, Bohnsack MT. Tuning the ribosome: The influence of rRNA modification on eukaryotic ribosome biogenesis and function. *RNA Biol* 2017; 14:1138–52.
17. Wells GR, Weichmann F, Colvin D, Sloan KE, Kudla G, Tollervey D, Watkins NJ, Schneider C. The PIN domain endonuclease Utp24 cleaves pre-ribosomal RNA at two coupled sites in yeast and humans. *Nucleic Acids Res* 2016; 44:5399–409.
18. Wells GR, Weichmann F, Sloan KE, Colvin D, Watkins NJ, Schneider C. The ribosome biogenesis factor yUtp23/hUTP23 coordinates key interactions in the yeast and human pre-40S particle and hUTP23 contains an essential PIN domain. *Nucleic Acids Res* 2017; 45:4796–809.
19. Warda AS, Freytag B, Haag S, Sloan KE, Gorlich D, Bohnsack MT. Effects of the Bowen-Conradi syndrome mutation in EMG1 on its nuclear import, stability and nucleolar recruitment. *Hum Mol Genet* 2016; 25:5353–64.

20. Kass S, Tyc K, Steitz JA, Sollner-Webb B. The U3 small nucleolar ribonucleoprotein functions in the first step of preribosomal RNA processing. *Cell* 1990; 60:897–908.
21. Sharma K, Venema J, Tollervey D. The 5' end of the 18S rRNA can be positioned from within the mature rRNA. *RNA* 1999; 5:678–86.
22. Hughes JM. Functional base-pairing interaction between highly conserved elements of U3 small nucleolar RNA and the small ribosomal subunit RNA. *J Mol Biol* 1996; 259:645–54.
23. Borovjagin A V, Gerbi SA. The spacing between functional Cis-elements of U3 snoRNA is critical for rRNA processing. *J Mol Biol* 2000; 300:57–74.
24. Barandun J, Chaker-Margot M, Hunziker M, Molloy KR, Chait BT, Klinge S. The complete structure of the small-subunit processome. *Nat Struct Mol Biol* 2017; 24:944–53.
25. Cheng J, Kellner N, Berninghausen O, Hurt E, Beckmann R. 3.2-Å-resolution structure of the 90S preribosome before A1 pre-rRNA cleavage. *Nat Struct Mol Biol* 2017; 24:954–64.
26. Sardana R, Liu X, Granneman S, Zhu J, Gill M, Papoulas O, Marcotte EM, Tollervey D, Correll CC, Johnson AW. The DEAH-box helicase Dhr1 dissociates U3 from the pre-rRNA to promote formation of the central pseudoknot. *PLoS Biol* 2015; 13:e1002083.
27. Sloan KE, Gleizes P-E, Bohnsack MT. Nucleocytoplasmic Transport of RNAs and RNA-Protein Complexes. *J Mol Biol* 2016; 428:2040–59.
28. Linder P, Jankowsky E. From unwinding to clamping - the DEAD box RNA helicase family. *Nat Rev Mol Cell Biol* 2011; 12:505–16.
29. Jarmoskaite I, Russell R. RNA helicase proteins as chaperones and remodelers. *Annu Rev Biochem* 2014; 83:697–725.
30. Liang X-H, Fournier MJ. The helicase Has1p is required for snoRNA release from pre-rRNA. *Mol Cell Biol* 2006; 26:7437–50.
31. Bohnsack MT, Kos M, Tollervey D. Quantitative analysis of snoRNA association with pre-ribosomes and release of snR30 by Rok1 helicase. *EMBO Rep* 2008; 9:1230–6.

32. Bohnsack MT, Martin R, Granneman S, Ruprecht M, Schleiff E, Tollervey D. Prp43 Bound at Different Sites on the Pre-rRNA Performs Distinct Functions in Ribosome Synthesis. *Mol Cell* 2009; 36:583–92.
33. Dembowski JA, Kuo B, Woolford JL. Has1 regulates consecutive maturation and processing steps for assembly of 60S ribosomal subunits. *Nucleic Acids Res* 2013; 41:7889–904.
34. Pertschy B, Schneider C, Gnadig M, Schafer T, Tollervey D, Hurt E. RNA helicase Prp43 and its co-factor Pfa1 promote 20 to 18 S rRNA processing catalyzed by the endonuclease Nob1. *J Biol Chem* 2009; 284:35079–91.
35. Martin R, Straub AU, Doebele C, Bohnsack MT. DExD/H-box RNA helicases in ribosome biogenesis. *RNA Biol* 2013; 10:4–18.
36. Srivastava L, Lapik YR, Wang M, Pestov DG. Mammalian DEAD box protein Ddx51 acts in 3' end maturation of 28S rRNA by promoting the release of U8 snoRNA. *Mol Cell Biol* 2010; 30:2947–56.
37. Kellner M, Rohrmoser M, Forne I, Voss K, Burger K, Muhl B, Gruber-Eber A, Kremmer E, Imhof A, Eick D. DEAD-box helicase DDX27 regulates 3' end formation of ribosomal 47S RNA and stably associates with the PeBoW-complex. *Exp Cell Res* 2015; 334:146–59.
38. Memet I, Doebele C, Sloan KE, Bohnsack MT. The G-patch protein NF-kappaB-repressing factor mediates the recruitment of the exonuclease XRN2 and activation of the RNA helicase DHX15 in human ribosome biogenesis. *Nucleic Acids Res* 2017; 45:5359–74.
39. Calo E, Flynn RA, Martin L, Spitale RC, Chang HY, Wysocka J. RNA helicase DDX21 coordinates transcription and ribosomal RNA processing. *Nature* 2015; 518:249–53.
40. Sloan KE, Leisegang MS, Doebele C, Ramirez AS, Simm S, Safferthal C, Kretschmer J, Schorge T, Markoutsas S, Haag S, et al. The association of late-acting snoRNPs with human pre-ribosomal complexes requires the RNA helicase DDX21. *Nucleic Acids Res* 2015; 43:553–64.
41. Larburu N, Montellese C, O'Donohue M-F, Kutay U, Gleizes P-E, Plisson-Chastang C. Structure of a human pre-40S particle points to a role for RACK1 in the final steps of 18S rRNA processing. *Nucleic Acids Res* 2016; 44:8465–78.

42. Ameismeier M, Cheng J, Berninghausen O, Beckmann R. Visualizing late states of human 40S ribosomal subunit maturation. *Nature* 2018; 558:249–53.
43. Wang M, Pestov DG. 5'-end surveillance by Xrn2 acts as a shared mechanism for mammalian pre-rRNA maturation and decay. *Nucleic Acids Res* 2011; 39:1811–22.
44. Zorbas C, Nicolas E, Wacheul L, Huvelle E, Heurgue-Hamard V, Lafontaine DLJ. The human 18S rRNA base methyltransferases DIMT1L and WBSCR22-TRMT112 but not rRNA modification are required for ribosome biogenesis. *Mol Biol Cell* 2015; 26:2080–95.
45. Carron C, O'Donohue MF, Choesmel V, Faubladiere M, Gleizes PE. Analysis of two human pre-ribosomal factors, bystin and hTsr1, highlights differences in evolution of ribosome biogenesis between yeast and mammals. *Nucleic Acids Res* 2011; 39:280–91.
46. McCaughan UM, Jayachandran U, Shchepachev V, Chen ZA, Rappsilber J, Tollervey D, Cook AG. Pre-40S ribosome biogenesis factor Tsr1 is an inactive structural mimic of translational GTPases. *Nat Commun* 2016; 7:11789.
47. Leulliot N, Bohnsack MT, Graille M, Tollervey D, Van tilbeurgh H. The yeast ribosome synthesis factor Emg1 is a novel member of the superfamily of alpha/beta knot fold methyltransferases. *Nucleic Acids Res* 2008; 36:629–39.
48. Meyer B, Wurm JP, Kotter P, Leisegang MS, Schilling V, Buchhaupt M, Held M, Bahr U, Karas M, Heckel A, et al. The Bowen-Conradi syndrome protein Nep1 (Emg1) has a dual role in eukaryotic ribosome biogenesis, as an essential assembly factor and in the methylation of Psi1191 in yeast 18S rRNA. *Nucleic Acids Res* 2011; 39:1526–37.
49. Haag S, Kretschmer J, Bohnsack MT. WBSCR22/Merm1 is required for late nuclear pre-ribosomal RNA processing and mediates N7-methylation of G1639 in human 18S rRNA. *RNA* 2015; 21:180–7.
50. Linder P, Jankowsky E. From unwinding to clamping - the DEAD box RNA helicase family. *Nat Rev Mol Cell Biol* 2011; 12:505–16.
51. Bohnsack MT, Tollervey D, Granneman S. Identification of RNA helicase target sites by UV cross-linking and analysis of cDNA [Internet]. 1st ed. Elsevier Inc.; 2012. Available from: <http://dx.doi.org/10.1016/B978-0-12-396546-2.00013-9>

52. Haag S, Kretschmer J, Sloan KE, Bohnsack MT. Crosslinking Methods to Identify RNA Methyltransferase Targets In Vivo. *Methods Mol Biol* 2017; 1562:269–81.
53. Sloan KE, Bohnsack MT. Unravelling the Mechanisms of RNA Helicase Regulation. *Trends Biochem Sci* 2018; 43:237–50.
54. Sardana R, Zhu J, Gill M, Johnson AW. Physical and functional interaction between the methyltransferase Bud23 and the essential DEAH-box RNA helicase Ecm16. *Mol Cell Biol* 2014; 34:2208–20.
55. L etoquart J, Huvelle E, Wacheul L, Bourgeois G, Zorbas C, Graille M, Heurgu e-Hamard V, Lafontaine DLJ. Structural and functional studies of Bud23-Trm112 reveal 18S rRNA N7-G1575 methylation occurs on late 40S precursor ribosomes. *Proc Natl Acad Sci U S A* 2014; 111:E5518-26.
56. Zhu J, Liu X, Anjos M, Correll CC, Johnson AW. Utp14 Recruits and Activates the RNA Helicase Dhr1 To Undock U3 snoRNA from the Preribosome. *Mol Cell Biol* 2016; 36:965–78.
57. Ounap K, Kasper L, Kurg A, Kurg R. The human WBSCR22 protein is involved in the biogenesis of the 40S ribosomal subunits in mammalian cells. *PLoS One* 2013; 8:e75686.
58. Choque E, Schneider C, Gadal O, Dez C. Turnover of aberrant pre-40S pre-ribosomal particles is initiated by a novel endonucleolytic decay pathway. *Nucleic Acids Res* 2018; 46:4699–714.
59. White J, Li Z, Sardana R, Bujnicki JM, Marcotte EM, Johnson AW. Bud23 methylates G1575 of 18S rRNA and is required for efficient nuclear export of pre-40S subunits. *Mol Cell Biol* 2008; 28:3151–61.
60. Heininger AU, Hackert P, Andreou AZ, Boon K-L, Memet I, Prior M, Clancy A, Schmidt B, Urlaub H, Schleiff E, et al. Protein cofactor competition regulates the action of a multifunctional RNA helicase in different pathways. *RNA Biol* 2016; 13:320–30.

FIGURE LEGENDS

Figure 1. Depletion of the nucleolar RNA helicase DHX37 affects early and late stages of 18S rRNA maturation. **(A)** HeLa cells were fixed and the localisation of DHX37 was determined by immunofluorescence using an antibody against endogenous DHX37 (green). Immunofluorescence against NSUN5 (red) served as a nucleolar marker and nuclear material was visualised by DAPI staining (blue). An overlay of the images is provided and a scale bar representing 10 μm is depicted. **(B)** HeLa cells were left untransfected (WT), or were transfected with non-target siRNA (siNT) or siRNAs targeting DHX37 (siDHX37_1 and siDHX37_2). After 72 h, cells were harvested, and proteins were analysed by western blotting using antibodies against DHX37 and tubulin. **(C)** Whole cell extracts from cells treated with non-target siRNAs (siNT) or a siRNA targeting DHX37 (siDHX37_1) were separated by sucrose density gradient centrifugation. The absorbance of each fraction at 260 nm was used to generate a profile on which the positions of the ribosomal and pre-ribosomal complexes are indicated. **(D)** Schematic view of the major pre-rRNA intermediates detected in human cells. Mature rRNA regions are shown as black rectangles, and internal (ITS) and external transcribed spacer (ETS) regions are represented by black lines. Cleavage sites relevant for maturation of the 18S rRNA are named above the 47S rRNA transcript and the hybridisation position of the 5' ITS1 probe used for northern blotting is indicated by the triangle. **(E)** Untransfected HeLa cells, or HeLa cells that had been treated with non-target siRNAs (siNT) or those targeting DHX37 (siDHX37_1) for 72 h were starved of phosphate then grown in media supplemented with [^{32}P]-orthophosphate for 1 h before growth in normal DMEM for 3 h. Total RNA was extracted, separated by denaturing agarose gel electrophoresis, transferred to a nylon membrane and nascent RNAs were detected using a phosphorimager. The mature 28S rRNA was visualised using methylene blue staining (MB). **(F)** Total RNA was extracted from wild-type (WT) HeLa cells or HeLa cells transfected with siRNAs as in (B). RNAs were separated by denaturing agarose gel electrophoresis, transferred to a nylon membrane and the mature 28S rRNA was visualised by methylene blue staining (MB). Northern blotting with a probe hybridising to the 5' end of ITS1 (5' ITS1) was used to detect precursors of the 18S RNA, which were visualised using a phosphorimager. Aberrant pre-rRNA species detected upon depletion of DHX37 are indicated by arrows. Experiments were performed at least in triplicate and representative data are shown.

Figure 2. Mapping of the aberrant 16S* and 38S* pre-rRNA intermediates that accumulate upon depletion of DHX37. **(A)** Schematic view of the 47S pre-rRNAs (black) and the aberrant 38S*, 16S* and 30SL5' pre-rRNA species not normally detected in human cells

(grey). Mature rRNA regions are shown as rectangles, and internal (ITS) and external transcribed spacer (ETS) regions are represented by lines. Cleavage sites are named above the 47S pre-rRNA and the hybridisation position of probes used for northern blotting are indicated. **(B,C)** RNA extracted from HeLa cells transfected with non-target siRNAs (siNT) or siRNAs targeting DHX37 (siDHX37_1) was separated by denaturing agarose gel electrophoresis, transferred to a nylon membrane and the mature 28S rRNA was detected by methylene blue staining (MB). Northern blotting was performed using probes hybridising to different positions within the 5' ETS and ITS1 (B) or the 18S rRNA (C) and pre-rRNAs were visualised using a phosphorimager. **(D)** RNA extracted from wildtype (WT) HeLa cells or cells that had been transfected with non-target siRNAs (siNT), or siRNAs targeting DHX37 (siDHX37_1) or XRN2 (siXRN2) was analysed as in (B, C) using a probe hybridising to the 5' end of ITS1. Experiments were performed at least in triplicate and representative data are shown.

Figure 3. Pre-rRNAs are degraded upon depletion of DHX37 and expression of catalytically inactive DHX37 leads to defects in A' cleavage and the conversion of 21S to 18SE. **(A)** C-terminally His₆-tagged DHX37 or DHX37 carrying a threonine to alanine substitution at amino acid 282 within the evolutionarily conserved "GKT" motif (DHX37_{T282A}) was recombinantly expressed in *E. coli* and purified. Purified proteins were separated by SDS-PAGE and visualised by Coomassie staining. **(B)** The amount of ATP hydrolysed by recombinant DHX37 or DHX37_{T282A} in the presence (+) or absence (-) of RNA was determined using an *in vitro* NADH-coupled ATPase assay. Experiments were performed in triplicate and error bars represent mean \pm standard deviation. **(C)** HEK293 cell lines were transfected with either non-target siRNAs (siNT) or siRNAs targeting DHX37 (siDHX37_1) and expression of the Flag tag, or C-terminally Flag-tagged DHX37 or DHX37_{T282A} was induced by addition of tetracycline 24 h before harvesting. Proteins were extracted and analysed by western blotting using antibodies against DHX37, tubulin and the Flag tag. **(D)** Total RNA extracted from HEK293 cell lines treated as described in (C) was separated by denaturing agarose gel electrophoresis, transferred to a nylon membrane and analysed by northern blotting using probes hybridising at the 5' end of ITS1 (left panel) or within the 5' ETS (right panel). Pre-rRNAs were detected using a phosphorimager and the mature 28S rRNA was visualised by methylene blue staining (MB).

Figure 4. DHX37 associates with the 3' region of the U3 snoRNA that contains the box C/D motifs. **(A)** HEK293 cells expressing DHX37-Flag or the Flag tag were grown in the presence of 4-thiouridine before crosslinking *in vivo* using light at 365 nm. RNA-protein complexes were tandem affinity purified under native and denaturing conditions, then RNAs co-purified with DHX37 were ligated to sequencing adaptors and labelled using [³²P]. Complexes were separated by denaturing PAGE, transferred to a nitrocellulose membrane

and labelled RNAs were detected by autoradiography. The regions of the membrane excised for subsequent analysis are indicated by boxes. **(B)** The region of the membrane containing DHX37-Flag-RNA complexes as indicated in (A), and a corresponding region of the lane containing the Flag sample, were excised. RNAs were isolated and subjected to reverse transcription and PCR amplification to generate a cDNA library upon which Illumina deep sequencing was performed. The obtained sequence reads were mapped to the human genome and, after normalisation, the relative number of reads derived from snoRNAs in the Flag and DHX37-Flag samples was determined. **(C)** The relative distribution of sequence reads derived from each box C/D snoRNA in the Flag and DHX37-Flag datasets is shown. The proportion of sequence reads mapping to the U3 snoRNA is highlighted in red while all other snoRNAs are shown in shades of grey. **(D)** Cell extracts prepared from HEK293 cells expressing Flag-DHX37 or the Flag tag were incubated with anti-Flag beads. After thorough washing steps, complexes were eluted and RNA was extracted. RNAs extracted from inputs (1%) and eluates were separated by denaturing PAGE, transferred to a nylon membrane and northern blotting was performed using probes hybridising to the U3 and U8 snoRNAs. RNAs were detected using a phosphorimager. **(E)** The normalised number of reads mapping to each nucleotide of the gene encoding the U3 snoRNA in the Flag (black) and DHX37-Flag (red) datasets is shown graphically (upper panel). The normalised number of mutations mapping to each position are indicated in the lower panel. A schematic representation of the U3 snoRNA is shown below with the relative positions of key features indicated.

Figure 5. The U3 snoRNA accumulates on pre-ribosomes upon expression of catalytically inactive DHX37. **(A)** HEK293 cells capable of expression of DHX37-Flag or DHX37_{T282A}-Flag were transfected with siRNAs against DHX37 and 24 h prior to harvesting, expression of the tagged proteins was induced by addition of tetracycline. To confirm equal expression levels, proteins were analysed by western blotting using antibodies against DHX37 and tubulin. **(B)** Whole cell extracts prepared from HEK293 cells treated as in (A) were separated by sucrose density gradient centrifugation. The optical density of each fraction at 260 nm was determined and used to generate a profile on which the peaks corresponding to ribosomal and pre-ribosomal complexes are indicated. RNA extracted from the gradient fractions described in (B) was separated by denaturing PAGE and transferred to a nylon membrane. Northern blotting was performed using a [³²P]-labelled probe hybridising to the U3 snoRNA. The experiments shown in this figure were performed in triplicate and representative data are shown.

Figure 6. UTP14A interacts with DHX37 and stimulates its ATPase activity *in vitro*. **(A)** Cell extracts prepared from HEK293 cells expressing either DHX37-Flag or the Flag tag were used for immunoprecipitation experiments in the presence (+) or absence (-) of RNase.

Inputs (1%) and eluates were separated by SDS-PAGE and analysed by western blotting using antibodies against DHX37, UTP14A, WBSCR22 and tubulin. **(B)** Recombinant DHX37-His₆ was incubated with either IgG sepharose (beads) or with IgG sepharose on which ZZ-UTP14A-His₁₀ had been immobilised. After washing steps, proteins were eluted, and inputs and eluates were separated by SDS-PAGE then analysed by western blotting using antibodies against DHX37 and UTP14A. **(C)** The amount of ATP hydrolysed by recombinant DHX37 in the presence (+) or absence (-) of RNA and the presence (+) or absence (-) of UTP14A was determined using an *in vitro* NADH-coupled ATPase assay. Experiments were performed in triplicate and error bars represent mean \pm standard deviation. **(D)** HeLa cells were left untransfected (WT), or were transfected with non-target siRNA (siNT) or siRNAs targeting UTP14A (siUTP14A_1 and siUTP14A_2). After 72 h, cells were harvested, and proteins were analysed by western blotting using antibodies against UTP14A (upper panel) and tubulin (lower panel). **(E)** Total RNA was extracted from wild-type (WT) HeLa cells or HeLa cells transfected with siRNAs as in (D). RNAs were separated by denaturing agarose gel electrophoresis, transferred to a nylon membrane and the mature 28S rRNA was visualised by methylene blue staining (MB). Northern blotting with a probe hybridising to the 5' end of ITS1 (5' ITS1) was used to detect precursors of the 18S RNA, which were visualised using a phosphorimager. **(F)** Whole cell extracts prepared from HEK293 cells treated with control siRNAs (siNT) or siRNAs targeting UTP14A (siUTP14A_1) were separated by sucrose density gradient centrifugation. The absorbance of each fraction at 260 nm was determined and used to generate a profile on which the peaks corresponding to ribosomal subunits (40S and 60S) and 80S monosomes are indicated. RNA extracted from the gradient fractions was separated by denaturing PAGE, transferred to a nylon membrane and northern blotting was performed using a [³²P]-labelled probe hybridising to the U3 snoRNA. Replica experiments have been performed and representative data is shown in this figure.

SUPPLEMENTARY MATERIAL

The human RNA helicase DHX37 is required for release of the U3 snoRNP from pre-ribosomal particles

Priyanka Choudhury, Philipp Hackert, Indira Memet, Katherine E. Sloan and Markus T. Bohnsack

SUPPLEMENTARY FIGURES

Supplementary Figure 1. Depletion of DHX37, DIMT1L or TSR1 leads to accumulation of the aberrant 16S* and 38S* pre-rRNA intermediates. **(A)** Secondary structure of the human mature 18S rRNA with the positions of northern blot probes and the 5' end of the 38S* pre-rRNA intermediate indicated. **(B)** HeLa cells were transfected with non-target siRNAs (siNT), siRNAs against DHX37 (siDHX37_1 or siDHX37_2), DIMT1L (siDIMT1L_1 or siDIMT1L_2) or TSR1 (siTSR1_1 or siTSR1_2) or were left untransfected (WT) and harvested after 72 h. Proteins were separated by SDS-PAGE, transferred to a nitrocellulose membrane and analysed by western blotting using antibodies against DHX37, DIMT1L, TSR1 and, as a loading control, tubulin. **(C)** Total RNA extracted from siRNA-treated cells as described in (A) was separated by denaturing agarose gel electrophoresis, transferred to a nylon membrane and analysed by northern blotting using a probe that hybridises to the 5' end of ITS1. The mature 28S rRNA was visualised by methylene blue staining (MB).

Supplementary Figure 2. The distribution of DHX37 between pre-ribosomal and non-ribosomal complexes. Cell extracts prepared from HeLa cells were separated by sucrose density gradient centrifugation. The absorbance of each fraction at 260 nm was used to generate a profile on which the positions of the 40S and 60S subunits, and the 80S monosomes are indicated (upper panel). The distribution of DHX37 was determined by western blotting using an antibody against the endogenous protein (lower panel).

Supplementary Figure 3. Sequence alignment of yeast Dhr1 and human DHX37. An alignment of the amino acid sequences of *S. cerevisiae* Dhr1 (Uniprot: Q04217) and *H. sapien* DHX37 (Uniprot: Q8IY37) is shown. Amino acids numbers are indicated to the left and right and the regions of Dhr1 that are known to form protein-protein interactions are indicated.

Supplementary Figure 4. DIMT1L and TSR1 co-precipitate with DHX37 from human cells but these interactions are RNA-dependent. **(A, B)** Whole cell extracts prepared from HEK293 cells expressing DHX37-Flag or the Flag tag were used for immunoprecipitation experiments on anti-Flag beads in the presence (+) or absence (-) of RNase treatment.

Inputs (1%) and eluates were separated by SDS-PAGE, transferred to a nitrocellulose membrane and analysed by western blotting using antibodies against DIMT1L (A), TSR1 (B) and tubulin (A and B).

Supplementary Figure 5. UTP14A does not stimulate ATP hydrolysis by the DEAH box RNA helicase DHX15. The amount of ATP hydrolysed by recombinant DHX15 in the presence (+) or absence (-) of RNA and the presence (+) or absence (-) of UTP14A was determined using an *in vitro* NADH-coupled ATPase assay. Experiments were performed in triplicate and error bars represent mean \pm standard deviation.

SUPPLEMENTARY TABLES

Supplementary Table 1. Normalised number of DHX37 CRAC sequencing reads mapping to snoRNAs

Box C/D snoRNA	Hits/million	Box snoRNA	H/ACA	Hits/million
SNORD1	20	SNORA1		10
SNORD3	7645	SNORA2		10
SNORD4	41	SNORA3		10
SNORD5	248	SNORA7		51
SNORD6	20	SNORA10		20
SNORD7	20	SNORA13		20
SNORD11	72	SNORA19		10
SNORD12	10	SNORA20		20
SNORD13	10	SNORA22		10
SNORD14	61	SNORA23		10
SNORD15	123	SNORA28		10
SNORD18	102	SNORA30		30
SNORD19	20	SNORA31		20
SNORD20	62	SNORA33		31
SNORD24	113	SNORA36		20
SNORD26	82	SNORA38		20
SNORD32	20	SNORA41		10
SNORD34	41	SNORA42		10
SNORD35	31	SNORA45		10
SNORD36	154	SNORA46		10
SNORD38	82	SNORA48		20
SNORD42	51	SNORA50		20
SNORD43	548	SNORA51		20
SNORD45	61	SNORA53		10
SNORD46	51	SNORA55		20
SNORD47	10	SNORA58		10
SNORD48	155	SNORA63		20
SNORD49	41	SNORA64		20
SNORD52	10	SNORA66		20
SNORD53	51	SNORA67		72
SNORD54	10	SNORA68		10
SNORD55	20	SNORA69		41
SNORD58	102	SNORA70		30
SNORD59	31	SNORA71		10
SNORD61	20	SNORA73		10
SNORD62	41	SNORA76		41
SNORD63	31	SNORA78		10
SNORD66	41	SNORA80		10
SNORD68	20	SNORA81		10
SNORD69	20			
SNORD70	20			
SNORD71	51			

SNORD72	51		
SNORD73	31		
SNORD76	227		
SNORD82	20		
SNORD83	40		
SNORD84	82		
SNORD85	72		
SNORD86	20		
SNORD87	10		
SNORD88	40		
SNORD90	10		
SNORD91	30		
SNORD93	10		
SNORD95	51		
SNORD96	155		
SNORD98	31		
SNORD99	41		
SNORD100	41		
SNORD101	62		
SNORD103	71		
SNORD104	41		
SNORD105	10		
SNORD110	20		
SNORD111	40		
SNORD117	51		
SNORD118	41		
SNORD119	51		
SNORD125	10		
SNORD126	20		

Supplementary Table 2. Sequences of siRNA used in this study

Name	siRNA target sequence (5'-3')	Reference
siNT	CGTACGCGGAATACTTCGA	61
siDHX37_1	AGAUCAACUUGGAUCAUUATT	Qiagen
siDHX37_2	GGAAGGUCAAGAAAACGCUATT	Qiagen
siXRN2_1	GGGAAGAAAUUUGGCAA	62
siDIMT1L_1	GGCUAGUAGCUGAACUUCA	44
siDIMT1L_2	GGAUGGUCUAGUAAGGAUA	44
siTSR1_1	GGAGAUUUGUGCUACGGAU	6
siTSR1_2	GCAUCUUGCUUUUCGAGAU	6
siUTP14A_1	CAGGAAGAACUAGCGGAUU	63
siUTP14A_2	GACGCCGGUUUCUCAUUA	63

Supplementary Table 3. Antibodies used in this study

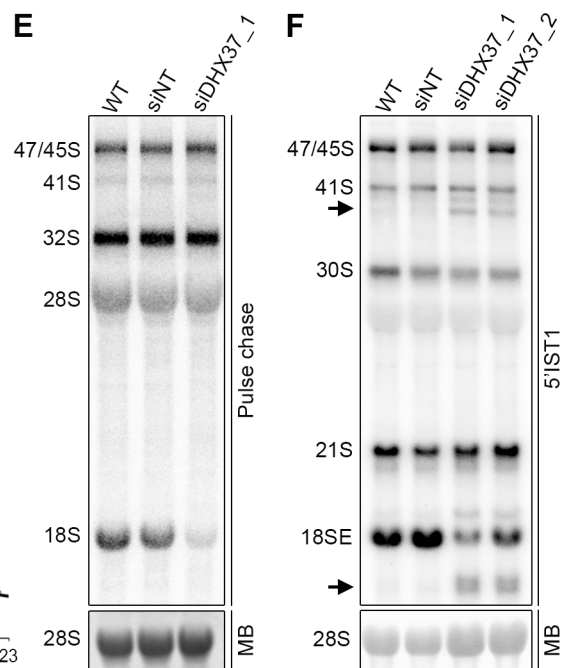
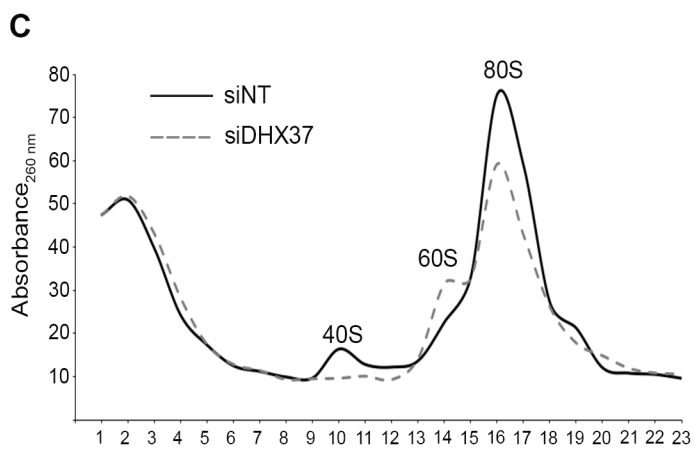
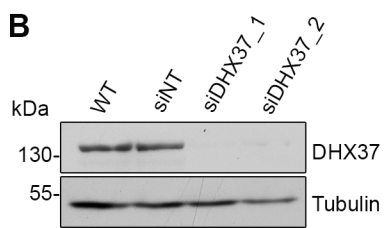
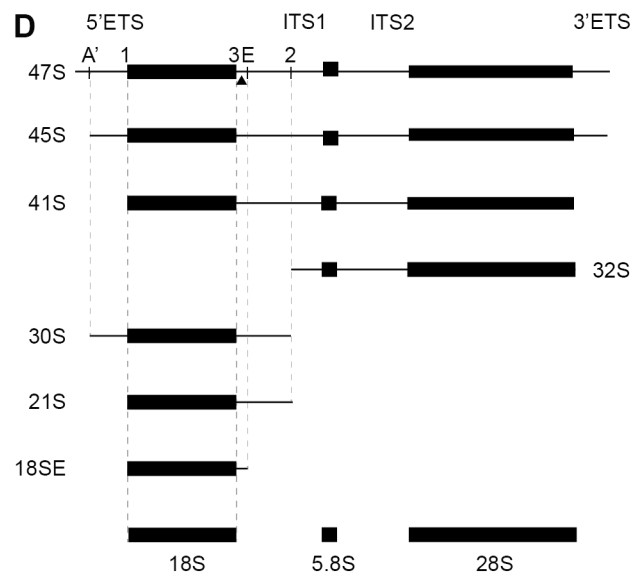
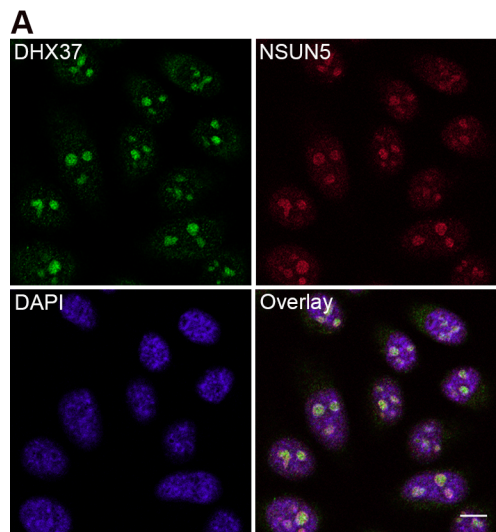
Name	Source
Anti-Flag	Sigma F3165
Anti-DHX37	Bethyl A300-857A
Anti-WBSCR22	Abgent AP20254b
Anti-NSUN5	Santa Cruz Sc-376147
Anti-DIMT1L	Sigma HP042944
Anti-TSR1	Proteintech 16887-1-AP
Anti-UTP14A	Proteintech 11474-1-AP
Anti-WBSCR22	Abgent AP20254b

Supplementary Table 4. Sequences of oligonucleotides used as northern blot probes in this study

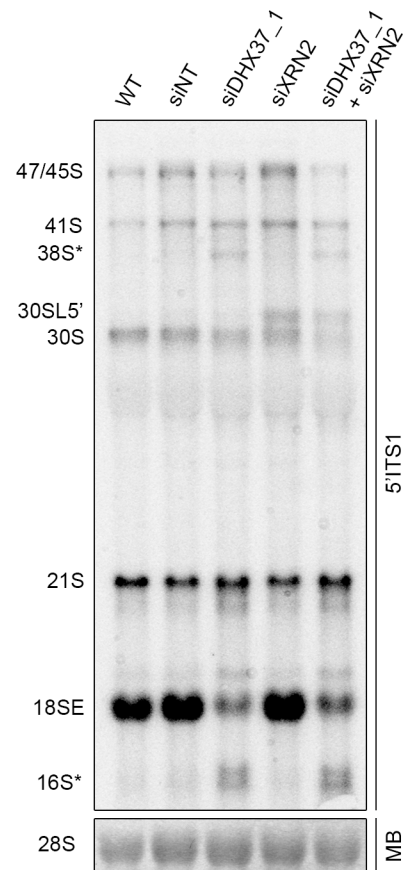
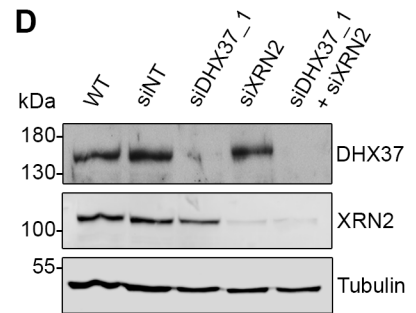
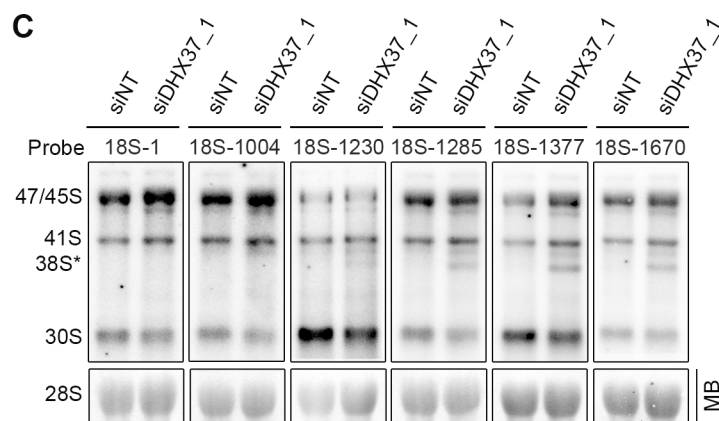
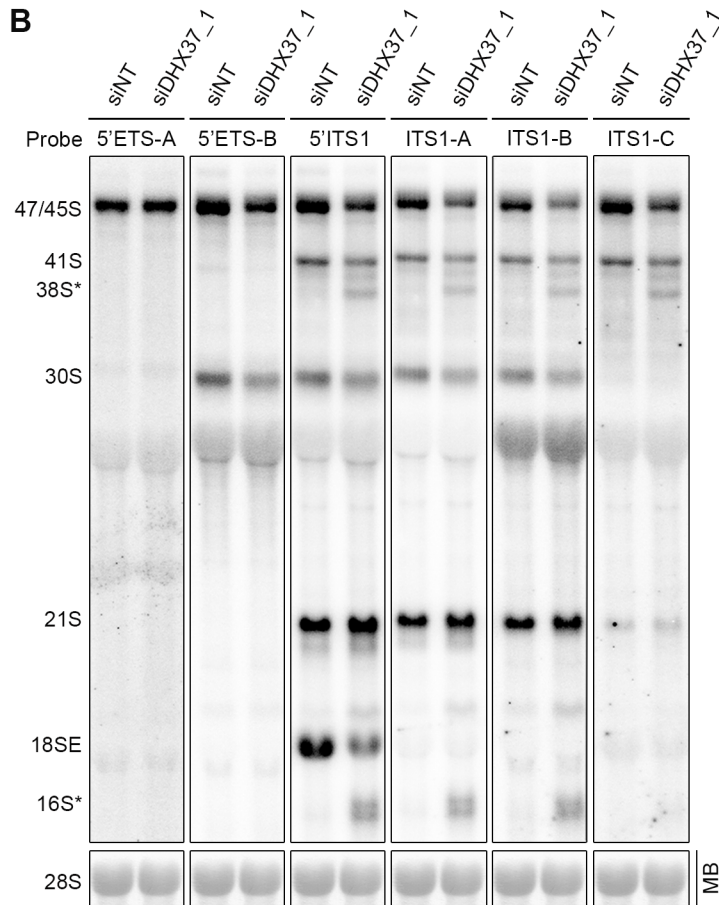
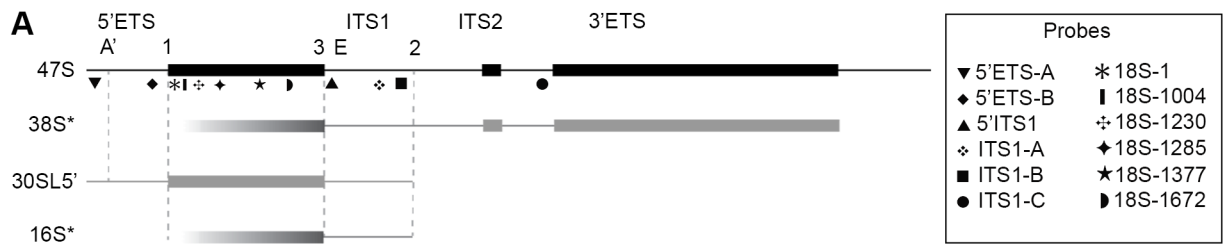
Name	Sequence (5'-3')
U3	GCTCTACACGTTTCAGAGAACTTCTCTAGTAACACACTATAGAAATGATC CC
U8	GTTCTAATCTGCCCTCCGGAAGGAGGAAACAGGAAACAGGTAAGGATTA TCCCACCC
5' ETS-A	CGGAGGCCCAACCTCTCCGACGACAGGTCCGCCAGAGGACAGCGTGTCA GC
5' ITS1	CCTCGCCCTCCGGGCTCCGTTAATGATC
5' ETS-B	GGTAAGGTAGAGCGCGGCGAGCC
ITS1-A	AGGGGTCTTTAAACCTCCGCGCCGGAACGCGCTAGGTAC
ITS1-B	GAGTCCGCGGTGGAG
ITS1-C	GGTTGCCTCAGGCCG
18A_1	CTGGCAGGATCAACCAGGTA
18S_1004	ATTAATGAAAACATTCTTGGCA
18S_1230	GTTGAGTCAAATTAAGCCGCAGG
18S_1285	AGCTATCAATCTGTCAATCC
18S_1377	CATGCCAGAGTCTCGTTCGTTA
18S_1670	CAAAGGGCAGGGACTTAATCAACG

SUPPLEMENTARY REFERENCES

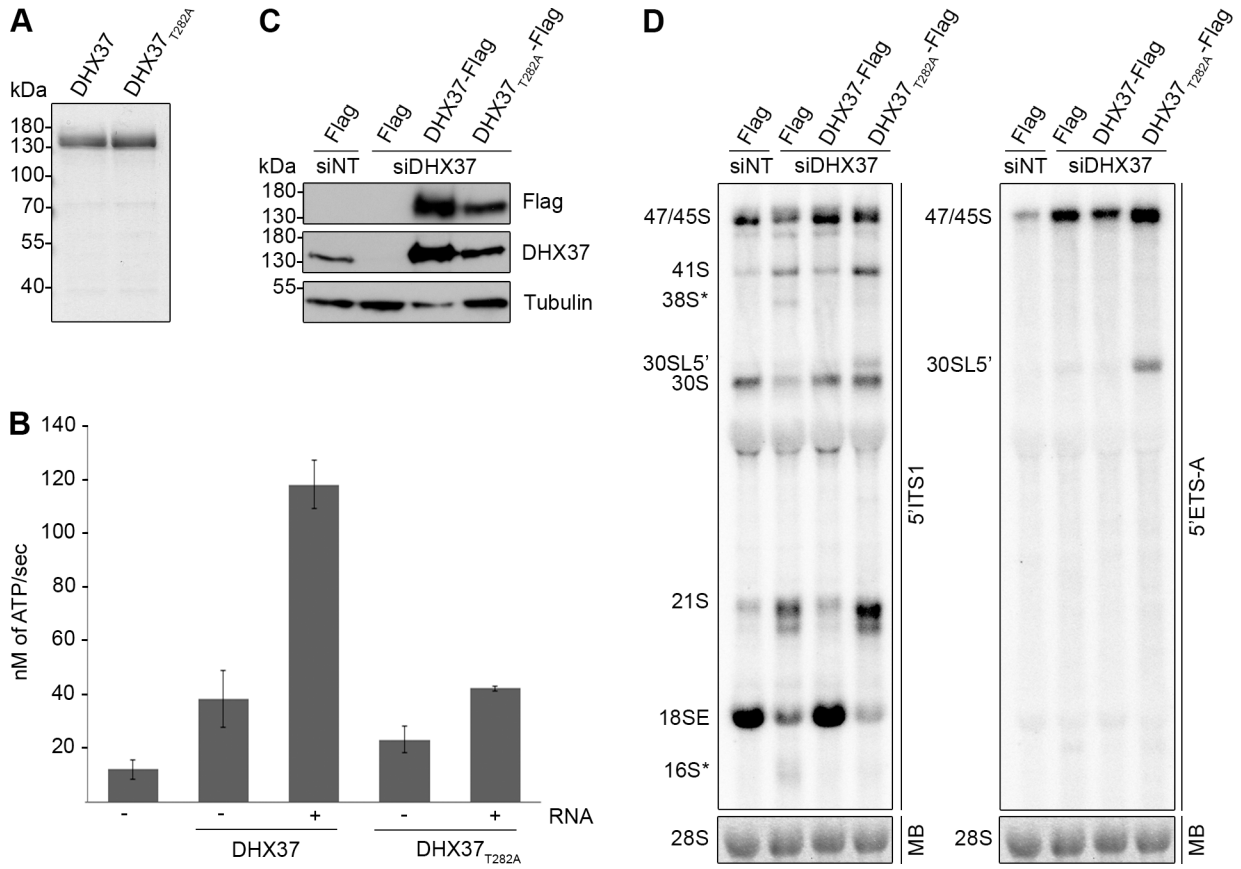
61. Elbashir SM, Harborth J, Weber K, Tuschl T. Analysis of gene function in somatic mammalian cells using small interfering RNAs. *Methods* 2002; 26:199-213.
62. West S, Gromak N, Proudfoot NJ. Human 5' → 3' exonuclease Xrn2 promotes transcription termination at co-transcriptional cleavage sites. *Nature* 2004; 432:522-525.
63. Hu L, Wang J, Liu Y, Zhang Y, Zhang L, Kong R, Zheng Z, Du X, Ke Y. A small ribosomal subunit (SSU) processome component, the human U3 protein 14A (hUTP14A) binds p53 and promotes p53 degradation. *J Biol Chem* 2011; 286:3119-28.



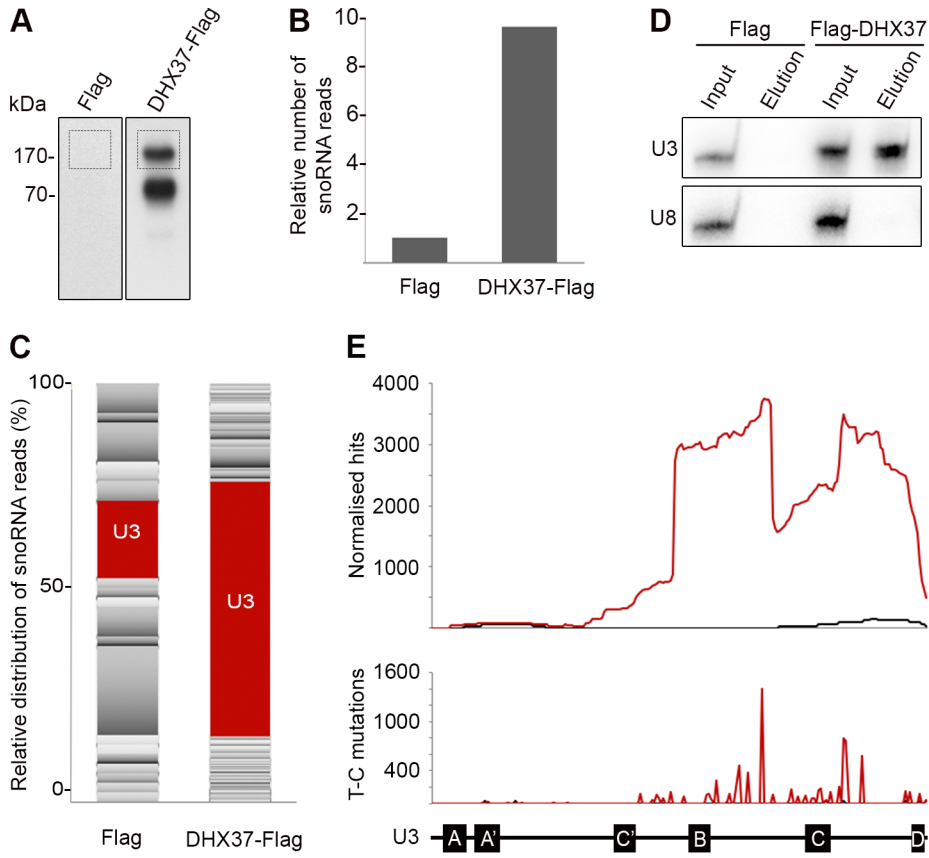
Choudhury et al., Figure 1



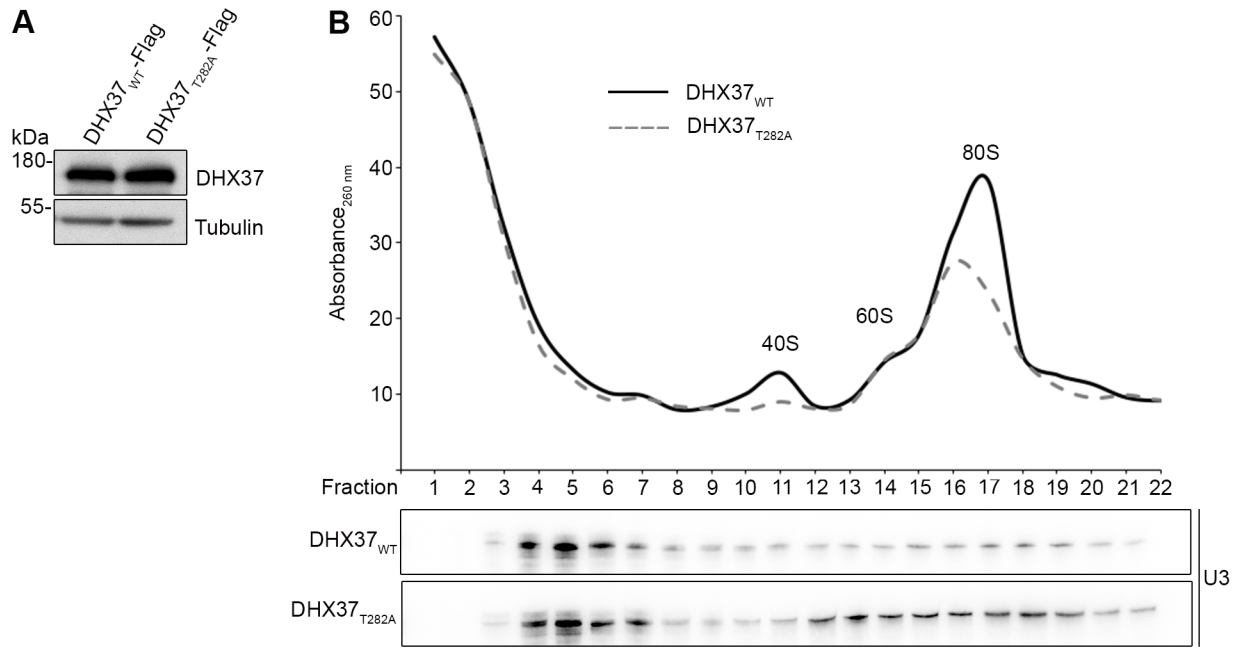
Choudhury et al., Figure 2



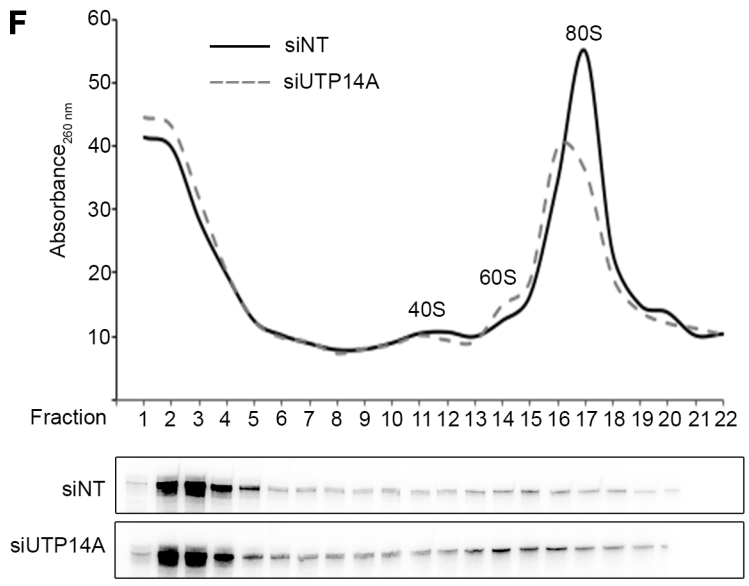
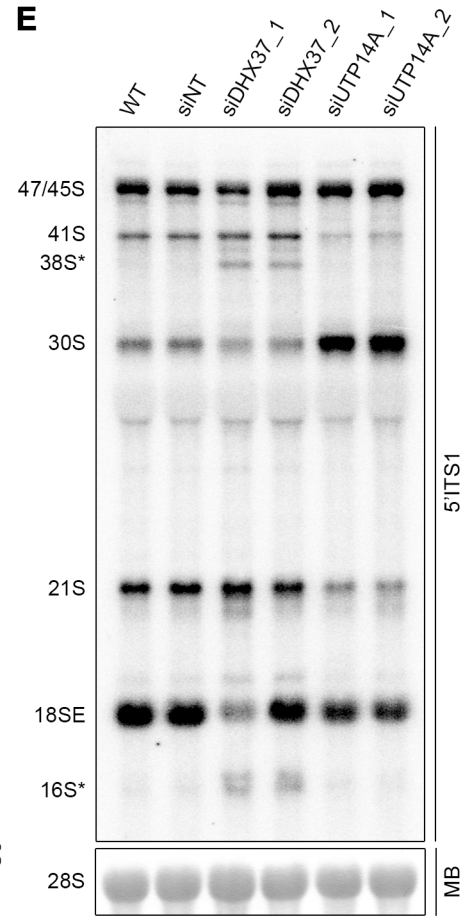
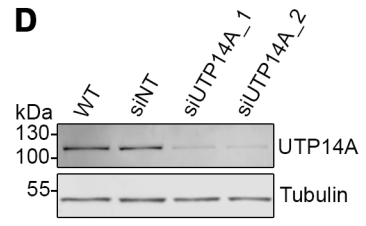
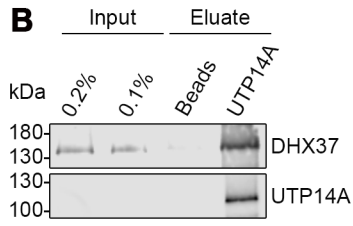
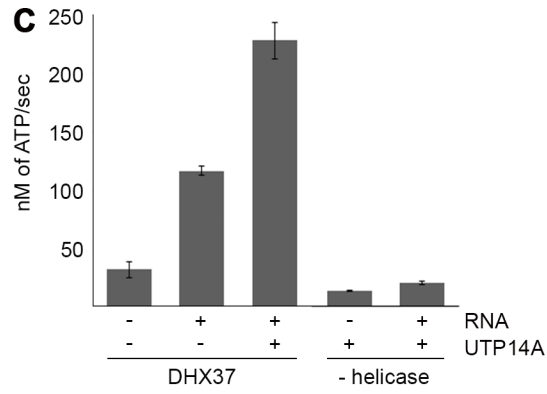
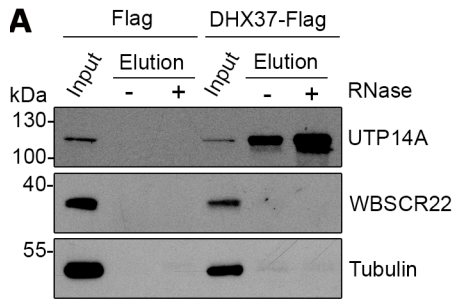
Choudhury et al., Figure 3



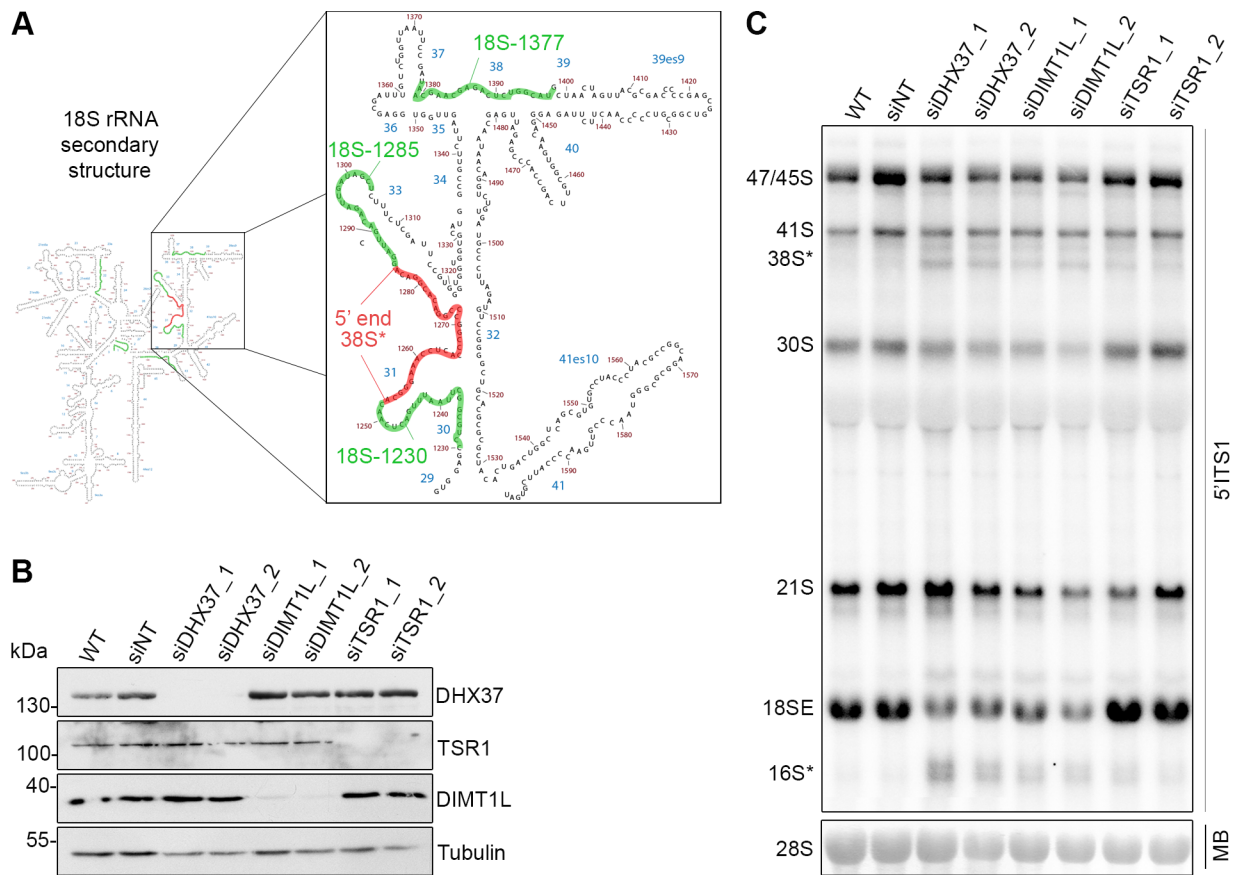
Choudhury et al., Figure 4



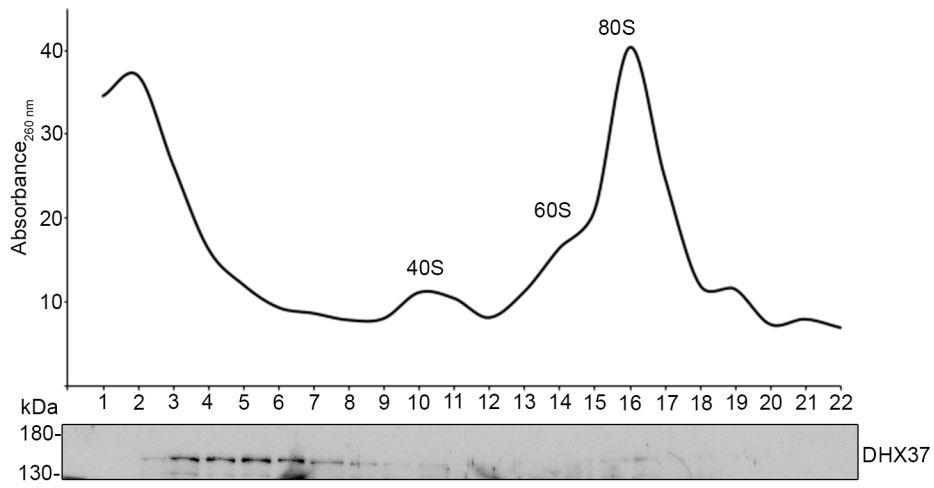
Choudhury et al., Figure 5



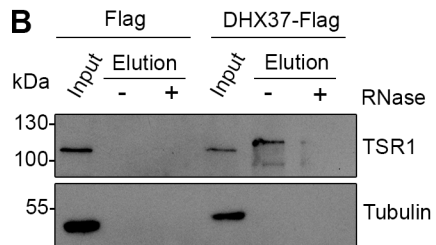
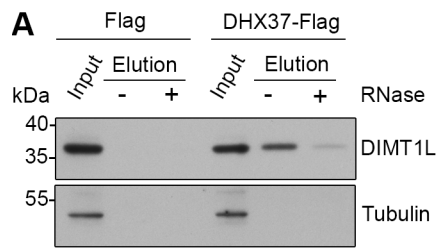
Choudhury et al., Figure 6



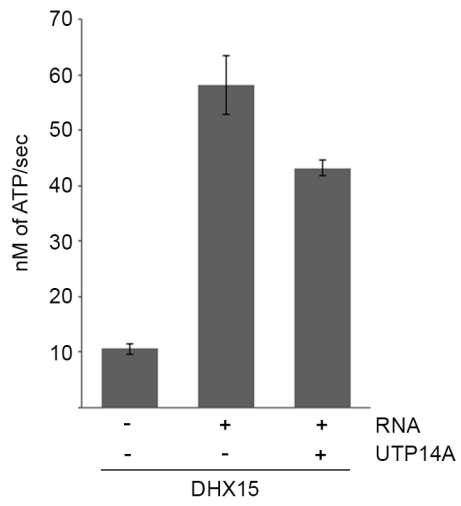
Choudhury et al., Supplementary Figure 1



Choudhury et al., Supplementary Figure 2



Choudhury et al., Supplementary Figure 4



Choudhury et al., Supplementary Figure 5

Chapter Four: The role of DDX55 in human ribosome biogenesis

4.1 Introduction

The eukaryotic ribosome is a large ribonucleoprotein complex, composed of the large and small subunits, 60S and 40S, respectively, which associate in the cytoplasm to form translation-competent 80S ribosomal complexes (Klinge et al., 2012). Ribosome biogenesis is one of the most dynamic and energy consuming processes in the cell with the production of approximately 2000 ribosomes per minute in yeast (Warner, 2001). In mammalian cells, owing to a higher degree of complexity, the number is significantly greater with the ribosome assembly machinery manufacturing approximately 7500 ribosomal subunits per minute (Lewis and Tollervey, 2000). In humans, ribosome assembly initiates in the nucleolus with the RNA polymerase I-mediated synthesis of the 47S pre-rRNA transcript. The primary transcript associates with a subset of ribosomal proteins and *trans*-acting ribosome assembly factors to form 90S pre-ribosomal complexes. An early cleavage within the pre-rRNA separates the precursors of the small and the large ribosomal subunits, which undergo independent maturation steps assisted by a diverse range of factors, for example, ATPase, GTPases, small nucleolar RNAs (snoRNAs) and RNA helicases before nuclear export (Anger et al., 2013; Ben-Shem et al., 2011). In yeast, more than 200 *trans*-acting factors have been identified, which associate with pre-ribosomal complexes and mediate important maturation events such as pre-rRNA folding, processing and structural remodelling (Woolford and Baserga, 2013). As the pathway of ribosomal assembly is conserved to a large extent amongst eukaryotes, homologues of known yeast biogenesis factors are generally expected to play similar roles in humans (Abdelhaleem et al., 2003). Although this appears to be true for a subset of biogenesis factors, a pioneering microscopy-based screen highlighted interesting differences in the assembly pathways of human and yeast ribosomal subunits (Wild et al., 2010). Furthermore, analysis of pre-rRNA processing defects due to RNAi-mediated depletion of putative ribosomal assembly factors identified 74 assembly factors in humans that lack homologues in yeast (Tafforeau et al., 2013). Proteomic analysis of nucleolar morphology and number have further contributed to the growing list of assembly factors in humans with no known yeast homologues (Ahmad et al., 2009; Andersen et al., 2002; Farley-Barnes et al., 2018). Therefore, the emergence of novel biogenesis factors in humans having additional or different roles than their yeast counterparts necessitates detailed characterization of the human ribosome assembly pathway.

RNA helicases are RNA-dependent NTPases that play key roles in mediating structural remodelling events during ribosome production (Martin et al., 2013). In yeast, 21 RNA helicases are known to associate transiently with pre-ribosomal complexes of which several (e.g. Prp43, Has1, Rok1, Dhr1) have been implicated in modulating snoRNA association with pre-ribosomal intermediates (Bohnsack et al., 2008, 2009; Martin et al., 2013; Sardana et al., 2015). Additionally, others (e.g. Prp43, Has1, Spb4, Mak5) have been shown to facilitate incorporation of ribosomal proteins/biogenesis factors and promote structural remodelling of pre-ribosomal subunits (Brüning et al., 2018; Dembowski et al., 2013; Pertschy et al., 2009). Detailed molecular characterization of several yeast RNA helicases has revealed that they fulfil similar roles in humans. For example, in humans, DHX37 (Dhr1) and SK2L2 (Mtr4) perform similar functions as their yeast counterparts (Choudhury et al., 2019; Schilders et al., 2007). However, RNA helicases have emerged to play additional or novel roles during human ribosome biogenesis. For instance, DHX15, in humans, has been implicated in the processing of metazoan-specific A' site (Memet et al., 2017) but does not seem to be required for late-stage processing events of 18S rRNA (Sloan et al., 2019). In contrast, its yeast homologue Prp43, in addition to its role in snoRNA release during pre-60S biogenesis, is involved in the cytoplasmic maturation phase of the 18S rRNA (Pertschy et al., 2009). Additionally, in humans, the DEAD-box helicase DDX51 is implicated in the release of U8 snoRNA from pre-rRNA subunits. Notably, DDX51 displays a high degree of homology with yeast DEAD-box protein Dbp6, although there is no yeast counterpart of U8 snoRNA suggesting that DDX51 might have acquired additional roles in higher eukaryotes (Srivastava et al., 2010). Likewise, the DEAD-box helicase eIF4AIII and its yeast orthologue Fal1, are implicated in SSU biogenesis. Moreover, in humans, eIF4AIII is also a major component of the EJC suggesting the acquisition of additional metazoan-specific function in the context of pre-mRNA splicing (Alexandrov et al., 2011). Recent reports have provided insights into the role of RNA helicases such as DDX21 with no known yeast homologues (Sloan et al., 2015). Genome-wide screens have suggested that RNAi-mediated depletion of several RNA helicases lead to impaired pre-rRNA processing during ribosome biogenesis (Tafforeau et al., 2013), however, the precise functions of many of these helicases are yet to be established.

In yeast, the DEAD-box helicase Spb4 associates with precursors of the large ribosomal subunit, promoting structural re-arrangement and has been implicated in the association of large subunit export adaptor, Arx1 (Brüning et al., 2018). Based on its homology to Spb4, DDX55 is anticipated to play a key role in ribosome biogenesis in humans, however, the precise role of DDX55 remains to be elucidated. Although the process of ribosome biogenesis is generally conserved amongst eukaryotes, growing evidence has highlighted

the different and/or additional roles of RNA helicases during biogenesis. Here, we aim to characterize DDX55 in humans and understand its function during ribosome assembly.

4.2 Material and Methods

4.2.1 Chemicals

Chemicals used in this study were purchased from Carl Roth GmbH & Co., AppliChem GmbH and Sigma-Aldrich Chemie GmbH unless stated otherwise.

All enzymes were purchased from Thermo Fischer Scientific or New England Biolabs. DNA and RNA oligonucleotides were supplied by Sigma-Aldrich and IDT, respectively.

4.2.2 Plasmids

Table 1 Plasmids used in this study

ID	Construct	CDS	Vector	Source
p1698	ZZ-DDX55-His ₇	NM_020936.3	pQE80 (A15)	This study
p1700	ZZ-DDX55 _{T60A} -His ₇	NM_020936.3	pQE80 (A15)	This study
p1699	ZZ- DDX55 _{ΔC-term} -His ₇	NM_020936.3	pQE80 (A15)	This study
p1019	DDX55-His ₆ -2xFlag	NM_020936.3	pcDNA5/FRT/TO	Bohnsack lab
p1702	DDX55 _{ΔC-term} -His ₆ -2xFlag	NM_020936.3	pcDNA5/FRT/TO	This study
p187	His ₆ -2xFlag	-	pcDNA5/FRT/TO	Bohnsack lab

4.2.3 Oligonucleotides

Table 2 Oligonucleotides used in this study

Name/Constructs	Forward/ reverse primer sequence (5'-3')	Application
ZZ-DDX55-His ₇	ATATATTCATGAGAATGGAGCATGTGACAGAGG	Cloning
	ATATATGGATCCGCAGTCATCTTCCAAATCTG	
ZZ- DDX55 _{ΔC-term} -His ₇	ATATATTCATGAGAATGGAGCATGTGACAGAGG	Cloning
	ATATATGGATCCGTCCGCTGTGTTTCTCTGGG	
ZZ-DDX55 _{T60A} -His ₇	CGGTCACAGGTAGTGGCAAAGCGCTCGCTTTTGTCATCC	Site-directed-mutagenesis
	GATGACAAAAGCGAGCGCTTTGCCACTACCTGTGACCG	
DDX55 _{ΔC-term} -His ₆ -2xFlag	ATATGGATCCACCATGGAGCATGTGACAGAGG	Cloning
	ATATGGCTAGCGCAGTCATCTTCCAAATCTG	

DDX55_seq	GAGGCAAGCATCAACACCATTCTG	Sequencing
-----------	--------------------------	------------

4.2.4 Small Interfering RNAs (siRNAs)

Table 3 siRNAs used in this study

Name	Sense sequence (5'-3')	Reference
siNT (non-target)	UCGUAAGUAAGCGCAACCC(dTdT)	Elbashir et al., 2001
DDX55_1	CAGUCUUGGAGUAGUCUAA(dTdT)	Tafforeau et al., 2013
DDX55_2	GGAGUUCCGCAAAUUGCAA(dTdT)	Tafforeau et al., 2013
DDX55_3	CCGACACGAUCCAUUUAA (dTdT)	Qiagen
DDX55_4	AGAGGGUUCUGAUAUUGAA(dTdT)	Qiagen

4.2.5 Antibodies

Table 4 Antibodies used in this study

Name	Company
Flag	Sigma-Aldrich
Tubulin	Sigma-Aldrich
IRDye 800 Donkey anti-rabbit	LI-COR
IRDye 680 Donkey anti-mouse	LI-COR
Goat-anti-mouse-Alexa594	Jackson ImmunoResearch
Goat-anti-rabbit-Alexa488	Jackson ImmunoResearch

4.2.6 Molecular Cloning

4.2.6.1 Amplification of gene of interest

To perform molecular cloning, standard recombinant DNA procedures were followed (Sambrook and Russell, 2001). In brief, the sequence of interest was amplified from HeLa cDNA or from a pre-existing template using specific primers. The PCR reaction components and conditions are summarized in Table 5.

Table 5 PCR components and amplification protocol

PCR reaction components		PCR amplification protocol		
5X HF Buffer	10 μ l	98°C (denaturation)	2 min	x 1
dNTPs (10 mM)	1 μ l	98°C (denaturation)	30 sec	x 35
Template DNA	2 μ l	58°C (annealing)	40 sec	
Forward Primer (10 mM)	1 μ l	72°C (elongation)	1 min/kb	
Reverse Primer (10 mM)	1 μ l	72°C (elongation)	10 min	x 1
Phusion Polymerase	1 μ l	4°C	Pause	-

10% of the PCR products were loaded on a 1% (w/v) agarose gel after resuspension in 6X DNA loading dye (0.2 % xylene cyanol, 0.2 % bromophenol blue, 60 % glycerol, 60 mM EDTA) to obtain a final concentration of 1X. The samples were loaded onto a 1% agarose gel containing SafeView DNA stain, and separated at 120 V for 45 min in TAE (40 mM Tris-HCl, 20 mM acetic acid, 1 mM EDTA). After visualisation of product using UV light, if a single product was obtained, the remaining PCR product was purified with NucleoSpin Gel and PCR Clean-Up kit (Machery-Nagel) following the manufacturer's instructions.

4.2.6.2 Restriction digestion and ligation

The purified PCR product (insert) and the vector backbone (2 μ g) were digested in 1X restriction enzyme buffer using 10 U of the appropriate restriction enzymes (Thermo Fischer Scientific), in a final volume of 20 μ l. Reactions were carried out at 37°C for 2 h. Vector dephosphorylation was performed by adding 1 μ l of alkaline phosphatase (Thermo Fischer Scientific) and further incubation for 20 min at 37°C. The digested vector backbone and insert were gel purified using NucleoSpin Gel and PCR Clean-Up kit (Machery-Nagel) following the manufacturer's instructions. Ligation reactions were set up containing 50 ng of vector backbone and a 5-fold molar excess of insert, together with 5 U of T4 DNA ligase in 1X ligation buffer. The reaction was carried out at 16°C, overnight.

4.2.6.3 Transformation of chemically competent *E. coli*

Chemically competent strains of *E. coli*, DH5 α (Thermo Fischer Scientific, amplification of plasmid DNA) or BL21 (DE3) CodonPlus-RIL (Agilent, recombinant protein expression) were used for transformation in this study. The ligation mix, or 100 ng of plasmid DNA, was added to 50 μ l of chemically competent cells and incubated for 20 min on ice. The mixture was then incubated at 42°C for 1 min followed by incubation on ice for 3 min. 800 μ l of Lysogeny Broth (LB) media was added to the mixture, which was further incubated for 1 h at 37°C, shaking. After 1 h, cells were pelleted by centrifugation (1,000 rcf, 3 min) and re-suspended in 50 μ l of LB media and spread on LB-agar plates containing appropriate antibiotics. In case of DH5 α transformed with plasmid harbouring ampicillin resistance, LB-agar plates containing 100 μ g/ml ampicillin were used. For BL21 (DE3) CodonPlus-RIL, LB-agar plates containing 100 μ g/ml ampicillin and 34 μ g/ml chloramphenicol were used. Plates were incubated overnight at 37°C.

4.2.6.4 Plasmid DNA extraction and sequencing

Single colonies from LB-agar plates were inoculated overnight in 4 ml LB media containing the appropriate antibiotic and grown at 37°C while shaking. The following day, cells were pelleted by centrifugation (11,000 rcf, 1 min) and plasmid isolation was carried out with NucleoSpin Plasmid kit (Machery-Nagel) according to manufacturer's protocol. Isolated plasmid DNA (approx. 60 ng) was sent for Sanger sequencing with gene/vector-specific primers to Eurofins Genomics. The obtained results were analysed using DNASTAR Lasergene 10 SeqMan software.

4.2.7 Human cell culture methods

4.2.7.1 Cell culture conditions

HeLa CCL-2 (ATCC) and HEK293 Flp-In T-REx (Thermo Fisher) were cultured in 1X Dulbecco's Modified Eagle Medium (DMEM, Thermo Fischer Scientific) supplemented with 10% foetal bovine serum (FBS, Merck) and 1:100 dilution of penicillin-streptomycin (stock concentration: 5000 U/ml; Thermo Fischer Scientific). Cells were incubated at 37°C with 5% CO₂.

4.2.7.2 Generation of stable cell lines

To generate inducible stable cell lines, HEK293 Flp-In T-REx cells were seeded (250,000 cells/well) in a 6 well plate and two wells were utilized for each cell line. The next day, cells were transfected with a reaction mixture consisting of 1.8 μ g of pOG44 plasmid encoding the Flp recombinase, 0.6 μ g of the appropriate pcDNA5-derived construct along with 91 μ l Opti-MEM (Thermo Fischer) and 9 μ l of X-tremeGENE 9 DNA transfection reagent (Roche).

48 h post transfection, cells were subjected to selection with 82.4 µg/ml Hygromycin B (Applichem) and 10 µg/ml Blastocidin S Hydrochloride (Applichem). After selection, cells were induced with 1 µg/ml tetracycline for 24 h, harvested using trypsin and resuspended in 4X SDS loading dye (200 mM Tris-HCl pH 6.8, 8% SDS, 50 mM EDTA, 4% β-mercaptoethanol, 0.08% bromophenol blue, 40% glycerol). The whole cell lysate was analysed by SDS-PAGE and western blotting.

4.2.7.3 siRNA transfection

HeLa cells were transfected with appropriate siRNAs using lipofectamine RNAiMAX (Thermo Fischer Scientific). 500 µl Opti-MEM was mixed with 50 nM siRNA and 5 µl lipofectamine RNAiMAX in a 6 well plate and incubated for 15 min. This was followed by addition of 100,000 HeLa cells (96 h knockdown) diluted in antibiotic-free media into the well containing the reaction mixture. The plate was gently shaken and incubated for 96 h at 37°C with 5% CO₂.

4.2.7.4 Immunofluorescence

HEK293 stable cell lines (30,000 cells/well) were grown on cover slips coated with 0.01% poly-L-lysine. Expression of the transgene was induced by the addition of 1 µg/ml tetracycline for 24 h. After induction, cells were fixed with 4% paraformaldehyde in PBS for 20 min and washed two times with PBS for 10 min. Cells were first permeabilized using 0.1% Triton X-100 in PBS for 20 min and then blocked with PBS containing 10% FBS (Merck) and 0.1% Triton X-100 for 2 h. Cells were incubated with primary antibodies (anti-Flag antibody and anti-UTP14A antibody (nucleolar marker)) diluted in 10% FBS in PBS for 2 h. The cover slips were washed 3 times, for 10 min each with PBS and subsequently incubated with Alexa Fluor 488-conjugated and Alexa Fluor 543-conjugated secondary antibodies for 1 h. The washing steps were repeated and the cover slips were mounted using VECTASHIELD (Vector Laboratories) containing DAPI for nuclear staining. Cells were analysed by confocal microscopy using a Nikon Eclipse Ti2 microscope.

4.2.7.5 Analysis of pre-ribosomal complexes by sucrose density centrifugation

HEK293 cells stably expressing full length DDX55 and DDX55_{ΔC-term} were grown to 70% confluency in 10 cm dishes. 24 h post induction with 1 µg/ml tetracycline, cells were harvested with trypsin and centrifuged for 3 min at 1000 rcf. The cell pellet was resuspended in 0.5 ml lysis buffer (50 mM Tris-HCl pH 7.4, 100 mM NaCl, 5 mM MgCl₂ and 1 mM DTT) supplemented with cOmplete, EDTA-free protease inhibitor (1 tablet per 3 ml lysis buffer, Roche). Cells were lysed by sonication using an amplitude of 20% (0.3 sec on, 0.7 sec off, 3x20 pulses). The lysate was cleared by centrifugation at 20,000 rcf for 20 min at 4°C and

10% of the total sample was reserved as input. A 10-45% sucrose gradient was used to separate ribosomal particles based on their densities. To prepare the sucrose gradients, 10% (w/v) sucrose solution was layered on top of 45% (w/v) sucrose solution and mixed using a gradient master (BioComp) protocol with the following settings: angle: 82°, speed: 19, rotation time: 1 min 25 sec. The gradient was then allowed to rest for 1 h at 4°C. Next, the cleared whole cell extract was loaded onto the prepared gradient and centrifuged at 23,500 rpm for 16 h at 4°C in a Beckman Coulter SW-40Ti rotor. After the overnight centrifugation step, gradients were fractionated into 530 µl samples. RNA profiles were generated by measuring the RNA content of each fraction at 254 nm using a NanoDrop ND-2000c (Thermo Fischer Scientific). Proteins in each fraction were precipitated by addition of TCA to a final concentration of 20%. The samples were thoroughly mixed by vortexing and incubated for 20 min on ice followed by centrifugation at 20,000 rcf for 20 min at 4°C. The supernatants were discarded and the pellets were washed with cold acetone, air dried and resuspended in 75 µl water and 25 µl of 4x SDS loading dye (8% SDS, 200 mM Tris-HCl pH 6.8, 4% 2-mercaptoethanol, 50 mM EDTA, 0.08% bromophenol blue and 40% glycerol).

4.2.8 RNA-based methods

4.2.8.1 RNA extraction

For a 6 well-plate of HeLa CCL2 or HEK293 cells, media was first removed from the wells, followed by a brief PBS wash to remove residual media. 500 µl of TRI-reagent (Sigma-Aldrich) was added directly onto the cells and the cell suspension was pipetted several times before transferring to a 1.5 ml tube. 100 µl chloroform was added to the mix and the sample was vortexed thoroughly for 2 min then incubated for 2-3 min before centrifugation at 20,000 rcf for 20 min at 4°C. The aqueous phase containing RNA was transferred to a new tube and was mixed thoroughly with equal volume of isopropanol. The mixture was incubated for 2-3 min at room temperature before centrifugation at 20,000 rcf for 20 min at 4°C to precipitate the RNA. The precipitated RNA pellet was washed with 75% ethanol, air dried and resuspended in 20 µl water to obtain a concentration of approximately 3 µg/µl.

4.2.8.2 Pulse chase metabolic labelling of newly synthesised RNA and northern blotting

siRNA-treated cells were grown in phosphate-free DMEM for 1 hour followed by a media exchange with phosphate-free DMEM supplemented with 15 µCi/mL [³²P]-labelled orthophosphate. Cells were further grown for 1 h. After incubation, the labelled media was removed, cells were washed with PBS and phosphate-containing DMEM was added into wells. Cells were harvested at specific time points (30 min, 60 min, 120 min, 180 min, 240

min) and total RNA was extracted. RNA samples were mixed with 5 volumes of glyoxal loading dye (72 ml DMSO, 24 ml glyoxal, 14.4 ml BTPE (10X), 7.2 ml 80% glycerol, 20 µg/ml ethidium bromide) and incubated for 1 h at 55°C. The samples were loaded onto a 1.2% agarose gel in 1X BTPE (10 mM PIPES, 30 mM Bis-Tris, 1 mM EDTA) and were separated for 16 h at 60 V. The gel was washed with 0.1 M NaOH for 20 min, followed by two washes of 15 min each with 0.5 M Tris-HCl pH 7.4 and 1.5 M NaCl. After a final washing step for 20 min with 6X SSC buffer (900 mM NaCl, 90 mM sodium citrate), RNA is transferred to Hybond-N membrane (GE-Healthcare) by capillary blotting. After transfer, RNA samples were crosslinked to the membrane at 254 nm with 2 cycles of 240 mJ/cm² in a Stratalinker UV Crosslinker (Stratagene) and the membrane containing labelled RNAs were then exposed to a phosphorimager screen (GE-Healthcare) and signals were detected with Typhoon FLA 9500 (GE-Healthcare). Northern blotting was carried out to detect actin mRNA which served as loading control. The membrane was pre-hybridized for 40 min with SES1 (0.25 M sodium phosphate pH 7.0, 7 % SDS, 1 mM EDTA) prior to incubation with 5' [³²P]-labelled DNA oligonucleotides. To prepare the labelled probes, 20 pmol of DNA oligonucleotide was incubated together with 10 U T4 polynucleotide kinase (Thermo Fisher Scientific) and 25 µCi [³²P]-ATP (PerkinElmer) in 1X T4 polynucleotide kinase buffer (Thermo Fisher Scientific). The mixture was incubated at 37°C for 30 min prior to its addition to the tube containing the membrane along with SES1. The labelled probe was incubated with the membrane overnight at 37°C. Next, the membrane was washed first with 6X SSC followed by 2X SSC + 0.1% SDS for 30 min each at 37°C. The dried membrane was then exposed to a phosphorimager screen and detected as above.

4.2.8.3 Crosslinking and analysis of cDNA

HEK293 stable cell lines expressing DDX55-Flag or the Flag-tag alone were induced with 1 µg/ml with tetracycline for 24 h followed by *in vivo* crosslinking (1.5×10^8 cells/ sample) at 254 nm with 2400 mJ/cm². Cells were harvested by addition of 200 µl of TNM150 buffer (50 mM Tris-HCl pH 7.8, 150 mM NaCl, 1.5 mM MgCl₂, 5 mM β-mercaptoethanol, 0.1% NP-40) supplemented with cComplete, EDTA-free protease inhibitor (Roche) and lysed by sonication using an amplitude of 40% (0.5 sec on, 0.5 sec off, 3x15 pulses). The lysate was cleared by centrifugation at 20000 rcf for 15 min at 4°C. The cleared lysate was incubated with 50 µl of pre-equilibrated anti-Flag M2 magnetic beads (Sigma Aldrich) for 2 h. Next, the beads were washed twice with TMN1000 buffer (50 mM Tris-HCl pH 7.8, 1000 mM NaCl, 1.5 mM MgCl₂, 5 mM β-mercaptoethanol, 0.1% NP-40) and three times with TNM150 buffer. Elution of bound RNA-protein complexes was carried out overnight at 4°C by addition of TMN150 buffer supplemented with 250 µg/ml Flag peptide (Sigma-Aldrich). Next, elutes were treated

with 0.1 U RNase-It (Agilent) and samples were incubated for 30 sec at 37 °C. The samples were then supplemented with 6 M Guanidinium hydrochloride, 300 mM NaCl and 10 mM imidazole before incubation with 100 µl Ni-NTA slurry pre-equilibrated with WB1 (50 mM Tris-HCl pH 7.8, 300 mM NaCl, 0.1% NP-40, 6 M guanidine hydrochloride, 10 mM imidazole, 5 mM β-mercaptoethanol) for 2 h at 4°C. The beads were washed twice with WB1 followed by three times with PNK buffer (50 mM Tris-HCl pH 7.8, 10 mM MgCl₂, 0.5% NP-40, 5 mM β-mercaptoethanol). Dephosphorylation was carried out with 8 U of TSAP (Promega) in PNK buffer for 30 min at 37°C and then the beads were washed once with WB1 and three times with PNK buffer. On-bead ligation of the Illumina RA3 3' adapter was carried out in PNK buffer containing 1 µM RA3 3' adapter, 800 U T4 RNA ligase II deletion mutant (Epicentre), 60 U RNasin (Promega) and 10 % PEG8000 (Sigma-Aldrich) at 16°C, overnight. The beads were washed as described before and radioactive labelling of the 5' ends of RNAs fragment was carried out. Phosphorylation was performed for 40 min, at 37°C with 80 U T4 PNK (NEB) and 40 µCi [³²P]-ATP, followed by addition of 1.25 mM ATP-lithium salt (Roche) and incubation for an additional 20 min. The samples were washed with WB1 and PNK buffer as before and 5' linker ligation was carried out overnight at 16°C. The reaction was carried out in PNK buffer containing 1.25 µM RA5 (N5) 5' linker, 40 U T4 RNA Ligase 1 (NEB) and 1 mM ATP. The samples were washed with WB2 (50 mM Tris pH 7.8, 50 mM NaCl, 10 mM imidazole, 0.1% NP-40, 5 mM β-mercaptoethanol) and the RNA-protein complexes were eluted by WB2 containing 150 mM imidazole. The samples were subjected to TCA precipitation (as described in 4.2.7.5) and separated on a 4-12% NuPAGE gel (Thermo Fischer Scientific) before transfer onto Hybond C membrane (Amersham). Radioactive signals were detected by autoradiography. Segments of the membrane carrying the radiolabelled RNA fragments were excised and RNAs were eluted from the membrane by incubating the membrane with WB2 supplemented with 1% SDS and 5 mM EDTA overnight at 55°C. RNA was extracted by addition of phenol:chloroform:isoamylalcohol (25:24:1) and 0.3 M sodium acetate pH 5.2. The samples were centrifuged at 20000 rcf for 5 min at RT. RNA was precipitated from the upper layer by addition of 20 µg glycogen and 3 volumes of 100% ethanol. The samples were incubated at -20°C overnight. Next, the samples were centrifuged at 20,000 rcf for 20 min at 4°C, and RNA pellet was washed with 70% ethanol and air dried. The pellet was resuspended in 1 µl RTP primer (10 mM), 2 µl dNTP mix (5 mM) and reverse transcription was carried out using Superscript III (Invitrogen) according to manufacturer's protocol. Next, PCR reactions were performed using 1 µl of the above reaction along with 1x LA Tag buffer + MgCl₂, 0.2 µM RPI (Illumina forward index primer), 0.2 µM RP1 (Illumina general reverse primer), 2.5 U TakaRa La Taq (Clontech) and 1.25 mM dNTPs. The PCR reaction conditions are summarized in

Table 6. The DNA was precipitated using 0.3 M sodium acetate pH 5.2 and 3 volumes of 100% ethanol as described above. The pellet obtained was resuspended in 1x gel loading dye (Qiagen) and the PCR products were separated on a 3% Metaphore agarose gel (Lonza) in 1x TBE. The PCR product was purified from the gel after excision using the MinElute gel extraction kit (Qiagen) according to manufacturer's protocol. The DNA concentration was determined using a Qubit Fluorometer (Thermo Fischer Scientific) and the cDNA library was subjected to Illumina deep sequencing. TestCRAC as well as full CRAC experiments and bioinformatics analyses have been performed in collaboration with Philipp Hackert and by Jens Kretschmer, respectively.

Table 6 PCR reaction conditions for CRAC

PCR reaction components		
95°C (denaturation)	2 min	x1
98°C (denaturation)	30 sec	x 40
60°C (annealing)	40 sec	
68°C (elongation)	40 sec	
72°C (elongation)	5 min	x 1

4.2.9 *In vitro* assays

4.2.9.1 Recombinant protein expression and purification

BL21 (DE3) CodonPlus-RIL strain of *E.coli* was transformed (4.2.6.3) with the plasmid of interest for recombinant protein expression. Single colonies were then grown in LB media overnight at 37°C to obtain stationary phase cultures. The following day, the overnight cultures were used to inoculate 1 l LB cultures, such that the O.D600 was 0.1. Cultures were grown at 37°C until an O.D600 of 0.6 was reached, indicative of an exponential growth phase. For induction of recombinant protein expression, 1 mM IPTG was added and cultures were further grown for 16 h at 18°C. The following day, cultures were harvested by centrifugation at 6,000 rcf for 20 min at 4°C. All subsequent purification steps were done on ice. The cell pellet was washed once with PBS before resuspension in 10 ml lysis buffer (50 mM Tris-HCl pH 7.0, 500 mM NaCl, 1 mM MgCl₂, 10% glycerol, 1 mM imidazole, 1 mM PMSF). For cell lysis, cells were sonicated for 30 sec, 4 cycles with an amplitude of 45%. Next, the lysate was cleared by centrifugation at 50,000 rcf for 20 min at 4°C. polyethyleneimine (PEI) was added to the clear lysate to a final concentration of 0.05% and further incubated for 15 min at 4°C. The lysate was again centrifuged at 50,000 rcf for 30

min at 4°C to precipitate nucleic acids. The lysate was then added to pre-equilibrated (with wash buffer I) cComplete His-tag purification resin (Roche) and incubated for 2 h. After incubation, the beads were washed with 10 ml wash buffer I (50 mM Tris-HCl pH 7.0, 500 mM NaCl, 1 mM MgCl₂, 10% glycerol, 30 mM imidazole). This was followed by a high salt wash with 10 ml wash buffer II (50 mM Tris-HCl pH 7.0, 1000 mM NaCl, 1 mM MgCl₂, 10% glycerol, 30 mM imidazole) followed by a final wash with 10 ml wash buffer I. Bound proteins were eluted with elution buffer (50 mM Tris-HCl pH 7.0, 500 mM NaCl, 1 mM MgCl₂, 10% glycerol, 300 mM imidazole). Elution fractions were spotted on to nitrocellulose membrane and stained with amido black. Protein-containing fractions were identified and pooled together, and glycerol was added to a final concentration of 20%. The protein sample was transferred to SpectraPore dialysis membrane with a cut off of 15 kDa. Dialysis was carried out overnight at 4°C in dialysis buffer (50 mM Tris-HCl pH 7.0, 150 mM NaCl, 1 mM MgCl₂, 20% glycerol). The following day, the dialysed protein sample was concentrated to an appropriate volume using a SpinX UF concentrator (Corning) with a molecular cut off of 30 kDa. Protein samples were aliquoted and stored at -80°C.

4.2.9.2 Steady-state ATPase assay

Hydrolysis of ATP was monitored with an NADH-coupled reaction (Kiiianitsa et al., 2003). Reactions were set up containing 1.5 μM protein sample, 45 mM Tris-HCl pH 7.4, 2 mM MgCl₂, 25 mM NaCl, 450 μM NADH, 1.5 mM phosphoenolpyruvate (PEP, Sigma-Aldrich), 4 mM ATP and 20 U/ml pyruvate kinase/lactate dehydrogenase (Sigma-Aldrich) supplemented with 1.5 μM RNA. Hydrolysis of ATP leads to a rise in ADP levels which when converted back into ATP results in the conversion of phosphoenolpyruvate to pyruvate by the action of pyruvate kinase. In the next step, the conversion of pyruvate to lactate by lactate dehydrogenase is concomitantly linked to the oxidation of NADH to NAD⁺. The decrease in absorbance of NADH at 340 nm was measured using a BioTEK Synergy HT microplate spectrophotometer. The rate of ATP hydrolysis was calculated using the following equation:

$$\text{ATPase rate} \left[\frac{\text{ATP}}{\text{min}} \right] = \frac{\frac{dA_{340}}{dt} \left[\frac{\text{OD}}{\text{min}} \right]}{K_{\text{path}} * \text{moles ATP}}$$

Wherein, K_{path} is the molar absorption coefficient for a defined optical path length which is defined as reaction volume (150 μl/well) and background NADH decomposition.

4.2.10 SDS-PAGE and western blotting

Protein samples were analysed by SDS-polyacrylamide gel electrophoresis (SDS-PAGE) following Laemmli's instructions (Laemmli, 1970). Samples were mixed with 4x SDS loading

dye (8% SDS, 200 mM Tris-HCl pH 6.8, 4% β -mercaptoethanol, 50 mM EDTA, 0.08% bromophenol blue and 40% glycerol) and heated at 95°C for 10 min. SDS-PAGE was carried out for 1.5 h with 25 mA/gel in a discontinuous system consisting of different stacking (125 mM Tris-HCl pH 6.8, 3.5 mM SDS) and resolving (375 mM Tris-HCl pH 8.8, 3.5 mM SDS) buffers in a Bio-rad system. The gels were either stained with Coomassie solution (0.1% Coomassie R-250, 10% acetic acid, 40% methanol) or transferred onto nitrocellulose membrane (GE-healthcare) via wet blotting. Proteins were transferred for 1 h at 100 V using a Bio-rad transfer set up in 1X western blotting buffer (25 mM Tris, 192 mM glycine, 0.05 % SDS, 20 % methanol). After transfer, the membrane was incubated for 1 h with blocking solution containing 5% milk in TBS (25 mM Tris-HCl pH 7.4, 137 mM NaCl, 2.7 mM KCl) with 0.1% Tween-20 (TBST-T) in order to avoid unspecific antibody binding to the membrane. After blocking, membrane was incubated with primary antibodies diluted in blocking solution and incubated overnight at 4°C. The membrane was washed three times, 10 min each time with TBST-T followed by incubation for 1 h with secondary antibodies diluted in blocking solution. Membranes were again washed as described above and the proteins were detected using Odyssey CLx imager (Li-COR Biosciences).

4.3 Results

4.3.1 DDX55 is an ATPase and a mutation in its conserved GKT motif inhibits its ATP hydrolysis capacity

In yeast, the DEAD-box helicase Spb4 was recently shown to be involved in ribosome biogenesis (Brüning et al., 2018). Based on its homology to DDX55, we speculated DDX55 to be a putative RNA helicase that may be involved in ribosome biogenesis in humans. Many RNA helicases hydrolyse nucleotide triphosphates (NTPs) in an RNA-dependent manner (Jarmoskaite and Russell, 2014; Linder and Jankowsky, 2011). Hence, we set out to explore if DDX55 is an ATPase. We, therefore, expressed recombinant, His-tagged DDX55 in *E. coli* cells and purified protein for performing *in vitro* ATP hydrolysis assays. In many RNA helicases, a characteristic glycine-lysine-threonine (GKT) sequence in the walker A motif is responsible for RNA binding and ATP hydrolysis. To confirm the specificity of any ATPase activity observed, a mutant form of DDX55 carrying a threonine to alanine substitution in the GKT motif at amino acid position 60 was also expressed and purified (Figure 4.1A).

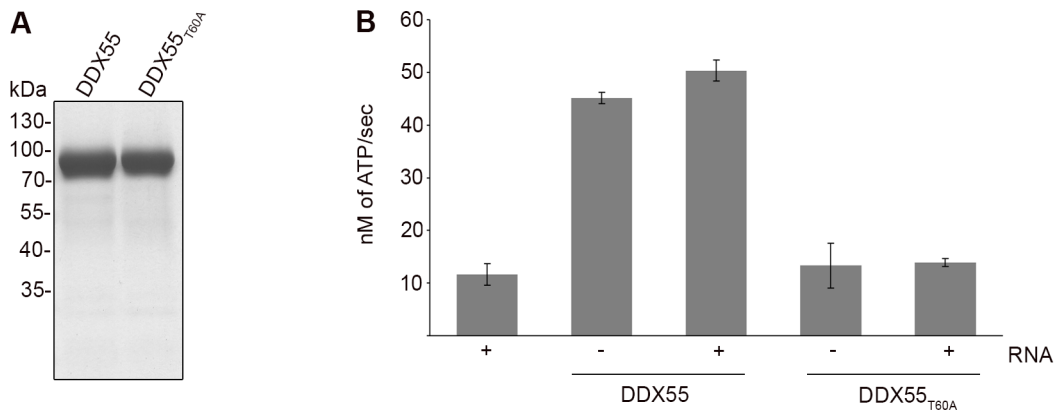


Figure 4.1. DDX55 is an ATPase. (A) ZZ-DDX55-His₇ and ZZ-DDX55_{T60A}-His₇ were expressed in *E. coli* and purified by affinity chromatography. The elution fractions containing protein were dialysed and concentrated. Proteins were separated by SDS-PAGE and visualized by Coomassie staining. **(B)** Rate of ATP hydrolysed by DDX55 and DDX55_{T60A} was determined by monitoring the absorbance at 340 nm. Reactions were carried out in the presence (+) or absence of RNA (-). Experiments were performed in triplicates and error bars represent mean \pm standard deviation.

ATP hydrolysis was then monitored with an NADH-coupled reaction and was performed with DDX55 or DDX55_{T60A} in the presence or absence of RNA. In comparison to the control sample containing no helicase, DDX55 exhibited strong ATP hydrolysis activity even in the absence of an RNA substrate and the addition of RNA resulted in mild stimulation of the ATPase activity. In contrast, the mutant variant of DDX55 only weakly hydrolysed ATP in

the absence of RNA and the addition of RNA into the reaction mixture did not stimulate ATP hydrolysis. This implies that DDX55 is an active ATPase and the T to A substitution within the conserved GKT motif is sufficient to abolish the ATPase activity of DDX55 (Figure 4.1B).

4.3.2 The human helicase DDX55 is required for ribosome biogenesis

4.3.2.1 DDX55 is localised in the nucleoplasm

Having established that DDX55 is an active ATPase, the next objective was to analyse DDX55 *in vivo* and investigate whether it has a role in ribosome biogenesis. First, we determined which sub-cellular compartment DDX55 is present in. Due to lack of a functional DDX55-specific antibody that could be used for immunofluorescence, an inducible HEK293 stable cell line expressing DDX55-Flag was generated and the localisation of Flag-tagged DDX55 was determined using an antibody against the Flag-tag. The SSU biogenesis factor, UTP14A and DAPI were used for visualisation of nucleoli and nuclear material, respectively. The localisation of DDX55 was observed to be predominantly nucleoplasmic and the helicase seemed to be largely excluded from the nucleoli (Figure 4.2), suggesting that DDX55 could be involved in late stages of ribosome biogenesis.

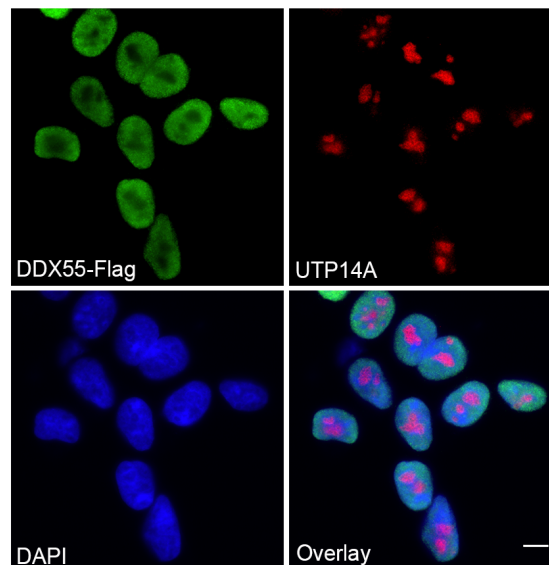


Figure 4.2. DDX55 predominantly exhibits a nucleoplasmic localisation. Expression of DDX55-Flag was induced in a HEK293 stable cell line for 24 h with tetracycline and cells were fixed with 4% paraformaldehyde for immunofluorescence microscopy. The localisation of DDX55 was determined using an antibody against the Flag-tag (green). UTP14A, an SSU biogenesis protein, served as nucleolar marker (red) and the nuclear material was visualized by staining with DAPI (blue). An overlay of images is presented for the purpose of co-localisation analysis. Scale bar represents 10 μm .

4.3.2.2 Depletion of DDX55 *in vivo* impairs ribosome biogenesis

To analyse the potential role of DDX55 in ribosome biogenesis, RNA interference (RNAi) was established using different siRNAs. HeLa cells were either left untreated or were treated with a non-target siRNA (siNT) or siRNAs targeting DDX55 (siRNA1-4). Cells were harvested 72 h after transfection and levels of DDX55 protein were determined using western blotting. In contrast to the cells treated with the non-target siRNA, there was a marked reduction in the DDX55 level upon treatment with siRNAs 1, 2 and 4 against DDX55. Furthermore, siRNA_2 and siRNA_4 were equally efficient in depleting DDX55 and were used for further experiments (Figure 4.3). Tubulin was used as a loading control.

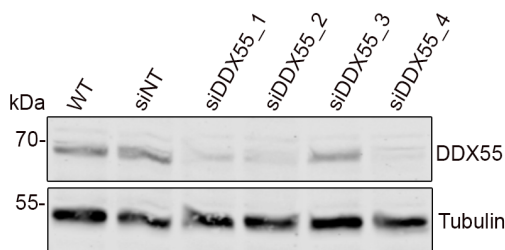


Figure 4.3. siRNA-mediated depletion of DDX55. HeLa cells were transfected with a non-target siRNA (siNT), siRNAs against DDX55 (1-4) or left untransfected (WT) for 72 h. Cells were harvested and proteins were separated by SDS-PAGE and analysed by western blotting with antibodies against DDX55 and tubulin.

Upon RNAi-mediated depletion of DDX55, the levels of newly synthesized (pre-) rRNAs were analysed by pulse-chase labelling. HeLa cells were transfected with non-target siRNA or siRNA targeting DDX55 (siRNA_2 or siRNA_4). After 96 h, cells were first grown in the presence of phosphate-free DMEM followed by growth in the presence of DMEM containing [³²P]-labelled orthophosphate which is incorporated into the nascent RNAs. After 1 h, labelled media were exchanged for DMEM and cells were harvested at specific time points. Extracted total RNA was separated on an agarose gel and transferred to a nylon membrane. The newly-synthesized, labelled rRNAs were detected by a phosphoimager. Steady-state levels of mature 18S and 28S rRNAs were visualized by methylene blue staining. Actin mRNA, which served as a loading control, was detected via northern blotting by using a radiolabelled probe. Depletion of DDX55 led to a marked reduction in the levels of newly synthesized 28S and 18S rRNAs when compared to the levels of actin mRNA. The steady state levels of mature 18S and 28S were also decreased as visualized by methylene blue staining (Figure 4.4). This indicates that loss of DDX55 results in impaired ribosome biogenesis in the cell.

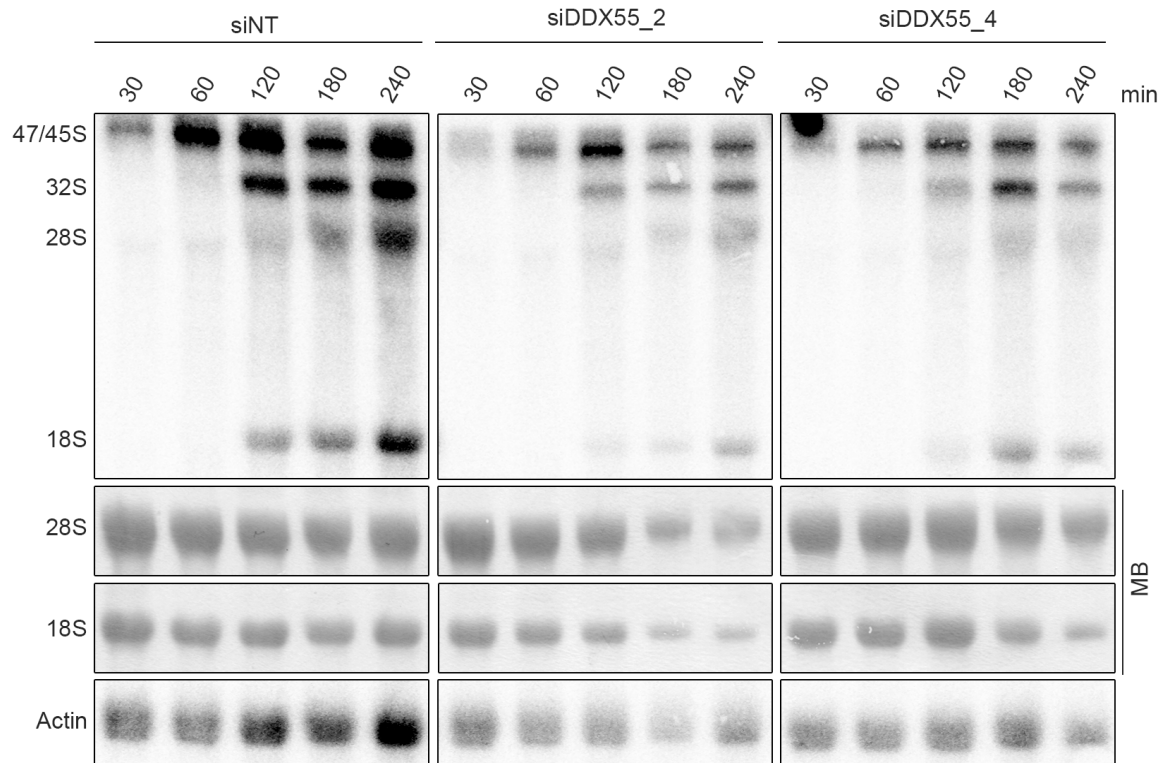


Figure 4.4. siRNA-mediated depletion of DDX55 impairs production of rRNAs. HeLa cells were transfected with a non-target siRNA (siNT) or siRNAs targeting DDX55 (siDDX55_2 and DDX55_4). After 96 h, cells were grown in phosphate-free media for 1 h, followed by growth in media containing [^{32}P]-labelled orthophosphate for labelling nascent RNAs. Labelled media was exchanged with complete DMEM and cells were harvested at specific time points. Total RNA was extracted and separated on 1.2% agarose gel and transferred to a nylon membrane. Nascent, labelled RNAs were detected using a phosphoimager. Steady-state levels of 28S and 18S were visualized by methylene blue (MB) staining. The actin mRNA, which was detected with a specific radiolabelled probe, served a loading control.

4.3.2.3 DDX55 crosslinks to helices 62 and 63 of the 28S rRNA sequence *in vivo*

In order to understand the precise role of RNA helicases in ribosome biogenesis, it is imperative to identify their binding site(s) on target RNAs *in vivo*. Crosslinking and analysis of cDNA (CRAC) was, therefore, employed to reveal the *in vivo* crosslinking site(s) of DDX55 (Bohnsack et al., 2012; Haag et al., 2017). HEK293 cells expressing either Flag-tagged DDX55 or the Flag-tag alone were crosslinked *in vivo* using UV light at 254 nm. After crosslinking, a two-step purification approach was utilized in order to ensure recovery of only RNA sequences, which were specifically bound by Flag-tagged DDX55 or by the Flag-tag. Purification was carried out first under native conditions using an immobilised anti-Flag antibody followed by a Ni-NTA-based purification under denaturing conditions. Crosslinked RNA was partially digested in order to trim away RNA sequences not directly in contact with Flag-tagged DDX55 or the Flag-tag alone and the trimmed RNA fragments were ligated to linkers and labelled with [^{32}P]. After elution, the covalently crosslinked RNA-protein

complexes were separated by denaturing PAGE, transferred to a nitrocellulose membrane and detected by autoradiography (Figure 4.5). RNA was extracted from the regions corresponding to the molecular weight of DDX55, reverse transcribed and PCR amplified to generate a cDNA library, which was utilized for next generation sequencing.

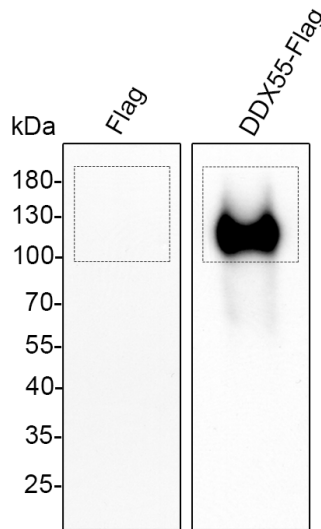


Figure 4.5. DDX55 crosslinks to RNA *in vivo*. HEK293 cells expressing either the Flag-tag control or DDX55-Flag were crosslinked *in vivo* using UV light at 254 nm. RNA-protein complexes were purified under both native and denaturing conditions. After RNase treatment, RNA sequences specifically associated with the protein were ligated to sequencing adaptors and labelled with [32P]. The RNA-protein complexes were eluted and separated by denaturing PAGE. After transfer to a nylon membrane, the labelled RNAs were detected by autoradiography. The regions along the dotted line were excised, RNA extracted and a cDNA library was generated for next generation sequencing.

The reads obtained after Illumina sequencing were bioinformatically mapped to the human genome. There was a prominent enrichment of reads corresponding to ribosomal RNA in the Flag-tagged DDX55 (31%) in comparison to the Flag-tag only (14%) (Figure 4.6), which is consistent with its role in ribosome biogenesis. An increase in the number of reads mapping to tRNA genes was also observed in case of DDX55-Flag (22%) compared to Flag-tag control (3%). However, as no specific tRNA was enriched this likely represents background. As tRNAs are abundant in nature, they are often non-specifically co-purified with RNA-binding protein and have been previously observed to be non-specifically enriched in other CRAC samples.

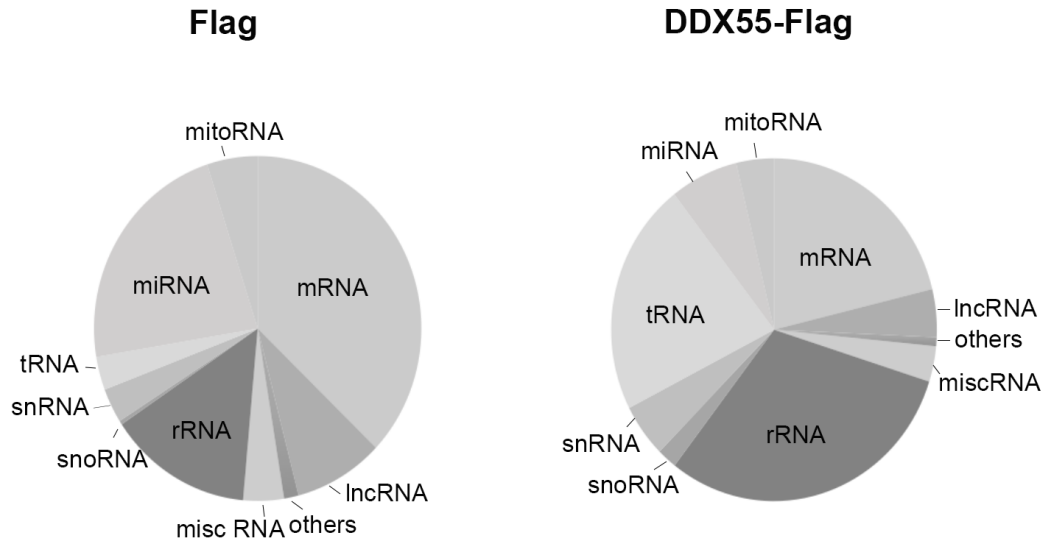


Figure 4.6. Flag-tagged DDX55 enriches ribosomal RNAs. *In vivo* crosslinked protein-RNA complexes were tandem affinity purified under native and denaturing conditions and crosslinked RNAs were partially digested, labelled with [32 P] and ligated to adaptors for generation of a cDNA library. The library was then subjected to Illumina deep sequencing and the reads obtained were mapped to the human genome. Pie charts represent the relative distribution of sequence reads mapping to different classes of RNA. Abbreviations: mRNA, messenger RNA; lncRNA, long non-coding RNA; snoRNA, small nucleolar RNA; snRNA, small nuclear RNA; tRNA, transfer RNA; mitoRNA, mitochondrial RNA; miRNA, microRNA; rRNA, ribosomal RNA; miscRNA, miscellaneous RNA.

As an increase in the number of reads mapping to the rDNA sequence was observed for DDX55, we next wanted to determine the specific crosslinking site within the rRNA. The number of reads at each nucleotide was normalized according to the total number of mapped reads per million and mapped at single nucleotide level on to the rDNA locus encoding the 47S pre-rRNA transcript. Increased accumulation of reads in specific peaks represents a specific crosslinking site for the analysed protein. In comparison to the Flag-tag control, a specific peak was obtained on the 28S rRNA sequence for DDX55, consistent with its role in LSU biogenesis (Figure 4.7).

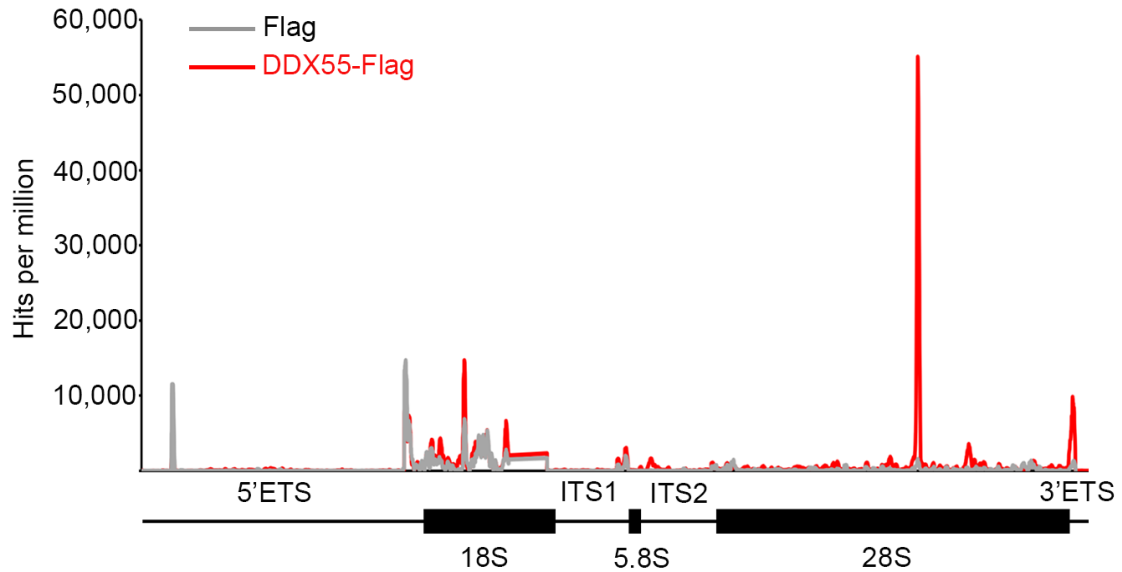


Figure 4.7. DDX55 crosslinks to a specific site within the 28S rRNA sequence. The sequence mapping to rDNA locus encoding the 47S ribosomal RNA transcript are shown. The reads obtained for Flag and DDX55-Flag are depicted in grey and red respectively. A schematic representation of the 47S rRNA is depicted below and wherein the mature rRNA sequences are depicted as rectangles and those of the spacer regions are depicted as lines.

In order to better understand the functional relevance of the distinct crosslinking site obtained, the DDX55-Flag CRAC data were mapped onto the secondary structure of mature LSU RNAs (Petrov et al., 2014). The number of sequence reads mapped to each nucleotide of the LSU RNAs is depicted as a colour gradient, with red representing the highest number of reads normalised to 100%. This revealed that DDX55 preferentially crosslinks to helices 62 and 63 of domain IV within 28S rRNA sequence, in the vicinity of the eukaryotic expansion segment 27 (ES27) (Figure 4.8). Interestingly, in yeast, Spb4 binds to helices 62 and 63 of the 25S rRNA sequence suggesting that the binding site of these helicases is evolutionarily conserved in eukaryotes (Brüning et al., 2018).

Additionally, the DDX55-CRAC data were mapped onto the available tertiary structure of the mature large ribosomal subunit (PDB 4V6X, Anger et al., 2013) in order to visualise the binding site of DDX55 relative to other ribosomal features (Figure 4.9).

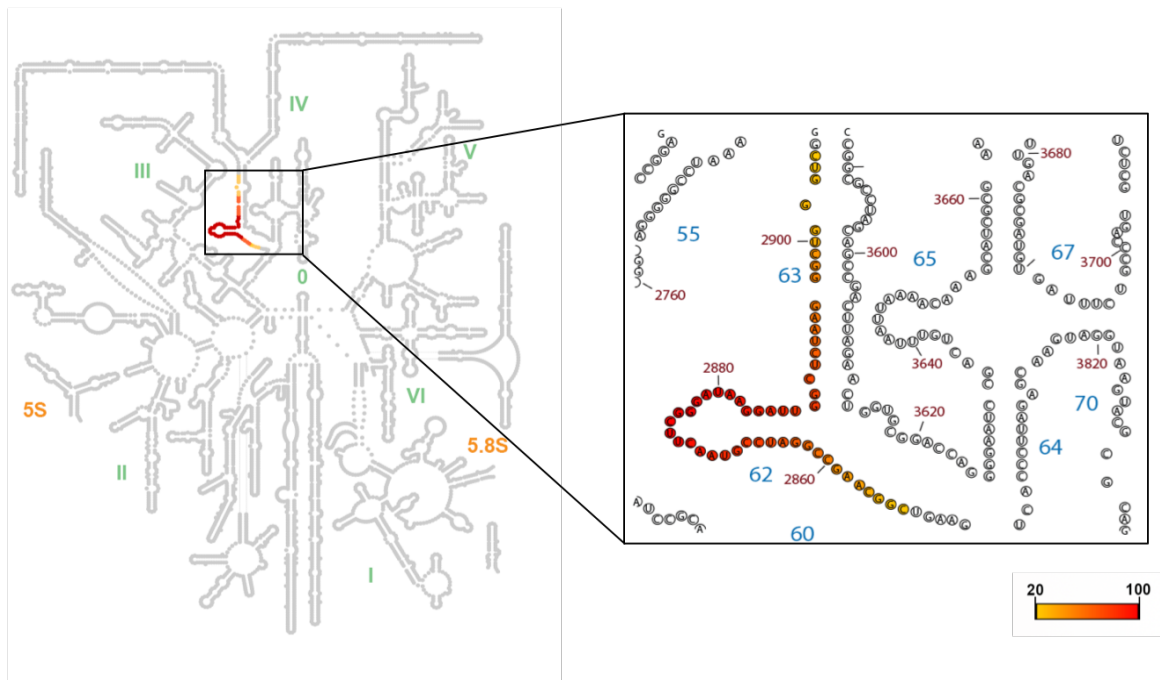


Figure 4.8. DDX55 crosslinks to helices 62 and 63 of the 28S rRNA. The sequence reads obtained for DDX55-Flag CRAC data were mapped on the secondary structure of LSU RNAs. 5S and 5.8S are labelled in brown. Various domains of 28S rRNA is depicted in green. Crosslinking sites are represented as a gradient ranging from yellow (lowest value, 20% above threshold) to red (highest value).

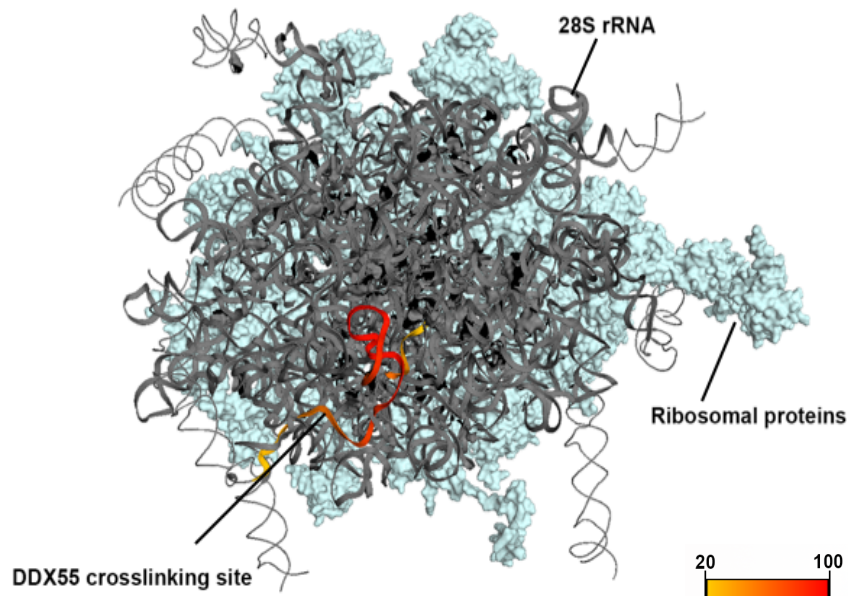


Figure 4.9. DDX55 crosslinks to helices 62 and 63 in domain IV of the 28S rRNA. The sequence reads obtained for DDX55-Flag CRAC data were mapped on the 3D structure of the 28S rRNA. Ribosomal proteins are depicted in blue. Crosslinking sites are represented as a gradient ranging from yellow (lowest value, 20% above threshold) to red (highest value).

4.3.3 C-terminal tail of DDX55 is required for its recruitment to pre-ribosomal subunits

Having established that DDX55 is an active ATPase that associates with pre-ribosomal complexes and is required for their maturation, we further explored the mechanism of DDX55 binding to RNA and its recruitment to ribosomal subunits. Interestingly, detailed sequence characterization revealed clusters of basic amino acid residues localised within the C-terminal tail region of DDX55 (Figure 4.10).

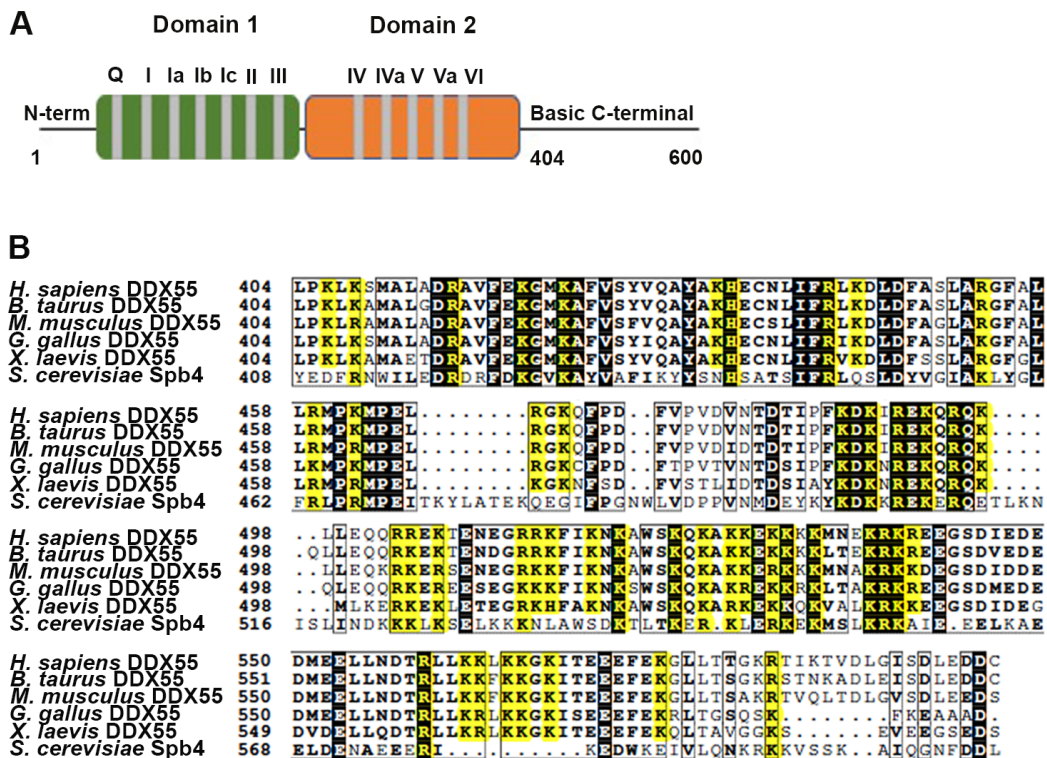


Figure 4.10. C-terminal extension of DDX55 contains conserved basic amino acid residues (A) Schematic representation of primary sequence of DDX55 depicting the two conserved RecA-like domains, domain 1 (green) and domain 2 (orange). Each domain consists of several conserved motifs coloured in grey. The N- and C-terminal extensions are denoted. **(B)** Sequence alignment of amino acid residues from the C-terminal tail region (residues 404-600) is represented from *S. cerevisiae* Spb4 (Uniprot: P25808); *H. sapiens* DDX55 (Uniprot: Q8NHQ9); *B. taurus* DDX55 (Uniprot: Q2NL08); *G. gallus* DDX55 (Uniprot: Q5ZLN8); *M. musculus* DDX55 (Uniprot: Q6ZPL9) and *X. laevis* DDX55 (Uniprot: Q6AZV7). Conserved amino acid are highlighted in black and basic amino acid residues are marked in yellow.

To enable potential functions of the C-terminal tail of DDX55 to be investigated, HEK293 stable cell lines expressing Flag-tagged full-length DDX55 and a C-terminally truncated version of DDX55, consisting of amino acids residues 1 to 403 were generated (DDX55_{ΔC-term}). Previous studies have suggested that basic C-terminal domains can contribute to the recruitment of helicases to their site of action by mediating interactions with RNA. For

example, the predominantly basic C-terminal extension of DEAD-box proteins Mss116 in yeast and CYT-19 in *Neurospora crassa* are involved in facilitating interaction of the helicase with its RNA or RNP targets (Mohr et al., 2008). *In vivo* crosslinking experiments were therefore carried out with cell lines expressing full-length or truncated DDX55 wherein the protein of interest was UV-crosslinked to associated RNAs. The RNAs after crosslinking were radiolabelled with [32 P], then protein-RNA complexes were separated by denaturing PAGE, transferred to a nitrocellulose membrane and detected by autoradiography. The elution fractions were also analysed by SDS-PAGE followed by western blotting with an anti-Flag antibody to confirm that similar amounts of the full-length and truncated DDX55 proteins were loaded (Figure 4.11A). In the case of Flag-tagged full-length DDX55, a strong signal migrating at the molecular weight of DDX55 was obtained, confirming the direct interaction of DDX55 with RNA *in vivo*. However, a significantly weaker signal was observed in the case of truncated DDX55, indicating a loss in RNA binding upon truncation of the C-terminal basic tail (Figure 4.11B).

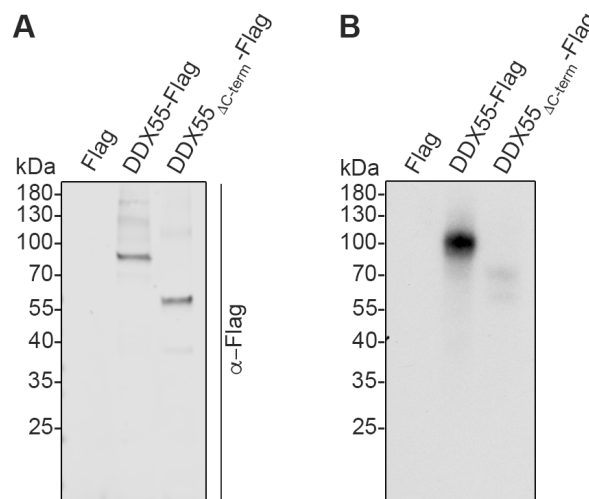


Figure 4.11. Deletion of the C-terminal tail of DDX55 leads to decreased RNA binding. HEK293 stable cell lines expressing DDX55-Flag or DDX55 $_{\Delta C-term}$ -Flag were crosslinked *in vivo* using UV light at 254 nm. RNA-protein complexes were purified first under native and then under denaturing conditions. Crosslinked RNA was partially digested and [32 P] labelled. Complexes were separated by denaturing PAGE and transferred onto nitrocellulose membranes. **(A)** The amount of Flag-tagged DDX55 and DDX55 $_{\Delta C-term}$ in the elution fractions was detected by western blotting with antibody against the Flag-tag. **(B)** Radiolabelled RNAs were detected by autoradiography.

Immunofluorescence microscopy was then performed in HEK293 stable cell lines expressing Flag-tagged DDX55 and the truncated Flag-tagged DDX55 $_{\Delta C-term}$ using an anti-Flag antibody in order to examine the effect of deleting the tail on the sub-cellular localisation of the helicase. Full-length DDX55 was predominantly present in the nuclear

compartment, co-localizing with the nuclear stain, DAPI, as previously observed (Figure 4.12A). In contrast, DDX55 lacking the C-terminal tail was largely excluded from the nuclear compartment and a dispersed signal was detected in the cytosol (Figure 4.12B).

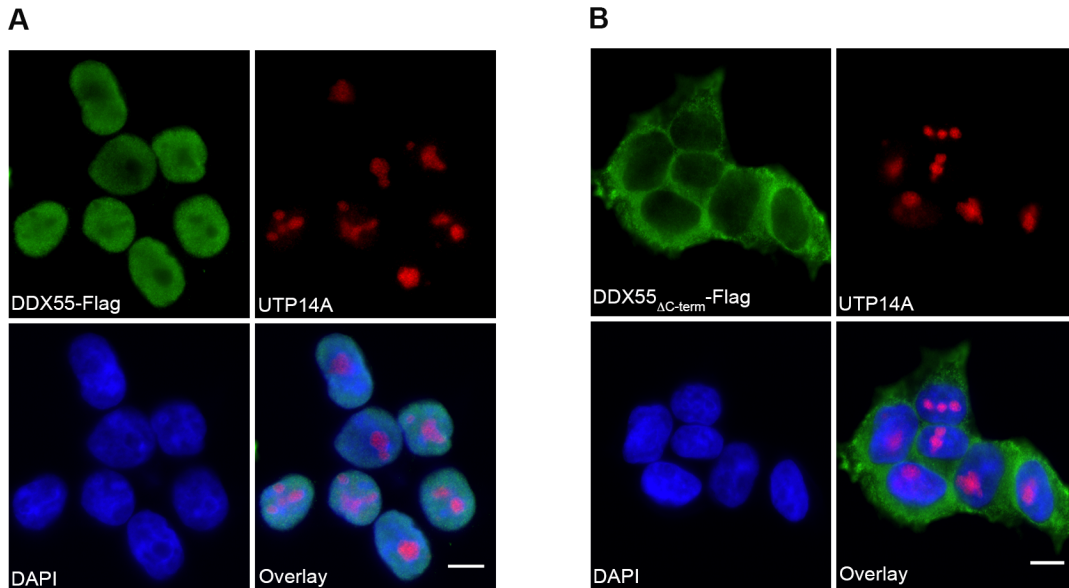


Figure 4.12. C-terminal truncation of DDX55 causes its mis-localisation to the cytoplasm. (A-B). Stable cell lines for the expression of DDX55-Flag (A) or DDX55 $_{\Delta C-term}$ -Flag (B) were induced with tetracycline for 24 h before fixing with 4% paraformaldehyde. The localisation of DDX55-Flag or DDX55 $_{\Delta C-term}$ -Flag were determined by immunofluorescence with an anti-Flag antibody (green). Immunofluorescence against UTP14A (red) served as a nucleolar marker. The nuclear material was visualized with DAPI (blue). An overlay of images is presented and the scale bar corresponds to 10 μ m.

As the C-terminal tail of DDX55 was observed to be important for RNA binding and nucleoplasmic localisation of the helicase *in vivo*, its potential role in recruitment of the helicase to the pre-ribosomal subunits was next analysed. Whole cell lysates from HEK293 stable cells lines expressing full length Flag-tagged DDX55 or the truncated DDX55 $_{\Delta C-term}$ -Flag were separated on sucrose density gradients. The absorbance of each fraction at 260 nm was measured to determine the RNA content and, thereby enable the fractions containing the large and small ribosomal subunits, and 80S monosomes to be identified. SDS-PAGE and western blotting with anti-Flag antibody was then used to analyse the distribution of the Flag-tagged proteins within the gradient. Full-length DDX55 was enriched in fractions containing 60S subunits, implying that it predominantly associates with pre-60S particles in the nucleus. As expected, there was a dramatic reduction in the amount of truncated DDX55 present in these fractions, demonstrating the requirement for the basic C-terminal tail of DDX55 for recruitment of the helicase to the right sub-cellular compartment and hence, its site of action in pre-60S complexes (Figure 4.13).

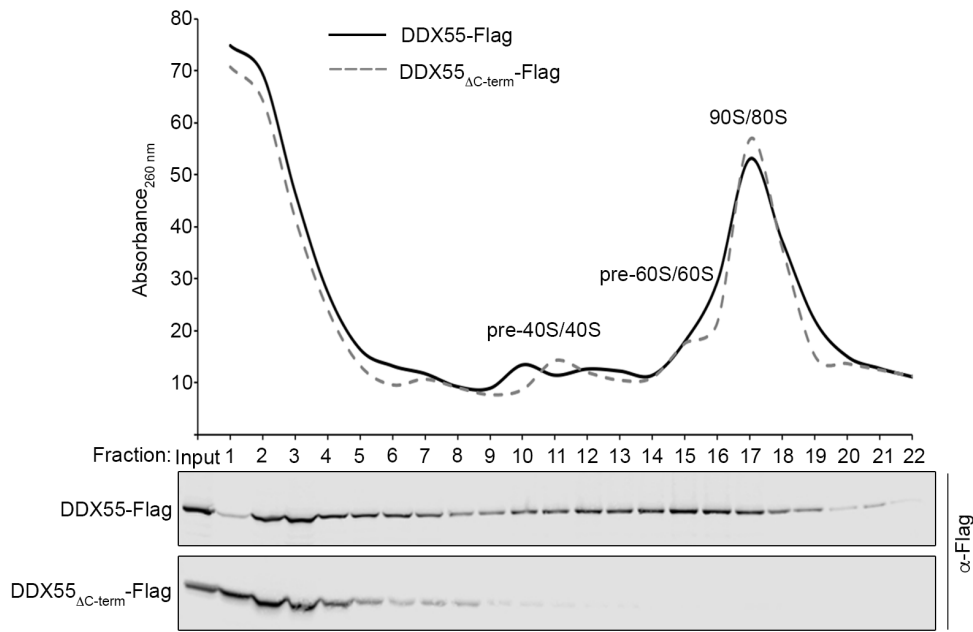


Figure 4.13. Deletion of the C-terminal basic tail of DDX55 results in reduced association with pre-ribosomal subunits. Flag-tagged DDX55 and DDX55_{ΔC-term}-Flag were expressed from HEK293 cells by addition of tetracycline. After 24 h, cells were harvested and whole cell extracts were prepared which were subjected to sucrose density gradient centrifugation. The absorbance of each fraction at 260 nm was measured to determine the RNA content and to generate a profile. The peaks corresponding to (pre)-ribosomal subunits are indicated. Proteins in each fraction (along with 10% input) were separated by SDS-PAGE and analysed by western blotting with an anti-Flag antibody.

4.4 Discussion

The pathway of ribosome assembly and maturation is characterized in much greater detail in yeast in comparison to that in humans. Hence, knowledge of ribosome biogenesis is largely derived from studies done in the yeast *S. cerevisiae*. Much of the knowledge on ribosome biogenesis in yeast is also applicable to higher eukaryotes due to a high degree of conservation of ribosome assembly factors and ribosomal proteins and similarities of the pre-rRNA processing pathways. However, a growing body of evidence indicates that the process of ribosome biogenesis has acquired greater complexity in humans in terms of additional pre-rRNA cleavage sites and ribosome assembly factors lacking yeast homologues. However, mechanistic details of ribosome biogenesis in humans is far from comprehensive with multiple ribosome assembly factors yet uncharacterized. Moreover, a group of genetic disorders, termed ribosomopathies, that are caused by mutations in genes encoding ribosomal proteins or assembly factors, further underscores the importance of a detailed understanding of the human ribosome assembly pathway.

In this study, the function of the putative RNA helicase DDX55, a homologue of yeast DEAD-box protein Spb4, was analysed in the process of ribosome assembly in humans. In yeast, Spb4 has been reported to hydrolyse ATP in an RNA-dependent manner (Brüning et al., 2018) and in line with this, *in vitro* ATPase assays confirm the hydrolysis of ATP by DDX55 and we observed a lack of ATP hydrolysis by the mutant demonstrating that the observed activity can be attributed to DDX55. However, surprisingly, and in contrast to Spb4, the addition of RNA did not significantly stimulate ATP hydrolysis. On the one hand, this could reflect a difference between the mechanism of action of the yeast and human proteins, but on the other hand, it could arise due to possible non-specific co-purification of nucleic acids from *E. coli* during recombinant protein purification. This is further supported by the observation that DDX55 exhibited strong ATP hydrolysis activity even in the absence of an *in vitro* RNA substrate. Stringent purification protocol specifically optimized for the removal of bound nucleic acids from the protein fractions could be a possible strategy to counter this issue.

Our data further suggest that lack of DDX55 in human cells can lead to impaired ribosome biogenesis. Consistent with this, *in vivo* crosslinking data revealed the physical association of DDX55 with pre-LSU, and crosslinking to a specific 28S rRNA sequence. Analogous to the pre-ribosome binding site identified for yeast Spb4 (Brüning et al., 2018), DDX55 crosslinks to helices 62 and 63 of 28S rRNA sequence suggesting that the helicase binding site is conserved from yeast to humans and further supporting the requirement for DDX55 for the maturation of pre-60S particles. In addition, similar to Spb4 in yeast, DDX55 does not crosslink to the 18S rRNA sequence in human cells. However, depletion of DDX55

resulted in mild defects in SSU biogenesis and while it is possible that DDX55 has a binding site in the 18S rRNA that was not identified by CRAC, it is likely that the effects of DDX55 depletion on 18S rRNA synthesis are indirect. We further demonstrated that DDX55 is a catalytically active enzyme and in order to demonstrate the requirement for the catalytic activity of DDX55 for ribosome biogenesis, RNAi-based rescue systems with cell lines expressing either wild-type or catalytically inactive DDX55 will be generated and used for analysing pre-rRNA processing.

In case of DEAH-box helicases, N- and C- terminal domains can serve as binding platforms for cofactors which can endow specificity to the intrinsically promiscuous helicase core. The OB-folds present in the conserved C-terminal domains of DEAH-box helicases are essential for binding to G-patch proteins which aid in the regulation as well as recruitment of helicases to their substrate RNAs. In the absence of such conserved domains in their C-terminal extensions, several DEAD-box helicases rely on their lysine rich C-terminal tail for targeting and/or tethering to their cognate RNA substrates. For example, the basic tail of yeast DEAD-box helicase Mss166 has been implicated in the binding of RNA and helps anchoring of the helicase to structured RNA substrates (Mohr et al., 2008). Interestingly, detailed investigation of the amino acid composition of DDX55 revealed the presence of a lysine-rich C-terminal domain, which is conserved amongst eukaryotes. Consistent with a role in the late steps of ribosome biogenesis, full-length DDX55 was predominantly localised in the nucleoplasm and co-sediments with pre-60S complexes. However, upon truncation of the C-terminal tail, the protein was largely excluded from the nucleus and was unable to associate with pre-ribosomal complexes. The C-terminal domain of DDX55 is reminiscent of the basic tails of other helicases that tether them to their RNA substrates, raising the possibility that the lysine-rich tail of DDX55 could similarly contribute to its association with target RNA substrates. However, bioinformatics analysis of the C-terminal domain of DDX55 revealed the presence of a nuclear localization signal (NLS). The loss of the NLS could be responsible for the cytoplasmic mis-localisation of the truncated protein and the loss of association with pre-ribosomal complexes. On a molecular level, elements within the C-terminal tail are likely to have two distinct functions. They are implicated in promoting nuclear import and/or can facilitate the interaction of the helicase with substrate RNA, a function similar to yeast Mss116. To gain further insights and explain the effects observed upon tail deletion, an *in vitro* fluorescence anisotropy approach, comparing the RNA-binding ability of the full length and truncated proteins could differentiate between these two roles and determine if the C-terminal tail is directly implicated in RNA-binding. To further investigate the function of the C-terminal domain of DDX55, the predicted bipartite NLS could be exchanged for a minimal NLS and the RNA-binding ability of DDX55 and its effective recruitment to pre-ribosomal complexes could be tested. Furthermore, the

contribution of C-terminal domain of DDX55 in the modulation of its catalytic activity *in vivo* also remains to be determined and methods such as *in vitro* ATPase assays together with RNAi-based rescue systems will be employed to address these open questions.

In yeast, Spb4 has been suggested to associate with pre-ribosomal particles in the nucleolus and is released relatively late prior to nuclear export of pre-60S particles (Brüning et al., 2018; de la Cruz et al., 1998). Recent reports suggest that Spb4 stably associates with helix 63 in 25S rRNA located at the base of ES27 which acts as a molecular hinge directing the position of a flexible arm that is involved in Arx1 binding to pre-60S particles. Binding of Spb4 likely promotes structural rearrangement enabling the recruitment of pre-60S export factor Arx1 (Brüning et al., 2018). Additionally, Nog2, which acts as a placeholder for the export adaptor Nmd3 (Matsuo et al., 2014; Sloan et al., 2016) is also dependent on Spb4 for its recruitment to pre-60S particles (Talkish et al., 2012). These findings implicate Spb4 in helping establish the export competence of pre-60S particles. Interestingly, in humans, DDX55 associates with late pre-ribosomal particles and in contrast to Spb4, it is predominantly excluded from the nucleolus (initial site of ribosome biogenesis) suggesting that the function or timing of this protein may differ in higher eukaryotes. Moreover, it remains to be determined if DDX55 is involved in preparing human pre-60S particles for export. This possibility is supported by the observation that DDX55 is localised predominantly in the nucleoplasm suggesting that it associates quite late with the pre-ribosomal complexes during the assembly pathway. This potential function will be explored by employing fluorescence microscopy-based approaches monitoring the mis-localisation of GFP-tagged ribosomal subunits upon DDX55 depletion (Wild et al., 2010). Additionally, mass-spectrometry (MS) based compositional analysis of late pre-60S particles upon RNAi-mediated depletion of DDX55 could provide further insights into a potential role of DDX55 in promoting the recruitment or release of *trans*-acting biogenesis factors.

Taken together, the results so far suggest the requirement for DDX55 for maturation of LSU and further highlight the importance of its C-terminal tail region for interaction with pre-ribosomal subunits. In the future, the various approaches described above will enable us to gain further mechanistic insights into the function of DDX55 in the context of LSU maturation and to understand the precise contribution of its basic C-terminal tail in regulating its function.

Chapter Five: Discussion

5.1 Distinct roles of RNA helicase in ribosome biogenesis

Ribosomes are essential in all domains of life and the assembly of such large macromolecular complexes involves the action of various types of *trans*-acting biogenesis factors that mediate modification, cleavage, folding and restructuring of the pre-ribosomal complexes. Therefore, it is not surprising that RNA helicases, which play key roles in diverse aspects of RNA metabolism, are extensively involved in the process of ribosome biogenesis. In bacteria, ribosome assembly is best characterized in *E. coli*. Of the five non-essential RNA helicases known in *E. coli*, four of them have been reported to play a role in ribosome assembly (Martin et al., 2013). Studies have also shown that in bacterial strains, defects arising due to a loss of all five RNA helicases can be successfully alleviated by growing them in alternative conditions (Jagessar and Jain, 2010). However, in eukaryotes, the increased size and complexity of ribosomal subunits have led to the emergence of a more complex ribosome assembly pathway. Not surprisingly, most RNA helicases involved in ribosome biogenesis in eukaryotes are essential due to the key roles they play in remodelling pre-ribosomal particles and the remodelling events driven by them often serve as checkpoint during the assembly pathway. Ribosome biogenesis is best characterized in yeast (Woolford and Baserga, 2013) and so far, 21 RNA helicases have been shown to contribute to yeast ribosome biogenesis (Martin et al., 2013). Detailed molecular characterization of RNA helicases has revealed the diverse range of activities carried out by them in the context of ribosome biogenesis. Several RNA helicases have been implicated in facilitating the association or removal of snoRNAs from pre-ribosomal complexes (Bohnsack et al., 2008, 2009; Koš and Tollervey, 2005; Liang and Fournier, 2006; Martin et al., 2013; Watkins and Bohnsack, 2012). For example, the DEAD-box helicase Has1 has been implicated in the removal of U14 snoRNA in yeast (Brüning et al., 2018; Liang and Fournier, 2006). The well-characterized DEAH-box protein Prp43 has been suggested to play a direct role in the unwinding of several snoRNAs that modify a cluster of nucleotides in 25S rRNA sequence (Bohnsack et al., 2009). In yeast, Dhr1 (DHX37 in humans) associates with early pre-ribosomal particles and is suggested to trigger the release of U3 snoRNA (Sardana et al., 2015). The binding of U3 to pre-rRNA sequences is important for proper cleavage events within 5'ETS and ITS1, resulting in the formation of the mature 5' end of 18S rRNA and separation of the pre-60S and pre-40S ribosomal subunits (Henras et al., 2008; Venema and Tollervey, 1995). The dissociation and release of the U3 snoRNA is also critical for the formation of the central pseudoknot, a key feature of the SSU (Henras et al., 2008). We observed that in human cells, DHX37 is required for

the maturation of 18S rRNA and plays a key role in the dissociation of U3 snoRNA from pre-ribosomal subunits, enabling the subsequent maturation of the SSU. Our CRAC data revealed direct interaction between DHX37 and the 3' hinge region of the U3 snoRNA, which is suggested to base-pair with 5'ETS sequences in the pre-rRNA. In accordance with this, expression of catalytically inactive DHX37 leads to impaired processing of the A' cleavage site within the 5' ETS resulting in the accumulation of aberrant pre-rRNAs.

Additionally, several RNA helicases are suggested to also contribute to the extensive pre-rRNA rearrangements that occur during ribosome assembly and which, for example, they facilitate efficient pre-rRNA cleavage, rRNA modification, or association/dissociation of different ribosomal proteins or biogenesis factors. For instance, in yeast, Kre33 is implicated in the acetylation of helix 34 and 35 within the 18S rRNA sequence. The conserved helicase domain of Kre33 was suggested to play a key role in the remodelling of 18S rRNA sequence in order for it to gain access and enable acetylation (Sharma et al., 2015). In addition to its role in the release of U14 snoRNA, Has1 has been reported to drive the remodelling of domain I of 25S rRNA enabling the incorporation of several RPs such as Rpl26, Rpl35 and Rpl37 (Brüning et al., 2018; Dembowski et al., 2013). The DEAD-box helicase Spb4 (DDX55 in humans), associates with pre-ribosomal complexes in the nucleolus and likely mediates structural rearrangement of the 25S pre-rRNA sequence (Brüning et al., 2018; de la Cruz et al., 1998). Interestingly and in contrast to Spb4, in humans, we observed DDX55 to be localized in the nucleoplasm suggesting its association with late-stage pre-ribosomal subunits. *In vivo* crosslinking data position both Spb4 and DDX55 in close proximity to helices 62 and 63 of 25S/28S rRNA sequences, implying that this binding site is conserved between yeast and humans. In yeast, remodelling activity of Spb4 at helices 62 and 63 of 25S rRNA has been suggested to promote the recruitment of the export adaptor Arx1. Interestingly, EBP1, the human homologue of Arx1, has been reported to associate with pre-60S particles. However, the precise binding sites of EBP1 on pre-ribosomal subunits is yet to be identified (Squatrito et al., 2004). It remains to be seen if DDX55 plays a role in the recruitment of export factors in the context of LSU biogenesis in humans. Although assumed to be highly conserved, an increasing body of evidence has highlighted key differences in the biogenesis pathway of yeast and human ribosomes implying that ribosome biogenesis has evolved to be more complex in humans. Hence, the list of assembly factors involved in ribosome biogenesis in humans is likely still incomplete (Sloan et al., 2013a; Tafforeau et al., 2013; Wild et al., 2010). Several RNA helicases that were previously functionally characterized in yeast, were shown to fulfil similar tasks in humans (Choudhury et al., 2019; Sekiguchi et al., 2006). However, there are now also examples of helicases which either lack a yeast homologue (DDX21) or play different roles in higher eukaryotes (DHX15) (Memet et al., 2017; Sloan et al., 2015). Moreover, RNAi-mediated

screens have identified several RNA helicases which are required for SSU and LSU biogenesis but are yet to be characterized in detail (Tafforeau et al., 2013). Thus, the molecular functions of most RNA helicases involved in ribosome biogenesis in higher eukaryotes are not well-understood and the emergence of ribosomopathies further emphasizes the need to characterize the human ribosome assembly pathway in detail.

5.2 Division of labour: DEAH-box versus DEAD-box helicases

Various aspects of gene expression such as pre-mRNA splicing or ribosome biogenesis require the contribution of RNA helicases belonging to either the DEAD-box or DEAH-box family of proteins. As observed in certain pathways, there seems to be a clear division of labour between proteins belonging to the two helicase families in assisting distinct assembly/disassembly steps, implying the requirement for different modes of strand separation. This is perhaps most evident in yeast pre-mRNA splicing, which requires the action of eight helicases which fall into the categories of DEAD-box, DEAH-box and Ski2-like helicases (Cordin and Beggs, 2013). The pre-catalytic steps are assisted by DEAD-box helicases which act as local 'unwindases' and typically bind to short duplex regions in an ATP-dependent manner. For example, during the first steps of splicing, the DEAD-box proteins Sub2 and Prp5 are implicated in branch point recognition by U2 snRNP by mediating local structural rearrangements. Prp5 is suggested to facilitate the transition of U2 snRNP between alternate conformation by restructuring an 8 bp helix. Subsequently, the DEAD-box helicase Prp28 is important for the unwinding of a 6 bp helix formed between the U1 snRNA and the 5' splice site, resulting in the release of the U1 snRNP. In contrast, DEAH-box helicases being processive enzymes, promote extensive structural rearrangements involving long-range interactions in the downstream catalytic steps (Gilman et al., 2017). For example, the DEAH-box helicase Prp2 is implicated in displacement of proteins from the branch point by translocating through the pre-mRNA in a 3'-5' manner. Likewise, a directional 3'-5' translocation has also been suggested for Prp22, resulting in the release of spliced mRNA. Lastly, the multi-functional DEAH-box helicase Prp43 promotes extensive re-structuring events leading to release of the intron lariat and recycling of the snRNPs (Cordin and Beggs, 2013; Fica and Nagai, 2017). In addition, DEAD-box proteins involved in local strand unwinding and duplex destabilization are key players in remodelling of carefully structured RNP complexes such as pre-ribosomes. Local destabilization within a layered RNP complex leads to large-scale structural rearrangements required for ribosome assembly and maturation, making DEAD-box helicases excellent candidates for this role (Jankowsky and Fairman, 2007). For instance, several DEAD-box helicases are suggested to promote unwinding of snoRNA-pre-rRNA base-pairing by mediating local unwinding (Martin et al., 2014).

Interestingly, although there is typically a clear demarcation between the molecular mechanisms of action of DEAD-box and DEAH-box helicases, studies have shown that there are a few exceptions. The DEAH-box helicase Prp43, in yeast, is exceptionally versatile, playing diverse roles in ribosome biogenesis and pre-mRNA splicing (Jarmoskaite and Russell, 2014). DEAH-box helicases are typified as unidirectional enzymes that bind to 3' single stranded sequences and translocate in a strict 3'-5' manner. *In vitro* studies have demonstrated that Prp43 does not require a 3' extension for unwinding of RNA and hence, can function in a manner similar to DEAD-box helicases by being directly recruited to structured, double stranded RNA sequences (Guenther and Jankowsky, 2009). Likewise, the yeast DEAH-box helicase Dhr1 was suggested to unwind RNA duplexes in a manner reminiscent of DEAD-box helicases. *In vitro* unwinding assays with ATP binding or hydrolysis mutants of Dhr1 indicated that the unwinding activity is dependent on ATP binding and that hydrolysis of bound ATP was only important for product release and dissociation of the helicase from the substrate (Sardana et al., 2015). This is in contrast to typical DEAH-box helicases as they rely on successive cycles of ATP hydrolysis for processive strand displacement but similar to the classical mechanism adopted by DEAD-box helicases for unwinding short duplexes. Recent structural insights provide mechanistic details of the RNA-dependent ATPase activity of the human homologue of Dhr1, DHX37. A crystal structure of DHX37 in the presence of a bound single stranded RNA substrate revealed that ATP binding to the conserved motifs within the helicase core domains induces a conformational shift resulting in formation of the 'closed' active conformation. This leads to a directional shift with the helicase engaging with the next 5' nucleotide in the substrate while releasing one base from the 3' side. Upon ATP hydrolysis, the helicase switches back to its inactive 'open' conformation and can associate with the next 5' terminal nucleotide. Hence, DHX37 is able to translocate in a 3'-5' unidirectional manner and ATP binding but not hydrolysis was suggested to provide the power stroke for translocation (Boneberg et al., 2019).

CRAC analysis of yeast DEAD-box helicase Spb4, identified two distinct crosslinking sites on the 25S rRNA sequence. However, crosslinking sites of helicases identified by approaches like CRAC do not necessarily represent the contact point of the active core of the helicase, but can also represent contacts formed by other regions of the protein. This can often be the case as it is likely that the active site makes only transient interactions with the RNA that are less likely to be captured by CRAC. Structural analysis of pre-ribosomal particles containing the helicase are required in order to identify RNA sequences that are directly contacted by the active site of the helicase. Dimethyl sulphate (DMS) structure probing experiments, aimed at uncoupling the functional relevance of the two sites identified in the case of Spb4, suggested that helices 62-63 are likely to serve as a binding platform

for the helicase whereas helix 101 may represent the remodelling site. Mapping of the CRAC data onto the 3D structure of pre-LSU particles showed that the two binding sites are present on the same face of the ribosome, albeit somewhat specially separated (Brüning et al., 2018). *In vivo*, however, DEAD-box helicases have been suggested to promote local strand separation raising the question of how DEAD-box helicases such as Spb4 are able to promote duplex destabilization at regions spatially distant from their binding sites. For long RNA substrates, some DEAD-box helicases have been shown to tether securely to RNA sequences spatially distinct from their remodelling targets, thereby enabling multiple rounds of helix capture, strand separation and ATP hydrolysis in the vicinity of their binding site. For example, yeast helicase Mss116 possess an arginine rich C-terminal extension that facilitates its anchoring onto the RNA substrate in order to perform multiple rounds of ATP hydrolysis (Mohr et al., 2008). Likewise, Spb4 contains numerous basic amino acid residues at the C-terminal tail extension, suggesting a similar mechanism of action. Interestingly, our CRAC data reveal a distinct binding site for DDX55 within the 28S rRNA sequence. The functional relevance of DDX55 binding to 28S rRNA sequence is still to be determined. However, taken together with its nucleoplasmic localisation, it is possible that DDX55 plays a role in late stages of pre-60S maturation as seen in the case of Spb4. Interestingly, detailed sequence characterization of DDX55 revealed the presence of C-terminal tail containing clusters of basic amino acid residues. Deletion of the C-terminal tail, downstream of the conserved core domain leads to mis-localization of the protein to the cytoplasm, thereby resulting in a loss of association with pre-60S particles as observed in sucrose density gradient experiments. *In vitro* studies such as fluorescence anisotropy experiments will provide clearer insights into the contribution of C-terminal tail in the binding and subsequent association of DDX55 with pre-ribosomal complexes.

Additionally, for several well-characterized DEAD-box proteins that display conventional non-processive methods of duplex unwinding, association with dedicated cofactors has been shown to drastically influence their properties. For example, in humans, the DEAD-box helicase eIF4A has been suggested to exhibit processive cycles of duplex unwinding in association with its partner proteins eIF4G and eIF4B (García-García et al., 2015). It is also likely that individual helicases have evolved specific properties distinctive from the classical enzymes of their respective families in order to perform a specialized task *in vivo*. Detailed biochemical and structural characterization of individual RNA helicases from the DEAD-box and DEAH-box families will therefore likely provide new insights into their precise mechanisms of action.

5.3 Regulation of RNA helicases

The conserved helicase core domains of DEAD-box proteins and DEAH-box proteins interact with the sugar phosphate backbone of their RNA substrates, thereby exhibiting an intrinsic lack of specificity. However, the existence of multi-functional helicases such as Prp43 and eIF4A highlight the ability of these enzymes to bind to specific RNA and/or RNP targets in the complex cellular environment. The N- and C-terminal auxiliary domains extending beyond the RecA-like domains have been implicated in influencing the target recognition and activity of these helicases. The C-terminal extensions of DEAD-box proteins is not conserved and often varies within the helicase family. In contrast, DEAH-box proteins possess a highly conserved C-terminus consisting of OB-fold, WH and the ratchet domain, which are implicated in substrate recognition and regulation through association with cofactors such as the G-patch family of proteins (Robert-Paganin et al., 2015). Alongside helicase cofactors such as the MIF4G and G-patch proteins that form family groups, several proteins that do not share any clear similarities with other cofactors and have evolved to influence the activity of specific helicases. For example, in yeast, the unwinding activity of DEAH-box helicase Dhr1 is stimulated by the 40S biogenesis factor Utp14. Additionally, Utp14 along with rRNA methyltransferase Bud23 has been reported to be required for the association of Dhr1 with the pre-ribosomal complexes (Zhu et al., 2016). Once recruited to pre-ribosomes, Dhr1 and Utp14 act synergistically leading to the efficient dissociation of U3 snoRNA from the pre-rRNA sequences (Zhu et al., 2016). Our data indicate a direct, RNA-independent interaction between UTP14A and DHX37 in humans, suggesting that this interaction is conserved between yeast and humans. *In vitro* ATPase assays further demonstrate that UTP14A stimulates the ATPase activity of DHX37 and RNAi-mediated depletion of UTP14A leads to accumulation of U3 snoRNA on pre-ribosomal complexes. This is in contrast to a previous observation that in yeast, Utp14 stimulates the unwinding activity of Dhr1 without altering its ATPase activity (Zhu et al., 2016), but is in accordance with recent reports investigating the mechanistic details of UTP14 dependent activation of DHX37 (Boneberg et al., 2019). Although the molecular mechanisms of Utp14/UTP14A mediated stimulation of Dhr1/DHX37 may therefore have diverged during evolution, the physiological function of the helicase and its cofactor seems to be conserved in higher eukaryotes. Fluorescence polarization assays used for monitoring RNA binding have further revealed the precise mechanism of DHX37 stimulation by UTP14A (Boneberg et al., 2019). A conserved motif in the central region of UTP14A has been implicated in the stimulation of RNA-dependent ATPase activity of DHX37 by enhancing the ATP-dependent RNA-binding ability of DHX37. Furthermore, structural studies of N-terminal truncated DHX37 reveal the presence of a unique alpha-helical C-terminal domain, which has not been previously observed in other proteins. Deletion of the C-terminus results in the loss of DHX37

association with UTP14A, indicating that this domain is crucial for efficient interaction with UTP14A. Moreover, fluorescence-based reporter assays indicated that although the C-terminal domain is not required for the nuclear import of DHX37, it plays an important role in the biogenesis of 40S ribosomal subunit *in vivo* (Boneberg et al., 2019).

Additionally, a diverse range of helicases are also regulated *in cis* by the action of auxiliary domains. Prominent examples include the yeast DEAD-box protein Mss116 and its *Neurospora crassa* orthologue CYT-19 wherein the basic C-terminal tail is implicated in the binding to RNA substrates. Interestingly, the proposed binding platform of Spb4 constitutes of a helical structure reminiscent of the secondary structure bound by the C-terminus of Mss116 (Brüning et al., 2018), implying a similar mode of recruitment. Our data suggest that the basic amino acid-rich C-terminal domain of DEAD-box protein DDX55 might also play a role in its recruitment to the pre-ribosomal subunits. However, it remains to be determined if the basic residues within the C-terminal domain directly contribute to the recruitment and regulation of DDX55. To determine the involvement of a possible *trans*-acting cofactor, immunoprecipitation experiments followed by mass-spectrometry could provide additional information regarding proteins that contribute to spatial and temporal regulation of the catalytic activity of DDX55. Alternatively, it is also possible that DDX55 is recruited and its activity is regulated by its basic C-terminal tail without the involvement of *trans*-acting effector proteins. Local duplex destabilization mediated by binding of a helicase within the context of a large RNP particle, like a pre-ribosome, can often lead to dissociation of bases downstream of the binding site leading to restructuring of the RNP complex. For example, in the case of Spb4, the binding site is suggested to be spatially separated from the site of action. However, the binding of Spb4 may also result in a structural rearrangement within its site of action, allowing the association of export adaptor protein Arx1 (Brüning et al., 2018). This phenomenon is analogous to the 'butterfly effect' whereby a miniscule localized change in a complex system ultimately manifests in a large effect. Unfortunately, the precise RNA targets of many DEAD and DEAH-box helicases are still unknown in humans. *In vivo* crosslinking based approaches such as CRAC are now increasingly being employed to identify targets of these helicases. Additionally, the newly available cryo-EM structures of large RNPs such as spliceosomes and pre-ribosomes significantly help identifying the targets of several helicases. Identifying RNA helicase cofactors remains extremely challenging, especially for proteins that function in large RNPs like pre-ribosomes, however, the development of improved protein-protein crosslinking and proximity labelling techniques will likely lead to the identification of additional RNA helicase cofactors in the future. Identification of target RNA substrates as well as their interactome will lead to a more comprehensive understanding of the regulatory networks governing the action of helicases *in vivo*.

5.4 Dynamics of RNA helicase association with pre-ribosomes.

RNA helicases associate with pre-ribosomal subunits and through their diverse range of functions, mediate remodelling of these complexes. However, it is often difficult to dissect the dynamics of helicase association with pre-ribosomal complexes. In humans, DHX37 is observed to associate with early pre-ribosomal particles where it functions in the removal of U3 snoRNP. Expression of catalytically inactive DHX37 leads to impaired processing at the A' cleavage site located within the 5' ETS region, likely reflecting the failure to release U3 snoRNA upon DHX37 depletion. Our studies further suggest that the association of DHX37 to early pre-ribosomal complexes is monitored by various quality control pathways and failure to recruit DHX37 along with the 40S biogenesis factors DIMT1L and TSR1 result in degradation of the pre-ribosomes. Interestingly, complementation assays further reveal that the catalytic activity of DHX37 is necessary for the processing of 21S pre-rRNA to generate 18S-E pre-rRNA during the late stages of ribosome biogenesis. Taken together, our results indicate that DHX37 is required for the early and late steps of 40S ribosomal biogenesis. A possible explanation coupling the early and late stage defects could be that the failure to release U3 snoRNA from early pre-ribosomal particles leads to defects in late stages of pre-rRNA processing. Additionally, in humans, the precise timing of U3 snoRNA release is not yet known. Alternatively, the defects in the late stages of pre-40S maturation can likely reflect an additional role for DHX37 in the pre-rRNA processing of 21S, independent of its function in the release of U3 snoRNA in the early steps of biogenesis. This raises an interesting question regarding the temporal regulation of DHX37. It is yet to be determined if DHX37 associates with the ribosome at an early stage and is released only after the successful processing of 21S to 18S-E or upon efficient dissociation of U3 snoRNA, or whether DHX37 is released from the pre-ribosomal subunits after U3 release and then re-associates during late-steps of ribosome biogenesis. Our data further suggest that UTP14A acts together with DHX37 in promoting the release of U3 snoRNA. Immunoprecipitation followed by mass-spectrometry analysis of the DHX37 interactome may reveal the presence of additional cofactors of DHX37 that could regulate the activity of DHX37 during later steps of biogenesis. These open questions regarding the timing of DHX37 association and link between the early and late stage defects can probably be best addressed by structural analysis of the helicase in association with pre-ribosomal complexes isolated during different stages of biogenesis. In addition, MS analyses of pre-ribosomal particles containing DHX37 can also provide information regarding the timing of its association. As DHX37, similar to Dhr1, does not stably associate with pre-ribosomal complexes, our *in vivo* crosslinking data did not reveal its binding site on the pre-rRNA. Performing CRAC experiments using catalytically inactive mutant of DHX37 could possibly

lead to a more stable association of the helicase with the pre-ribosomal complexes, thereby providing additional information regarding the pre-rRNA target sites of DHX37.

In contrast to DHX37, the DEAD-box helicase DDX55, binds to pre-ribosomes during the late steps of ribosome biogenesis. *In vivo* crosslinking data suggest its direct association with the 28S rRNA sequence. The DDX55 binding site is observed to be conserved between yeast and humans and the late association of DDX55 with pre-60S complexes could indicate a possible role in establishing export competence of pre-60S complexes. While it is likely that late-acting RNA helicases like DDX55 remodel RNA sequences present on the surface of pre-ribosomal particles, it is also possible that they influence RNA structures buried deep within the RNP complex. Recent reports have proposed a 'winching' model for DEAH-box helicases that may explain the mechanism by which helicases are able to gain access to their target substrates within the context of large RNPs. Based on biochemical studies from yeast DEAH-box helicases Prp16 and Prp22, it was proposed that helicases can load onto 3' exposed extensions and upon encountering a block in translocation, they are able to pull on the RNA strand. This results in disruption in base-pairing without the helicase accessing the buried regions within the RNP (Semlow et al., 2016). This model highlights how DEAH-box helicases can act from a distance without having to translocate through their substrates and it is likely that this mechanism can also be employed by other members of the DEAH-box family of helicases. In contrast, DEAD-box helicases need direct association with or in the vicinity their duplex substrate and are not capable of acting from a distance as the winching model proposes. Auxiliary domains consisting of flexible basic C-terminal tail extensions or RNA recognition motifs in some cases have been proposed to anchor the helicase at an exposed region proximal to the remodelling site within the RNP complex. Once securely anchored to the RNA substrate, the helicase core gains access to the target site and remodels it (Diges and Uhlenbeck, 2001; Karginov et al., 2005; Mohr et al., 2008). An alternative possibility could be via the assistance of various cofactors that can help in the recruitment of helicases within the context of an RNP complex. Alternatively, the remodelling sites, if present on the surface of the pre-ribosomes, are easily accessible to DEAD-box helicases for binding.

Another complexity that arises as a result of RNA helicases acting in the context of large RNPs is the difficulty in distinguishing the direct consequences of RNA helicase action from indirect effects. A key example is the case of RNA helicases mediating snoRNA release from pre-ribosomal complexes. Depletion of more than one helicase can lead to the accumulation of a specific snoRNA on pre-ribosomes (Bohnsack et al., 2008; Koš and Tollervey, 2005; Liang and Fournier, 2006; Martin et al., 2014). For example, in yeast, DEAD-box helicases Dpb4 and Has1 have both been implicated in the release of U14 snoRNA from pre-ribosomes. U14 is required for guiding the 2'-O-methylation in 18S rRNA

and also for mediating pre-rRNA rearrangement required for processing (Dunbar and Baserga, 1998; Liang and Fournier, 1995). CRAC analyses have established the physical association of Has1 with U14, implying the direct role of Has1 in the release of U14 (Brüning et al., 2018; Liang and Fournier, 2006). However, so far, there is no direct evidence of Dbp4 interaction with Has1. Moreover, U14 was not found to be present in particles associated with Dbp4 (Soltanieh et al., 2015). Hence, it is likely that depletion of Dpb4 leads to remodelling events within the pre-ribosomal subunit, which indirectly retains U14. The yeast RNA helicase Rok1 is implicated in the unwinding and release of snR30 from pre-ribosomal complexes (Bohnsack et al., 2008). *In vivo* crosslinking data revealed that Rok1 associates with snR30 and promotes direct unwinding of snR30-pre-rRNA base-pairing (Martin et al., 2014). The strongest evidence indicating a direct role for a helicase in unwinding snoRNA-pre-rRNA base-pairing is supported by the data reported for Prp43. Crosslinking data revealed that Prp43 contacts the snoRNAs as well as their base-pairing sites on the pre-rRNAs sequences indicating a direct role in unwinding and release of snoRNAs (Bohnsack et al., 2009). Likewise, in humans, DDX51 is required for the displacement of U8 snoRNA from pre-ribosomes. However, as there is no evidence of direct binding between U8 and DDX51, it is also possible that instead of being directly involved in the unwinding of a U8 snoRNA-pre-rRNA duplex, DDX51 mediates structural rearrangements in distant areas of the pre-ribosome that indirectly lead to U8 snoRNA release (Srivastava et al., 2010). In yeast, Dhr1 crosslinks to the 5' region of the U3 snoRNA sequence which associates with the 18S rRNA sequence. However, Dhr1 was also reported to promote the unwinding of a duplex formed between 3' region of U3 and the 5'ETS of pre-rRNA. Hence, it is yet to be determined if Dhr1 acts to unwind both these duplexes *in vivo* or the disruption of one duplex is sufficient to promote the dissociation of U3 from pre-ribosomes (Sardana et al., 2015). Our CRAC data suggest a direct physical contact between 3' hinge region of U3 snoRNA that is predicted to base-pair with 5'ETS region and DHX37, implying that DHX37 may have a direct role in the dissociating U3 snoRNA from the pre-ribosomal subunits. The development of methods that allow visualisation of RNA helicases within pre-ribosomes, and structural analyses of helicases in the context of RNP complexes will be important approaches for better dissecting the precise roles of RNA helicases *in vivo*.

Bibliography

- Abaeva, I.S., Marintchev, A., Pisareva, V.P., Hellen, C.U.T., and Pestova, T. V (2011). Bypassing of stems versus linear base-by-base inspection of mammalian mRNAs during ribosomal scanning. *EMBO J.* 30, 115–129.
- Abdelhaleem, M., Maltais, L., and Wain, H. (2003). The human DDX and DHX gene families of putative RNA helicases. *Genomics* 81, 618–622.
- Ahmad, Y., Boisvert, F.-M., Gregor, P., Cobley, A., and Lamond, A.I. (2009). NOPdb: Nucleolar Proteome Database--2008 update. *Nucleic Acids Res.* 37, D181-4.
- Aitken, C.E., and Lorsch, J.R. (2012). A mechanistic overview of translation initiation in eukaryotes. *Nat. Struct. Mol. Biol.* 19, 568–576.
- Alexandrov, A., Colognori, D., and Steitz, J.A. (2011). Human eIF4AIII interacts with an eIF4G-like partner, NOM1, revealing an evolutionarily conserved function outside the exon junction complex. *Genes Dev.* 25, 1078–1090.
- Alexandrov, A., Colognori, D., Shu, M.-D., and Steitz, J.A. (2012). Human spliceosomal protein CWC22 plays a role in coupling splicing to exon junction complex deposition and nonsense-mediated decay. *PNAS* 109, 21313–21318.
- Ameismeier, M., Cheng, J., Berninghausen, O., and Beckmann, R. (2018). Visualizing late states of human 40S ribosomal subunit maturation. *Nature* 558, 249–253.
- Andersen, J.S., Lyon, C.E., Fox, A.H., Leung, A.K.L., Lam, Y.W., Steen, H., Mann, M., and Lamond, A.I. (2002). Directed proteomic analysis of the human nucleolus. *Curr. Biol.* 12, 1–11.
- Andreou, A.Z., and Klostermeier, D. (2014). eIF4B and eIF4G Jointly Stimulate eIF4A ATPase and Unwinding Activities by Modulation of the eIF4A Conformational Cycle. *J. Mol. Biol.* 426, 51–61.
- Anger, A.M., Armache, J.-P., Berninghausen, O., Habeck, M., Subklewe, M., Wilson, D.N., and Beckmann, R. (2013). Structures of the human and *Drosophila* 80S ribosome. *Nature* 497, 80–85.

Ansel, K.M., Pastor, W.A., Rath, N., Lapan, A.D., Glasmacher, E., Wolf, C., Smith, L.C., Papadopoulou, N., Lamperti, E.D., Tahiliani, M., et al. (2008). Mouse Eri1 interacts with the ribosome and catalyzes 5.8S rRNA processing. *Nat. Struct. Mol. Biol.* *15*, 523–530.

Aravind, L., and Koonin, E. V (1999). Novel predicted RNA-binding domains associated with the translation machinery. *J. Mol. Evol.* *48*, 291–302.

Arcus, V. (2002). OB-fold domains: a snapshot of the evolution of sequence, structure and function. *Curr. Opin. Struct. Biol.* *12*, 794–801.

Armistead, J., Khatkar, S., Meyer, B., Mark, B.L., Patel, N., Coghlan, G., Lamont, R.E., Liu, S., Wiechert, J., Cattini, P.A., et al. (2009). Mutation of a Gene Essential for Ribosome Biogenesis, *EMG1*, Causes Bowen-Conradi Syndrome. *Am. J. Hum. Genet.* *84*, 728–739.

Bai, D., Zhang, J., Li, T., Hang, R., Liu, Y., Tian, Y., Huang, D., Qu, L., Cao, X., Ji, J., et al. (2016). The ATPase hCINAP regulates 18S rRNA processing and is essential for embryogenesis and tumour growth. *Nat. Commun.* *7*, 12310.

Banroques, J., Cordin, O., Doère, M., Linder, P., and Tanner, N.K. (2008). A conserved phenylalanine of motif IV in superfamily 2 helicases is required for cooperative, ATP-dependent binding of RNA substrates in DEAD-box proteins. *Mol. Cell. Biol.* *28*, 3359–3371.

Barandun, J., Chaker-Margot, M., Hunziker, M., Molloy, K.R., Chait, B.T., and Klinge, S. (2017). The complete structure of the small-subunit processome. *Nat. Struct. Mol. Biol.* *24*, 944–953.

Beltrame, M., and Tollervey, D. (1995). Base pairing between U3 and the pre-ribosomal RNA is required for 18S rRNA synthesis. *EMBO J.* *14*, 4350–4356.

Ben-Shem, A., Garreau de Loubresse, N., Melnikov, S., Jenner, L., Yusupova, G., and Yusupov, M. (2011). The Structure of the Eukaryotic Ribosome at 3.0 Å Resolution. *Science* (80-.). *334*, 1524–1529.

Bohnsack, K.E., and Bohnsack, M.T. (2019). Uncovering the assembly pathway of human ribosomes and its emerging links to disease. *EMBO J.* e100278.

Bohnsack, M.T., Kos, M., and Tollervey, D. (2008). Quantitative analysis of snoRNA

association with pre-ribosomes and release of snR30 by Rok1 helicase. *EMBO Rep.* 9, 1230–1236.

Bohnsack, M.T., Martin, R., Granneman, S., Ruprecht, M., Schleiff, E., and Tollervey, D. (2009a). Prp43 Bound at Different Sites on the Pre-rRNA Performs Distinct Functions in Ribosome Synthesis. *Mol. Cell* 36, 583–592.

Bohnsack, M.T., Martin, R., Granneman, S., Ruprecht, M., Schleiff, E., and Tollervey, D. (2009b). Prp43 Bound at Different Sites on the Pre-rRNA Performs Distinct Functions in Ribosome Synthesis. *Mol. Cell* 36, 583–592.

Bohnsack, M.T., Tollervey, D., and Granneman, S. (2012). Identification of RNA Helicase Target Sites by UV Cross-Linking and Analysis of cDNA. *Methods Enzymol.* 511, 275–288.

Boneberg, F.M., Brandmann, T., Kobel, L., van den Heuvel, J., Bargsten, K., Bammert, L., Kutay, U., and Jinek, M. (2019). Molecular mechanism of the RNA helicase DHX37 and its activation by UTP14A in ribosome biogenesis. *RNA* 25, 685–701.

Boon, K.-L., Auchynnikava, T., Edwalds-Gilbert, G., Barrass, J.D., Droop, A.P., Dez, C., and Beggs, J.D. (2006). Yeast Ntr1/Spp382 Mediates Prp43 Function in Postspliosomes. *Mol. Cell. Biol.* 26, 6016–6023.

Booy, E.P., McRae, E.K.S., Howard, R., Deo, S.R., Ariyo, E.O., Džananovic, E., Meier, M., Stetefeld, J., and McKenna, S.A. (2016). RNA Helicase Associated with AU-rich Element (RHAU/DHX36) Interacts with the 3'-Tail of the Long Non-coding RNA BC200 (BCYRN1). *J. Biol. Chem.* 291, 5355–5372.

Boria, I., Garelli, E., Gazda, H.T., Aspesi, A., Quarello, P., Pavesi, E., Ferrante, D., Meerpohl, J.J., Kartal, M., Da Costa, L., et al. (2010). The ribosomal basis of diamond-blackfan anemia: mutation and database update. *Hum. Mutat.* 31, 1269–1279.

Bortoluzzi, S., D'alessi, F., Romualdi, C., and Danieli, G.A. (2001). Differential expression of genes coding for ribosomal proteins in different human tissues.

Bourgeois, C.F., Mortreux, F., and Auboeuf, D. (2016). The multiple functions of RNA helicases as drivers and regulators of gene expression. *Nat. Rev. Mol. Cell Biol.* 17, 426–438.

- Brüning, L., Hackert, P., Martin, R., Davila Gallezio, J., Aquino, G.R.R., Urlaub, H., Sloan, K.E., and Bohnsack, M.T. (2018). RNA helicases mediate structural transitions and compositional changes in pre-ribosomal complexes. *Nat. Commun.* *9*, 5383.
- Büttner, K., Nehring, S., and Hopfner, K.-P. (2007). Structural basis for DNA duplex separation by a superfamily-2 helicase. *Nat. Struct. Mol. Biol.* *14*, 647–652.
- Caruthers, J.M., and McKay, D.B. (2002). Helicase structure and mechanism. *Curr. Opin. Struct. Biol.* *12*, 123–133.
- Chen, S.S., and Williamson, J.R. (2013). Characterization of the ribosome biogenesis landscape in *E. coli* using quantitative mass spectrometry. *J. Mol. Biol.* *425*, 767–779.
- Chen, W., Shulha, H.P., Ashar-Patel, A., Yan, J., Green, K.M., Query, C.C., Rhind, N., Weng, Z., and Moore, M.J. (2014a). Endogenous U2·U5·U6 snRNA complexes in *S. pombe* are intron lariat spliceosomes. *RNA* *20*, 308.
- Chen, Y.-L., Capeyrou, R., Humbert, O., Mouffok, S., Kadri, Y.A., Lebaron, S., Henras, A.K., and Henry, Y. (2014b). The telomerase inhibitor Gno1p/PINX1 activates the helicase Prp43p during ribosome biogenesis. *Nucleic Acids Res.* *42*, 7330–7345.
- Chen, Y., Potratz, J.P., Tijerina, P., Del Campo, M., Lambowitz, A.M., and Russell, R. (2008). DEAD-box proteins can completely separate an RNA duplex using a single ATP. *Proc. Natl. Acad. Sci. U. S. A.* *105*, 20203–20208.
- Cheng, J., Kellner, N., Berninghausen, O., Hurt, E., and Beckmann, R. (2017). 3.2-Å-resolution structure of the 90S preribosome before A1 pre-rRNA cleavage. *Nat. Struct. Mol. Biol.* *24*, 954–964.
- Choesmel, V., Bacqueville, D., Rouquette, J., Noaillac-Depeyre, J., Fribourg, S., Cretien, A., Leblanc, T., Tchernia, G., Da Costa, L., and Gleizes, P.-E. (2006). Impaired ribosome biogenesis in Diamond-Blackfan anemia. *Blood* *109*, 1275–1283.
- Choudhury, P., Hackert, P., Memet, I., Sloan, K.E., and Bohnsack, M.T. (2019). The human RNA helicase DHX37 is required for release of the U3 snoRNP from pre-ribosomal particles. *RNA Biol.* *16*, 1–15.

Christian, H., Hofele, R. V, Urlaub, H., and Ficner, R. (2014). Insights into the activation of the helicase Prp43 by biochemical studies and structural mass spectrometry. *Nucleic Acids Res.* 42, 1162–1179.

Ciganda, M., and Williams, N. (2011). Eukaryotic 5S rRNA biogenesis. *Wiley Interdiscip. Rev. RNA* 2, 523–533.

Collins, R., Karlberg, T., Lehtiö, L., Schütz, P., van den Berg, S., Dahlgren, L.-G., Hammarström, M., Weigelt, J., and Schüler, H. (2009). The DEXD/H-box RNA helicase DDX19 is regulated by an α -helical switch. *J. Biol. Chem.* 284, 10296–10300.

Cordin, O., and Beggs, J.D. (2013). RNA helicases in splicing. *RNA Biol.* 10, 83–95.

Da Costa, L., Narla, A., and Mohandas, N. (2018). An update on the pathogenesis and diagnosis of Diamond-Blackfan anemia. *F1000Research* 7.

Couté, Y., Kindbeiter, K., phane Belin, S., gis Dieckmann, R., Duret, L., Bezin, L., Sanchez, J.-C., and Diaz, J.-J. (2008a). ISG20L2, a Novel Vertebrate Nucleolar Exoribonuclease Involved in Ribosome Biogenesis* □ S.

Couté, Y., Kindbeiter, K., Belin, S., Dieckmann, R., Duret, L., Bezin, L., Sanchez, J.-C., and Diaz, J.-J. (2008b). ISG20L2, a Novel Vertebrate Nucleolar Exoribonuclease Involved in Ribosome Biogenesis. *Mol. Cell. Proteomics* 7, 546–559.

Danilova, N., and Gazda, H.T. (2015). Ribosomopathies: how a common root can cause a tree of pathologies. *Dis. Model. Mech.* 8, 1013–1026.

Dardenne, E., Polay Espinoza, M., Fattet, L., Germann, S., Lambert, M.-P., Neil, H., Zonta, E., Mortada, H., Gratadou, L., Deygas, M., et al. (2014). RNA Helicases DDX5 and DDX17 Dynamically Orchestrate Transcription, miRNA, and Splicing Programs in Cell Differentiation. *Cell Rep.* 7, 1900–1913.

Daugeron, M.-C., and Linder, P. (2001). Characterization and mutational analysis of yeast Dbp8p, a putative RNA helicase involved in ribosome biogenesis. *Nucleic Acids Res.* 29, 1144–1155.

Decatur, W.A., and Fournier, M.J. (2002). rRNA modifications and ribosome function.

Trends Biochem. Sci. 27, 344–351.

Dembowski, J.A., Ramesh, M., McManus, C.J., and Woolford, J.L. (2013). Identification of the binding site of Rlp7 on assembling 60S ribosomal subunits in *Saccharomyces cerevisiae*. *RNA* 19, 1639–1647.

Diges, C.M., and Uhlenbeck, O.C. (2001). *Escherichia coli* DbpA is an RNA helicase that requires hairpin 92 of 23S rRNA. *EMBO J.* 20, 5503–5512.

Donati, G., Peddigari, S., Mercer, C.A., and Thomas, G. (2013). 5S Ribosomal RNA Is an Essential Component of a Nascent Ribosomal Precursor Complex that Regulates the Hdm2-p53 Checkpoint. *Cell Rep.* 4, 87–98.

Dunbar, D.A., and Baserga, S.J. (1998). The U14 snoRNA is required for 2'-O-methylation of the pre-18S rRNA in *Xenopus* oocytes. *RNA* 4, 195–204.

Dutca, L.M., Gallagher, J.E.G., and Baserga, S.J. (2011). The initial U3 snoRNA:pre-rRNA base pairing interaction required for pre-18S rRNA folding revealed by in vivo chemical probing. *Nucleic Acids Res.* 39, 5164–5180.

Elbashir, S.M., Harborth, J., Lendeckel, W., Yalcin, A., Weber, K., and Tuschl, T. (2001). Duplexes of 21-nucleotide RNAs mediate RNA interference in cultured mammalian cells. *Nature* 411, 494–498.

Enright, C.A., Maxwell, E.S., Eliceiri, G.L., and Sollner-Webb, B. (1996). 5'ETS rRNA processing facilitated by four small RNAs: U14, E3, U17, and U3. *RNA* 2, 1094–1099.

Fairman-Williams, M.E., Guenther, U.-P., and Jankowsky, E. (2010). SF1 and SF2 helicases: family matters. *Curr. Opin. Struct. Biol.* 20, 313–324.

Farley-Barnes, K.I., McCann, K.L., Ogawa, L.M., Merkel, J., Surovtseva, Y. V., and Baserga, S.J. (2018). Diverse Regulators of Human Ribosome Biogenesis Discovered by Changes in Nucleolar Number. *Cell Rep.* 22, 1923–1934.

Faza, M.B., Chang, Y., Occhipinti, L., Kemmler, S., and Panse, V.G. (2012). Role of Mex67-Mtr2 in the Nuclear Export of 40S Pre-Ribosomes. *PLoS Genet.* 8, e1002915.

Fedoriw, A.M., Starmer, J., Yee, D., and Magnuson, T. (2012). Nucleolar Association and Transcriptional Inhibition through 5S rDNA in Mammals. *PLoS Genet.* 8, e1002468.

Ferreira-Cerca, S., Pöll, G., Gleizes, P.-E., Tschochner, H., and Milkereit, P. (2005). Roles of Eukaryotic Ribosomal Proteins in Maturation and Transport of Pre-18S rRNA and Ribosome Function. *Mol. Cell* 20, 263–275.

Ferreira-Cerca, S., Pöll, G., Kühn, H., Neueder, A., Jakob, S., Tschochner, H., and Milkereit, P. (2007). Analysis of the In Vivo Assembly Pathway of Eukaryotic 40S Ribosomal Proteins. *Mol. Cell* 28, 446–457.

Fica, S.M., and Nagai, K. (2017). Cryo-electron microscopy snapshots of the spliceosome: structural insights into a dynamic ribonucleoprotein machine. *Nat. Struct. Mol. Biol.* 24, 791–799.

Fischer, N., and Weis, K. (2002). The DEAD box protein Dhh1 stimulates the decapping enzyme Dcp1. *EMBO J.* 21, 2788–2797.

Flygare, J., Aspesi, A., Bailey, J.C., Miyake, K., Caffrey, J.M., Karlsson, S., and Ellis, S.R. (2006). Human RPS19, the gene mutated in Diamond-Blackfan anemia, encodes a ribosomal protein required for the maturation of 40S ribosomal subunits. *Blood* 109, 980–986.

Fu, X.-D., and Ares, M. (2014). Context-dependent control of alternative splicing by RNA-binding proteins. *Nat. Rev. Genet.* 15, 689–701.

García-García, C., Frieda, K.L., Feoktistova, K., Fraser, C.S., and Block, S.M. (2015). RNA BIOCHEMISTRY. Factor-dependent processivity in human eIF4A DEAD-box helicase. *Science* 348, 1486–1488.

Gartmann, M., Blau, M., Armache, J.-P., Mielke, T., Topf, M., and Beckmann, R. (2010). Mechanism of eIF6-mediated Inhibition of Ribosomal Subunit Joining. *J. Biol. Chem.* 285, 14848–14851.

Ghalei, H., Schaub, F.X., Doherty, J.R., Noguchi, Y., Roush, W.R., Cleveland, J.L., Stroupe, M.E., and Karbstein, K. (2015). Hrr25/CK1 δ -directed release of Ltv1 from pre-40S ribosomes is necessary for ribosome assembly and cell growth. *J. Cell Biol.* 208, 745–759.

Gilman, B., Tijerina, P., and Russell, R. (2017). Distinct RNA-unwinding mechanisms of DEAD-box and DEAH-box RNA helicase proteins in remodeling structured RNAs and RNPs. *Biochem. Soc. Trans.* 45, 1313–1321.

Gorbalenya, A.E., and Koonin, E. V. (1993). Helicases: amino acid sequence comparisons and structure-function relationships. *Curr. Opin. Struct. Biol.* 3, 419–429.

Gross, T., Siepmann, A., Sturm, D., Windgassen, M., Scarcelli, J.J., Seedorf, M., Cole, C.N., and Krebber, H. (2007). The DEAD-Box RNA Helicase Dbp5 Functions in Translation Termination. *Science* (80-.). 315, 646–649.

Guenther, U.-P., and Jankowsky, E. (2009). Helicase Multitasking in Ribosome Assembly. *Mol. Cell* 36, 537–538.

Güttler, T., and Görlich, D. (2011). Ran-dependent nuclear export mediators: a structural perspective. *EMBO J.* 30, 3457–3474.

Haag, S., Kretschmer, J., Sloan, K.E., and Bohnsack, M.T. (2017). Crosslinking Methods to Identify RNA Methyltransferase Targets In Vivo. (Humana Press, New York, NY), pp. 269–281.

Halaby, M.-J., Li, Y., Harris, B.R., Jiang, S., Miskimins, W.K., Cleary, M.P., and Yang, D.-Q. (2015). Translational Control Protein 80 Stimulates IRES-Mediated Translation of p53 mRNA in Response to DNA Damage. *Biomed Res. Int.* 2015, 708158.

Hamann, F., Enders, M., and Ficner, R. (2019). Structural basis for RNA translocation by DEAH-box ATPases. *Nucleic Acids Res.* 47, 4349–4362.

He, Y., Andersen, G.R., and Nielsen, K.H. (2010). Structural basis for the function of DEAH helicases. *EMBO Rep.* 11, 180–186.

He, Y., Staley, J.P., Andersen, G.R., and Nielsen, K.H. (2017). Structure of the DEAH/RHA ATPase Prp43p bound to RNA implicates a pair of hairpins and motif Va in translocation along RNA. *RNA* 23, 1110–1124.

Heininger, A.U., Hackert, P., Andreou, A.Z., Boon, K.-L., Memet, I., Prior, M., Clancy, A., Schmidt, B., Urlaub, H., Schleiff, E., et al. (2016). Protein cofactor competition regulates the

action of a multifunctional RNA helicase in different pathways. *RNA Biol.* 13, 320–330.

Henras, A.K., Soudet, J., G erus, M., Lebaron, S., Caizergues-Ferrer, M., Mougin, A., and Henry, Y. (2008). The post-transcriptional steps of eukaryotic ribosome biogenesis. *Cell. Mol. Life Sci.* 65, 2334–2359.

Henras, A.K., Plisson-Chastang, C., O'Donohue, M.-F., Chakraborty, A., and Gleizes, P.-E. (2015). An overview of pre-ribosomal RNA processing in eukaryotes. *Wiley Interdiscip. Rev. RNA* 6, 225–242.

Henras, A.K., Plisson-Chastang, C., Humbert, O., Romeo, Y., and Henry, Y. (2017). Synthesis, Function, and Heterogeneity of snoRNA-Guided Posttranscriptional Nucleoside Modifications in Eukaryotic Ribosomal RNAs. In *The Enzymes*, pp. 169–213.

Hilbert, M., Karow, A.R., and Klostermeier, D. (2009). The mechanism of ATP-dependent RNA unwinding by DEAD box proteins. *Biol. Chem.* 390, 1237–1250.

Hilbert, M., Kebbel, F., Gubaev, A., and Klostermeier, D. (2011). eIF4G stimulates the activity of the DEAD box protein eIF4A by a conformational guidance mechanism. *Nucleic Acids Res.* 39, 2260–2270.

Hilliker, A., Gao, Z., Jankowsky, E., and Parker, R. (2011). The DEAD-box protein Ded1 modulates translation by the formation and resolution of an eIF4F-mRNA complex. *Mol. Cell* 43, 962–972.

Hooper, C., and Hilliker, A. (2013). Packing them up and dusting them off: RNA helicases and mRNA storage. *Biochim. Biophys. Acta - Gene Regul. Mech.* 1829, 824–834.

Hughes, J.M., and Ares, M. (1991). Depletion of U3 small nucleolar RNA inhibits cleavage in the 5' external transcribed spacer of yeast pre-ribosomal RNA and impairs formation of 18S ribosomal RNA. *EMBO J.* 10, 4231–4239.

Huh, W.-K., Falvo, J. V., Gerke, L.C., Carroll, A.S., Howson, R.W., Weissman, J.S., and O'Shea, E.K. (2003). Global analysis of protein localization in budding yeast. *Nature* 425, 686–691.

Jagessar, K.L., and Jain, C. (2010). Functional and molecular analysis of *Escherichia coli*

strains lacking multiple DEAD-box helicases. *RNA* 16, 1386–1392.

Jankowsky, E., and Fairman, M.E. (2007). RNA helicases — one fold for many functions. *Curr. Opin. Struct. Biol.* 17, 316–324.

Jarmoskaite, I., and Russell, R. (2014). RNA Helicase Proteins as Chaperones and Remodelers. *Annu. Rev. Biochem.* 83, 697–725.

Karginov, F. V., Caruthers, J.M., Hu, Y., McKay, D.B., and Uhlenbeck, O.C. (2005). YxiN Is a Modular Protein Combining a DEx^D/H Core and a Specific RNA-binding Domain. *J. Biol. Chem.* 280, 35499–35505.

Khajuria, R.K., Munschauer, M., Ulirsch, J.C., Panse, V.G., Carr, S.A., and Sankaran Correspondence, V.G. (2018). Ribosome Levels Selectively Regulate Translation and Lineage Commitment in Human Hematopoiesis In Brief. *Cell* 173, 90-103.e19.

Kiianitsa, K., Solinger, J.A., and Heyer, W.-D. (2003). NADH-coupled microplate photometric assay for kinetic studies of ATP-hydrolyzing enzymes with low and high specific activities. *Anal. Biochem.* 321, 266–271.

King, T.H., Liu, B., McCully, R.R., and Fournier, M.J. (2003). Ribosome structure and activity are altered in cells lacking snoRNPs that form pseudouridines in the peptidyl transferase center. *Mol. Cell* 11, 425–435.

Klinge, S., and Woolford, J.L. (2019). Ribosome assembly coming into focus. *Nat. Rev. Mol. Cell Biol.* 20, 116–131.

Klinge, S., Voigts-Hoffmann, F., Leibundgut, M., Arpagaus, S., and Ban, N. (2011). Crystal Structure of the Eukaryotic 60S Ribosomal Subunit in Complex with Initiation Factor 6. *Science* (80-.). 334, 941–948.

Klinge, S., Voigts-Hoffmann, F., Leibundgut, M., and Ban, N. (2012). Atomic structures of the eukaryotic ribosome. *Trends Biochem. Sci.* 37, 189–198.

Knight, S., Vulliamy, T., Morgan, B., Devriendt, K., Mason, P., and Dokal, I. (2001). Identification of novel DKC1 mutations in patients with dyskeratosis congenita: implications for pathophysiology and diagnosis. *Hum. Genet.* 108, 299–303.

Koš, M., and Tollervey, D. (2005). The Putative RNA Helicase Dbp4p Is Required for Release of the U14 snoRNA from Preribosomes in *Saccharomyces cerevisiae*. *Mol. Cell* 20, 53–64.

Kressler, D., Doère, M., Rojo, M., and Linder, P. (1999). Synthetic lethality with conditional *dbp6* alleles identifies *rsa1p*, a nucleoplasmic protein involved in the assembly of 60S ribosomal subunits. *Mol. Cell. Biol.* 19, 8633–8645.

de la Cruz, J., Kressler, D., Rojo, M., Tollervey, D., and Linder, P. (1998). Spb4p, an essential putative RNA helicase, is required for a late step in the assembly of 60S ribosomal subunits in *Saccharomyces cerevisiae*. *RNA* 4, 1268–1281.

de la Cruz, J., Karbstein, K., and Woolford, J.L. (2015). Functions of Ribosomal Proteins in Assembly of Eukaryotic Ribosomes In Vivo. *Annu. Rev. Biochem.* 84, 93–129.

Laemmli, U.K. (1970). Cleavage of structural proteins during the assembly of the head of bacteriophage T4. *Nature* 227, 680–685.

Lafontaine, D.L., Preiss, T., and Tollervey, D. (1998). Yeast 18S rRNA dimethylase Dim1p: a quality control mechanism in ribosome synthesis? *Mol. Cell. Biol.* 18, 2360–2370.

Landry-Voyer, A.-M., Bilodeau, S., Bergeron, D., Dionne, K.L., Port, S.A., Rouleau, C., Boisvert, F.-M., Kehlenbach, R.H., and Bachand, F. (2016). Human PDCD2L Is an Export Substrate of CRM1 That Associates with 40S Ribosomal Subunit Precursors. *Mol. Cell. Biol.* 36, 3019–3032.

Larburu, N., Montellese, C., O'Donohue, M.-F., Kutay, U., Gleizes, P.-E., and Plisson-Chastang, C. (2016). Structure of a human pre-40S particle points to a role for RACK1 in the final steps of 18S rRNA processing. *Nucleic Acids Res.* 44, 8465–8478.

Lattmann, S., Giri, B., Vaughn, J.P., Akman, S.A., and Nagamine, Y. (2010). Role of the amino terminal RHAU-specific motif in the recognition and resolution of guanine quadruplex-RNA by the DEAH-box RNA helicase RHAU. *Nucleic Acids Res.* 38, 6219–6233.

Lazdins, I.B., Delannoy, M., and Sollner-Webb, B. (1997). Analysis of nucleolar transcription and processing domains and pre-rRNA movements by in situ hybridization. *Chromosoma*

105, 481–495.

Lebaron, S., Papin, C., Capeyrou, R., Chen, Y.-L., Froment, C., Monsarrat, B., Caizergues-Ferrer, M., Grigoriev, M., and Henry, Y. (2009). The ATPase and helicase activities of Prp43p are stimulated by the G-patch protein Pfa1p during yeast ribosome biogenesis. *EMBO J.* 28, 3808–3819.

Leeds, N.B., Small, E.C., Hiley, S.L., Hughes, T.R., and Staley, J.P. (2006). The Splicing Factor Prp43p, a DEAH Box ATPase, Functions in Ribosome Biogenesis. *Mol. Cell. Biol.* 26, 513–522.

Léger-Silvestre, I., Milkereit, P., Ferreira-Cerca, S., Saveanu, C., Rousselle, J.-C., Choismel, V., Guinefoleau, C., Gas, N., and Gleizes, P.-E. (2004). The ribosomal protein Rps15p is required for nuclear exit of the 40S subunit precursors in yeast. *EMBO J.* 23, 2336–2347.

Lewis, J.D., and Tollervey, D. (2000). Like attracts like: getting RNA processing together in the nucleus. *Science* 288, 1385–1389.

Li, H.D., Zagorski, J., and Fournier, M.J. (1990). Depletion of U14 small nuclear RNA (snR128) disrupts production of 18S rRNA in *Saccharomyces cerevisiae*. *Mol. Cell. Biol.* 10, 1145–1152.

Liang, W.Q., and Fournier, M.J. (1995). U14 base-pairs with 18S rRNA: a novel snoRNA interaction required for rRNA processing. *Genes Dev.* 9, 2433–2443.

Liang, X. -h., and Fournier, M.J. (2006). The Helicase Has1p Is Required for snoRNA Release from Pre-rRNA. *Mol. Cell. Biol.* 26, 7437–7450.

Lin, D., Pestova, T. V., Hellen, C.U.T., and Tiedge, H. (2008). Translational Control by a Small RNA: Dendritic BC1 RNA Targets the Eukaryotic Initiation Factor 4A Helicase Mechanism. *Mol. Cell. Biol.* 28, 3008.

Linder, P. (2006). Dead-box proteins: a family affair—active and passive players in RNP-remodeling. *Nucleic Acids Res.* 34, 4168–4180.

Linder, P., and Jankowsky, E. (2011). From unwinding to clamping — the DEAD box RNA

helicase family. *Nat. Rev. Mol. Cell Biol.* *12*, 505–516.

Littlefield, J.W., and Dunn, D.B. (1958a). Natural occurrence of thymine and three methylated adenine bases in several ribonucleic acids. *Nature* *181*, 254–255.

Littlefield, J.W., and Dunn, D.B. (1958b). The occurrence and distribution of thymine and three methylated-adenine bases in ribonucleic acids from several sources. *Biochem. J.* *70*, 642–651.

Liu, J.M., and Ellis, S.R. (2006). Ribosomes and marrow failure: Coincidental association or molecular paradigm? *Blood* *107*, 4583–4588.

Liu, F., Putnam, A., and Jankowsky, E. (2008). ATP hydrolysis is required for DEAD-box protein recycling but not for duplex unwinding. *Proc. Natl. Acad. Sci.* *105*, 20209–20214.

Liu, Y., Deisenroth, C., and Zhang, Y. (2016). RP-MDM2-p53 Pathway: Linking Ribosomal Biogenesis and Tumor Surveillance. *Trends in Cancer* *2*, 191–204.

Lo, K.-Y., Li, Z., Bussiere, C., Bresson, S., Marcotte, E.M., and Johnson, A.W. (2010). Defining the pathway of cytoplasmic maturation of the 60S ribosomal subunit. *Mol. Cell* *39*, 196–208.

Long, E.O., and Dawid, I.B. (1980). Repeated Genes in Eukaryotes. *Annu. Rev. Biochem.* *49*, 727–764.

Ludwig, L.S., Gazda, H.T., Eng, J.C., Eichhorn, S.W., Thiru, P., Ghazvinian, R., George, T.I., Gotlib, J.R., Beggs, A.H., Sieff, C.A., et al. (2014). Altered translation of GATA1 in Diamond-Blackfan anemia. *Nat. Med.* *20*, 748–753.

Luo, M.-J., Zhou, Z., Magni, K., Christoforides, C., Rappsilber, J., Mann, M., and Reed, R. (2001). Pre-mRNA splicing and mRNA export linked by direct interactions between UAP56 and Aly. *Nature* *413*, 644–647.

Lygerou, Z., Allmang, C., Tollervey, D., and Seraphin, B. (1996). Accurate Processing of a Eukaryotic Precursor Ribosomal RNA by Ribonuclease MRP in Vitro. *Science* (80-.). *272*, 268–270.

Lykke-Andersen, S., and Jensen, T.H. (2015). Nonsense-mediated mRNA decay: an intricate machinery that shapes transcriptomes. *Nat. Rev. Mol. Cell Biol.* *16*, 665–677.

Mallam, A.L., Jarmoskaite, I., Tijerina, P., Campo, M. Del, Seifert, S., Guo, L., Russell, R., and Lambowitz, A.M. (2011). Solution structures of DEAD-box RNA chaperones reveal conformational changes and nucleic acid tethering by a basic tail. *Proc. Natl. Acad. Sci.* *108*, 12254–12259.

Mallam, A.L., Del Campo, M., Gilman, B., Sidote, D.J., and Lambowitz, A.M. (2012). Structural basis for RNA-duplex recognition and unwinding by the DEAD-box helicase Mss116p. *Nature* *490*, 121–125.

Malygin, A.A., Parakhnevitch, N.M., Ivanov, A. V., Eperon, I.C., and Karpova, G.G. (2007). Human ribosomal protein S13 regulates expression of its own gene at the splicing step by a feedback mechanism. *Nucleic Acids Res.* *35*, 6414–6423.

Manojlovic, Z., and Stefanovic, B. (2012). A novel role of RNA helicase A in regulation of translation of type I collagen mRNAs. *RNA* *18*, 321–334.

Martin, R., Straub, A.U., Doebele, C., and Bohnsack, M.T. (2013). DExD/H-box RNA helicases in ribosome biogenesis. *RNA Biol.* *10*, 4–18.

Martin, R., Hackert, P., Ruprecht, M., Simm, S., Brüning, L., Mirus, O., Sloan, K.E., Kudla, G., Schleiff, E., and Bohnsack, M.T. (2014). A pre-ribosomal RNA interaction network involving snoRNAs and the Rok1 helicase. *RNA* *20*, 1173–1182.

Matsuo, Y., Granneman, S., Thoms, M., Manikas, R.-G., Tollervey, D., and Hurt, E. (2014). Coupled GTPase and remodelling ATPase activities form a checkpoint for ribosome export. *Nature* *505*, 112–116.

Melnikov, S., Ben-Shem, A., Garreau de Loubresse, N., Jenner, L., Yusupova, G., and Yusupov, M. (2012). One core, two shells: bacterial and eukaryotic ribosomes. *Nat. Struct. Mol. Biol.* *19*, 560–567.

Memet, I., Doebele, C., Sloan, K.E., and Bohnsack, M.T. (2017). The G-patch protein NF- κ B-repressing factor mediates the recruitment of the exonuclease XRN2 and activation of the RNA helicase DHX15 in human ribosome biogenesis. *Nucleic Acids Res.* *45*, gkx013.

Michelle, L., Cloutier, A., Toutant, J., Shkreta, L., Thibault, P., Durand, M., Garneau, D., Gendron, D., Lapointe, E., Couture, S., et al. (2012). Proteins associated with the exon junction complex also control the alternative splicing of apoptotic regulators. *Mol. Cell. Biol.* 32, 954–967.

Michot, B., Joseph, N., Mazan, S., and Bachellerie, J.P. (1999). Evolutionarily conserved structural features in the ITS2 of mammalian pre-rRNAs and potential interactions with the snoRNA U8 detected by comparative analysis of new mouse sequences. *Nucleic Acids Res.* 27, 2271–2282.

Mills, E.W., and Green, R. (2017). Ribosomopathies: There's strength in numbers. *Science* (80-.). 358, eaan2755.

Mohr, G., Del Campo, M., Mohr, S., Yang, Q., Jia, H., Jankowsky, E., and Lambowitz, A.M. (2008). Function of the C-terminal Domain of the DEAD-box Protein Mss116p Analyzed in Vivo and in Vitro. *J. Mol. Biol.* 375, 1344–1364.

Montellese, C., Montel-Lehry, N., Henras, A.K., Kutay, U., Gleizes, P.-E., and O'Donohue, M.-F. (2017). Poly(A)-specific ribonuclease is a nuclear ribosome biogenesis factor involved in human 18S rRNA maturation. *Nucleic Acids Res.* 45, 6822–6836.

Moy, R.H., Cole, B.S., Yasunaga, A., Gold, B., Shankarling, G., Varble, A., Molleston, J.M., tenOever, B.R., Lynch, K.W., and Cherry, S. (2014). Stem-Loop Recognition by DDX17 Facilitates miRNA Processing and Antiviral Defense. *Cell* 158, 764–777.

Mukhopadhyay, R., Jia, J., Arif, A., Ray, P.S., and Fox, P.L. (2009). The GAIT system: a gatekeeper of inflammatory gene expression. *Trends Biochem. Sci.* 34, 324–331.

Mullineux, S.-T., and Lafontaine, D.L.J. (2012). Mapping the cleavage sites on mammalian pre-rRNAs: where do we stand? *Biochimie* 94, 1521–1532.

Murzin, A.G. (1993). OB(oligonucleotide/oligosaccharide binding)-fold: common structural and functional solution for non-homologous sequences. *EMBO J.* 12, 861.

Naoko Tanaka, and Schwer, B. (2005). Characterization of the NTPase, RNA-Binding, and RNA Helicase Activities of the DEAH-Box Splicing Factor Prp22†.

Napetschnig, J., Kassube, S.A., Debler, E.W., Wong, R.W., Blobel, G., and Hoelz, A. (2009). Structural and functional analysis of the interaction between the nucleoporin Nup214 and the DEAD-box helicase Ddx19. *Proc. Natl. Acad. Sci.* *106*, 3089–3094.

Narla, A., and Ebert, B.L. (2010). Ribosomopathies: human disorders of ribosome dysfunction. *Blood* *115*, 3196–3205.

O'Donohue, M.-F., Choessel, V., Faublader, M., Fichant, G., and Gleizes, P.-E. (2010). Functional dichotomy of ribosomal proteins during the synthesis of mammalian 40S ribosomal subunits. *J. Cell Biol.* *190*, 853–866.

Oeffinger, M., Dlakic, M., and Tollervey, D. (2004). A pre-ribosome-associated HEAT-repeat protein is required for export of both ribosomal subunits. *Genes Dev.* *18*, 196–209.

Oie, S., Matsuzaki, K., Yokoyama, W., Tokunaga, S., Waku, T., Han, S.-I., Iwasaki, N., Mikogai, A., Yasuzawa-Tanaka, K., Kishimoto, H., et al. (2014). Hepatic rRNA Transcription Regulates High-Fat-Diet-Induced Obesity. *Cell Rep.* *7*, 807–820.

Ozgur, S., Buchwald, G., Falk, S., Chakrabarti, S., Prabu, J.R., and Conti, E. (2015). The conformational plasticity of eukaryotic RNA-dependent ATPases. *FEBS J.* *282*, 850–863.

Pause, A., and Sonenberg, N. (1992). Mutational analysis of a DEAD box RNA helicase: the mammalian translation initiation factor eIF-4A. *EMBO J.* *11*, 2643–2654.

Peculis, B.A., and Steitz, J.A. (1993). Disruption of U8 nucleolar snRNA inhibits 5.8S and 28S rRNA processing in the *Xenopus* oocyte. *Cell* *73*, 1233–1245.

Pelava, A., Schneider, C., and Watkins, N.J. (2016). The importance of ribosome production, and the 5S RNP-MDM2 pathway, in health and disease. *Biochem. Soc. Trans.* *44*, 1086–1090.

Pertschy, B., Saveanu, C., Zisser, G., Lebreton, A., Tengg, M., Jacquier, A., Liebming, E., Nobis, B., Kappel, L., van der Klei, I., et al. (2007). Cytoplasmic recycling of 60S preribosomal factors depends on the AAA protein Drg1. *Mol. Cell. Biol.* *27*, 6581–6592.

Pertschy, B., Schneider, C., Gnädig, M., Schäfer, T., Tollervey, D., and Hurt, E. (2009). RNA Helicase Prp43 and Its Co-factor Pfa1 Promote 20 to 18 S rRNA Processing Catalyzed

by the Endonuclease Nob1. *J. Biol. Chem.* *284*, 35079–35091.

Petrov, A.S., Bernier, C.R., Hsiao, C., Norris, A.M., Kovacs, N.A., Waterbury, C.C., Stepanov, V.G., Harvey, S.C., Fox, G.E., Wartell, R.M., et al. (2014). Evolution of the ribosome at atomic resolution. *Proc. Natl. Acad. Sci. U. S. A.* *111*, 10251–10256.

Phipps, K.R., Charette, J.M., and Baserga, S.J. (2011). The small subunit processome in ribosome biogenesis—progress and prospects. *Wiley Interdiscip. Rev. RNA* *2*, 1–21.

Pillet, B., Mitterer, V., Kressler, D., and Pertschy, B. (2017). Hold on to your friends: Dedicated chaperones of ribosomal proteins. *BioEssays* *39*, e201600153.

Polprasert, C., Schulze, I., Sekeres, M.A., Makishima, H., Przychodzen, B., Hosono, N., Singh, J., Padgett, R.A., Gu, X., Phillips, J.G., et al. (2015). Inherited and Somatic Defects in DDX41 in Myeloid Neoplasms. *Cancer Cell* *27*, 658–670.

Ponting, C.P. (2000). Novel eIF4G domain homologues linking mRNA translation with nonsense-mediated mRNA decay. *Trends Biochem. Sci.* *25*, 423–426.

Preti, M., O'Donohue, M.-F., Montel-Lehry, N., Bortolin-Cavaillé, M.-L., Choessel, V., and Gleizes, P.-E. (2013). Gradual processing of the ITS1 from the nucleolus to the cytoplasm during synthesis of the human 18S rRNA. *Nucleic Acids Res.* *41*, 4709–4723.

Putnam, A.A., and Jankowsky, E. (2013). DEAD-box helicases as integrators of RNA, nucleotide and protein binding. *Biochim. Biophys. Acta - Gene Regul. Mech.* *1829*, 884–893.

Pyle, A.M. (2008). Translocation and Unwinding Mechanisms of RNA and DNA Helicases. *Annu. Rev. Biophys.* *37*, 317–336.

Raman, N., Weir, E., and Müller, S. (2016). The AAA ATPase MDN1 Acts as a SUMO-Targeted Regulator in Mammalian Pre-ribosome Remodeling. *Mol. Cell* *64*, 607–615.

Robert-Paganin, J., Réty, S., and Leulliot, N. (2015a). Regulation of DEAH/RHA Helicases by G-Patch Proteins. *Biomed Res. Int.* *2015*.

Robert-Paganin, J., Réty, S., and Leulliot, N. (2015b). Regulation of DEAH/RHA Helicases

by G-Patch Proteins. *Biomed Res. Int.* 2015, 1–9.

Robledo, S., Idol, R.A., Crimmins, D.L., Ladenson, J.H., Mason, P.J., and Bessler, M. (2008). The role of human ribosomal proteins in the maturation of rRNA and ribosome production. *RNA* 14, 1918–1929.

Rodríguez-Galán, O., García-Gómez, J.J., and de la Cruz, J. (2013). Yeast and human RNA helicases involved in ribosome biogenesis: Current status and perspectives. *Biochim. Biophys. Acta - Gene Regul. Mech.* 1829, 775–790.

Rogers, G.W., Richter, N.J., and Merrick, W.C. (1999). Biochemical and Kinetic Characterization of the RNA Helicase Activity of Eukaryotic Initiation Factor 4A. *J. Biol. Chem.* 274, 12236–12244.

Rosado, I. V, Kressler, D., and de la Cruz, J. (2007). Functional analysis of *Saccharomyces cerevisiae* ribosomal protein Rpl3p in ribosome synthesis. *Nucleic Acids Res.* 35, 4203–4213.

Rudolph, M.G., and Klostermeier, D. (2015). When core competence is not enough: functional interplay of the DEAD-box helicase core with ancillary domains and auxiliary factors in RNA binding and unwinding. *Biol. Chem.* 396.

Sardana, R., Liu, X., Granneman, S., Zhu, J., Gill, M., Papoulas, O., Marcotte, E.M., Tollervey, D., Correll, C.C., and Johnson, A.W. (2015). The DEAH-box Helicase Dhr1 Dissociates U3 from the Pre-rRNA to Promote Formation of the Central Pseudoknot. *PLOS Biol.* 13, e1002083.

Schilders, G., Egberts, W.V., Raijmakers, R., and Pruijn, G.J.M. (2007). C1D is a major autoantibody target in patients with the polymyositis–scleroderma overlap syndrome. *Arthritis Rheum.* 56, 2449–2454.

Schillewaert, S., Wacheul, L., Lhomme, F., and Lafontaine, D.L.J. (2012). The evolutionarily conserved protein Las1 is required for pre-rRNA processing at both ends of ITS2. *Mol. Cell. Biol.* 32, 430–444.

Schütz, P., Bumann, M., Oberholzer, A.E., Bieniossek, C., Trachsel, H., Altmann, M., and Baumann, U. (2008). Crystal structure of the yeast eIF4A-eIF4G complex: an RNA-helicase

controlled by protein-protein interactions. *Proc. Natl. Acad. Sci. U. S. A.* *105*, 9564–9569.

Sekiguchi, T., Hayano, T., Yanagida, M., Takahashi, N., and Nishimoto, T. (2006). NOP132 is required for proper nucleolus localization of DEAD-box RNA helicase DDX47. *Nucleic Acids Res.* *34*, 4593.

Semlow, D.R., and Staley, J.P. (2012). Staying on message: ensuring fidelity in pre-mRNA splicing. *Trends Biochem. Sci.* *37*, 263–273.

Semlow, D.R., Blanco, M.R., Walter, N.G., and Staley, J.P. (2016). Spliceosomal DEAH-Box ATPases Remodel Pre-mRNA to Activate Alternative Splice Sites. *Cell* *164*, 985–998.

Senger, B., Lafontaine, D.L., Graindorge, J.S., Gadai, O., Camasses, A., Sanni, A., Garnier, J.M., Breitenbach, M., Hurt, E., and Fasiolo, F. (2001). The nucle(ol)ar Tif6p and Efl1p are required for a late cytoplasmic step of ribosome synthesis. *Mol. Cell* *8*, 1363–1373.

Sentenac, A. (1985). Eukaryotic RNA polymerases. *CRC Crit. Rev. Biochem.* *18*, 31–90.

Sharma, K., and Tollervey, D. (1999). Base pairing between U3 small nucleolar RNA and the 5' end of 18S rRNA is required for pre-rRNA processing. *Mol. Cell. Biol.* *19*, 6012–6019.

Sharma, S., Langhendries, J.-L., Watzinger, P., Kötter, P., Entian, K.-D., and Lafontaine, D.L.J. (2015). Yeast Kre33 and human NAT10 are conserved 18S rRNA cytosine acetyltransferases that modify tRNAs assisted by the adaptor Tan1/THUMP1. *Nucleic Acids Res.* *43*, 2242–2258.

SHWACHMAN, H., DIAMOND, L.K., OSKI, F.A., and KHAW, K.T. (1964). THE SYNDROME OF PANCREATIC INSUFFICIENCY AND BONE MARROW DYSFUNCTION. *J. Pediatr.* *65*, 645–663.

Simsek, D., Tiu, G.C., Flynn, R.A., Byeon, G.W., Leppek, K., Xu, A.F., Chang, H.Y., and Barna, M. (2017). The Mammalian Ribo-interactome Reveals Ribosome Functional Diversity and Heterogeneity. *Cell* *169*, 1051-1065.e18.

Singleton, M.R., Dillingham, M.S., and Wigley, D.B. (2007). Structure and Mechanism of Helicases and Nucleic Acid Translocases. *Annu. Rev. Biochem.* *76*, 23–50.

Sloan, K.E., and Bohnsack, M.T. (2018). Unravelling the Mechanisms of RNA Helicase Regulation. *Trends Biochem. Sci.* *43*, 237–250.

Sloan, K.E., Mattijssen, S., Lebaron, S., Tollervey, D., Pruijn, G.J.M., and Watkins, N.J. (2013a). Both endonucleolytic and exonucleolytic cleavage mediate ITS1 removal during human ribosomal RNA processing. *J. Cell Biol.* *200*, 577–588.

Sloan, K.E., Bohnsack, M.T., and Watkins, N.J. (2013b). The 5S RNP couples p53 homeostasis to ribosome biogenesis and nucleolar stress. *Cell Rep.* *5*, 237–247.

Sloan, K.E., Bohnsack, M.T., Schneider, C., and Watkins, N.J. (2014). The roles of SSU processome components and surveillance factors in the initial processing of human ribosomal RNA. *RNA* *20*, 540–550.

Sloan, K.E., Leisegang, M.S., Doebele, C., Ramírez, A.S., Simm, S., Safferthal, C., Kretschmer, J., Schorge, T., Markoutsas, S., Haag, S., et al. (2015). The association of late-acting snoRNPs with human pre-ribosomal complexes requires the RNA helicase DDX21. *Nucleic Acids Res.* *43*, 553–564.

Sloan, K.E., Gleizes, P.-E., and Bohnsack, M.T. (2016). Nucleocytoplasmic Transport of RNAs and RNA–Protein Complexes. *J. Mol. Biol.* *428*, 2040–2059.

Sloan, K.E., Warda, A.S., Sharma, S., Entian, K.-D., Lafontaine, D.L.J., and Bohnsack, M.T. (2017). Tuning the ribosome: The influence of rRNA modification on eukaryotic ribosome biogenesis and function. *RNA Biol.* *14*, 1138–1152.

Sloan, K.E., Knox, A.A., Wells, G.R., Schneider, C., and Watkins, N.J. (2019). Interactions and activities of factors involved in the late stages of human 18S rRNA maturation. *RNA Biol.* *16*, 196–210.

Smith, J.E., Cooperman, B.S., and Mitchell, P. (1992). Methylation sites in *Escherichia coli* ribosomal RNA: localization and identification of four new sites of methylation in 23S rRNA. *Biochemistry* *31*, 10825–10834.

Soltanieh, S., Osheim, Y.N., Spasov, K., Trahan, C., Beyer, A.L., and Dragon, F. (2015). DEAD-Box RNA Helicase Dbp4 Is Required for Small-Subunit Processome Formation and Function. *Mol. Cell. Biol.* *35*, 816–830.

Song, C., Hotz-Wagenblatt, A., Voit, R., and Grummt, I. (2017). SIRT7 and the DEAD-box helicase DDX21 cooperate to resolve genomic R loops and safeguard genome stability. *Genes Dev.* 31, 1370–1381.

Squatrito, M., Mancino, M., Donzelli, M., Areces, L.B., and Draetta, G.F. (2004). EBP1 is a nucleolar growth-regulating protein that is part of pre-ribosomal ribonucleoprotein complexes. *Oncogene* 23, 4454–4465.

Srivastava, L., Lapik, Y.R., Wang, M., and Pestov, D.G. (2010). Mammalian DEAD box protein Ddx51 acts in 3' end maturation of 28S rRNA by promoting the release of U8 snoRNA. *Mol. Cell. Biol.* 30, 2947–2956.

Stage-Zimmermann, T., Schmidt, U., and Silver, P.A. (2000). Factors Affecting Nuclear Export of the 60S Ribosomal Subunit In Vivo. *Mol. Biol. Cell* 11, 3777–3789.

Steckelberg, A.-L., Boehm, V., Gromadzka, A.M., and Gehring, N.H. (2012). CWC22 Connects Pre-mRNA Splicing and Exon Junction Complex Assembly. *Cell Rep.* 2, 454–461.

Steitz, J.A., Berg, C., Hendrick, J.P., La Branche-Chabot, H., Metspalu, A., Rinke, J., and Yario, T. (1988). A 5S rRNA/L5 complex is a precursor to ribosome assembly in mammalian cells. *J. Cell Biol.* 106, 545–556.

Sun, Q., Zhu, X., Qi, J., An, W., Lan, P., Tan, D., Chen, R., Wang, B., Zheng, S., Zhang, C., et al. (2017). Molecular architecture of the 90S small subunit pre-ribosome. *Elife* 6.

Svitkin, Y. V., Pause, A., Haghghat, A., Pyronnet, S., Witherell, G., Belsham, G.J., and Sonenberg, N. (2001). The requirement for eukaryotic initiation factor 4A (eIF4A) in translation is in direct proportion to the degree of mRNA 5' secondary structure. *RNA* 7, 382–394.

Tafforeau, L., Zorbas, C., Langhendries, J.-L., Mullineux, S.-T., Stamatopoulou, V., Mullier, R., Wacheul, L., and Lafontaine, D.L.J. (2013). The Complexity of Human Ribosome Biogenesis Revealed by Systematic Nucleolar Screening of Pre-rRNA Processing Factors. *Mol. Cell* 51, 539–551.

Takei, S., Togo-Ohno, M., Suzuki, Y., and Kuroyanagi, H. (2016). Evolutionarily conserved

autoregulation of alternative pre-mRNA splicing by ribosomal protein L10a. *Nucleic Acids Res.* *44*, 5585–5596.

Talkish, J., Zhang, J., Jakovljevic, J., Horsey, E.W., and Woolford, J.L. (2012). Hierarchical recruitment into nascent ribosomes of assembly factors required for 27SB pre-rRNA processing in *Saccharomyces cerevisiae*. *Nucleic Acids Res.* *40*, 8646–8661.

Talwar, T., Vidhyasagar, V., Qing, J., Guo, M., Kariem, A., Lu, Y., Singh, R.S., Lukong, K.E., and Wu, Y. (2017). The DEAD-box protein DDX43 (HAGE) is a dual RNA-DNA helicase and has a K-homology domain required for full nucleic acid unwinding activity. *J. Biol. Chem.* *292*, 10429–10443.

Tanaka, N., Aronova, A., and Schwer, B. (2007). Ntr1 activates the Prp43 helicase to trigger release of lariat-intron from the spliceosome. *Genes & Dev.* *21*, 2312–2325.

Tanner, N.K., Cordin, O., Banroques, J., Doère, M., and Linder, P. (2003). The Q motif: a newly identified motif in DEAD box helicases may regulate ATP binding and hydrolysis. *Mol. Cell* *11*, 127–138.

Tauchert, M.J., Fourmann, J.-B., Lührmann, R., and Ficner, R. (2017). Structural insights into the mechanism of the DEAH-box RNA helicase Prp43. *Elife* *6*.

Theobald, D.L., Mitton-Fry, R.M., and Wuttke, D.S. (2003). Nucleic Acid Recognition by OB-Fold Proteins. *Annu. Rev. Biophys. Biomol. Struct.* *32*, 115–133.

Tieg, B., and Krebber, H. (2013). Dbp5 — From nuclear export to translation. *Biochim. Biophys. Acta - Gene Regul. Mech.* *1829*, 791–798.

Tomecki, R., Labno, A., Draskowska, K., Cysewski, D., and Dziembowski, A. (2015). hUTP24 is essential for processing of the human rRNA precursor at site A₁, but not at site A₀. *RNA Biol.* *12*, 1010–1029.

Trainor, P.A., Dixon, J., and Dixon, M.J. (2009). Treacher Collins syndrome: etiology, pathogenesis and prevention. *Eur. J. Hum. Genet.* *17*, 275–283.

Turner, A.J., Knox, A.A., and Watkins, N.J. (2012). Nucleolar disruption leads to the spatial separation of key 18S rRNA processing factors. *RNA Biol.* *9*, 175–186.

Udem, S.A., and Warner, J.R. (1972). Ribosomal RNA synthesis in *Saccharomyces cerevisiae*. *J. Mol. Biol.* *65*, 227–242.

Venema, J., and Tollervey, D. (1995). Processing of pre-ribosomal RNA in *Saccharomyces cerevisiae*. *Yeast* *11*, 1629–1650.

Vincent, M., Geneviève, D., Ostertag, A., Marlin, S., Lacombe, D., Martin-Coignard, D., Coubes, C., David, A., Lyonnet, S., Vilain, C., et al. (2016). Treacher Collins syndrome: a clinical and molecular study based on a large series of patients. *Genet. Med.* *18*, 49–56.

Walbott, H., Mouffok, S., Capeyrou, R., Lebaron, S., Humbert, O., van Tilbeurgh, H., Henry, Y., and Leulliot, N. (2010). Prp43p contains a processive helicase structural architecture with a specific regulatory domain. *EMBO J.* *29*, 2194–2204.

Walker, J.E., Saraste, M., Runswick, M.J., and Gay, N.J. (1982). Distantly related sequences in the alpha- and beta-subunits of ATP synthase, myosin, kinases and other ATP-requiring enzymes and a common nucleotide binding fold. *EMBO J.* *1*, 945–951.

Wang, M., and Pestov, D.G. (2011). 5'-end surveillance by Xrn2 acts as a shared mechanism for mammalian pre-rRNA maturation and decay. *Nucleic Acids Res.* *39*, 1811–1822.

Wang, Z., Murigneux, V., and Le Hir, H. (2014). Transcriptome-wide modulation of splicing by the exon junction complex. *Genome Biol.* *15*, 551.

Warkocki, Z., Schneider, C., Mozaffari-Jovin, S., Schmitzová, J., Höbartner, C., Fabrizio, P., and Lührmann, R. (2015). The G-patch protein Spp2 couples the spliceosome-stimulated ATPase activity of the DEAH-box protein Prp2 to catalytic activation of the spliceosome. *Genes Dev.* *29*, 94–107.

Warner, J.R. (2001). Nascent ribosomes. *Cell* *107*, 133–136.

Watkins, N.J., and Bohnsack, M.T. (2012). The box C/D and H/ACA snoRNPs: key players in the modification, processing and the dynamic folding of ribosomal RNA. *Wiley Interdiscip. Rev. RNA* *3*, 397–414.

Weaver, P.L., Sun, C., and Chang, T.H. (1997). Dbp3p, a putative RNA helicase in

Saccharomyces cerevisiae, is required for efficient pre-rRNA processing predominantly at site A3. *Mol. Cell. Biol.* 17, 1354–1365.

Wells, G.R., Weichmann, F., Colvin, D., Sloan, K.E., Kudla, G., Tollervey, D., Watkins, N.J., and Schneider, C. (2016). The PIN domain endonuclease Utp24 cleaves pre-ribosomal RNA at two coupled sites in yeast and humans. *Nucleic Acids Res.* 44, 9016–9016.

Wen, X., Tannukit, S., and Paine, M. (2008). TFIP11 Interacts with mDEAH9, an RNA Helicase Involved in Spliceosome Disassembly. *Int. J. Mol. Sci.* 9, 2105–2113.

Wild, T., Horvath, P., Wyler, E., Widmann, B., Badertscher, L., Zemp, I., Kozak, K., Csucs, G., Lund, E., and Kutay, U. (2010). A protein inventory of human ribosome biogenesis reveals an essential function of exportin 5 in 60S subunit export. *PLoS Biol.* 8, e1000522.

Witten, J.T., and Ule, J. (2011). Understanding splicing regulation through RNA splicing maps. *Trends Genet.* 27, 89–97.

Woolford, J.L., and Baserga, S.J. (2013). Ribosome Biogenesis in the Yeast *Saccharomyces cerevisiae*. *Genetics* 195, 643–681.

Yang, Q., Fairman, M.E., and Jankowsky, E. (2007). DEAD-box-protein-assisted RNA Structure Conversion Towards and Against Thermodynamic Equilibrium Values. *J. Mol. Biol.* 368, 1087–1100.

Yoneyama, M., and Fujita, T. (2008). Structural Mechanism of RNA Recognition by the RIG-I-like Receptors. *Immunity* 29, 178–181.

Yoon, A. (2006). Impaired Control of IRES-Mediated Translation in X-Linked Dyskeratosis Congenita. *Science* (80-.). 312, 902–906.

Zang, S., Lin, T.-Y., Chen, X., Gencheva, M., Newo, A.N.S., Yang, L., Rossi, D., Hu, J., Lin, S.-B., Huang, A., et al. (2014). GPKOW is essential for pre-mRNA splicing in vitro and suppresses splicing defect caused by dominant-negative DHX16 mutation in vivo. *Biosci. Rep.* 34, e00163.

Zemp, I., Wandrey, F., Rao, S., Ashiono, C., Wyler, E., Montellese, C., and Kutay, U. (2014). CK1 and CK1 are components of human 40S subunit precursors required for cytoplasmic

40S maturation. *J. Cell Sci.* 127, 1242–1253.

Zhang, Y., You, J., Wang, X., and Weber, J. (2015). The DHX33 RNA Helicase Promotes mRNA Translation Initiation. *Mol. Cell. Biol.* 35, 2918–2931.

Zhang, Y., O'leary, M.N., Morris, D.R., Kennedy, B.K., and Wiest Correspondence, D.L. (2017). Ribosomal Proteins Rpl22 and Rpl22i1 Control Morphogenesis by Regulating Pre-mRNA Splicing. *CellReports* 18, 545–556.

Zhu, J., Liu, X., Anjos, M., Correll, C.C., and Johnson, A.W. (2016). Utp14 Recruits and Activates the RNA Helicase Dhr1 To Undock U3 snoRNA from the Preribosome. *Mol. Cell. Biol.* 36, 965–978.

Zorbas, C., Nicolas, E., Wacheul, L., Huvelle, E., Heurgué-Hamard, V., and Lafontaine, D.L.J. (2015). The human 18S rRNA base methyltransferases DIMT1L and WBSCR22-TRMT112 but not rRNA modification are required for ribosome biogenesis. *Mol. Biol. Cell* 26, 2080–2095.

List of Figures

Figure 1.1 Ribosome biogenesis in humans.....	1
Figure 1.2 Schematic representation of yeast 35S pre-rRNA transcript.....	2
Figure 1.3 Overview of pre-rRNA processing in humans.....	5
Figure 1.4 SF1 and SF2 superfamily of helicases.....	13
Figure 1.5 Structural characterization of DEAD-box and DEAH-box helicases.....	15
Figure 4.1 DDX55 is an ATPase.....	91
Figure 4.2 DDX55 predominantly exhibits a nucleoplasmic localisation.....	92
Figure 4.3 siRNA-mediated depletion of DDX55.....	93
Figure 4.4 siRNA-mediated depletion of DDX55 impairs production of rRNAs.....	94
Figure 4.5 DDX55 crosslinks to RNA <i>in vivo</i>	95
Figure 4.6 Flag-tagged DDX55 enriches ribosomal RNAs.....	96
Figure 4.7 DDX55 crosslinks to a specific site within the 28S rRNA sequence.....	97
Figure 4.8 DDX55 crosslinks to helices 62 and 63 of the 28S rRNA.....	98
Figure 4.9 DDX55 crosslinks to helices 62 and 63 in domain IV of the 28S rRNA.....	98
Figure 4.10 C-terminal extension of DDX55 contains conserved basic amino acid residues.....	99
Figure 4.11 Deletion of C-terminal tail of DDX55 leads to decreased RNA binding.....	100
Figure 4.12 C-terminal truncation of DDX55 causes its mis-localisation to the cytoplasm.....	101
Figure 4.13 Deletion of the C-terminal basic tail of DDX55 results in reduced association with pre-ribosomal subunits.....	102

List of Tables

Table 1 Plasmids used in this study.....	80
Table 2 Oligonucleotides used in this study.....	80
Table 3 siRNAs used in this study	81
Table 4 Antibodies used in this study	81
Table 5 PCR components and amplification protocol	82
Table 6 PCR reaction conditions for CRAC	88

Abbreviations

ATP	Adenosine triphosphate
bp	Base-pair
CRAC	Cross-linking and analysis of cDNA
DAPI	4',6-diamidino-2-phenylindole
DMEM	Dulbecco's Modified Eagle Medium
DNA	Deoxyribonucleic acid
ETS	External transcribed spacer
ITS	Internal transcribed spacer
lncRNA	Long non-coding RNA
miRNA	MicroRNA
miscRNA	Miscellaneous RNA
mRNA	Messenger RNA
mtRNA	Mitochondrial RNA
NLS	Nuclear localization signal
nt	Nucleotide
NTP	Nucleoside triphosphate
PAGE	Polyacrylamide gel electrophoresis
PCR	Polymerase chain reaction
PDB	Protein data bank
pre-mRNA	Precursor mRNA
pre-rRNA	Precursor rRNA

RBF	Ribosome biogenesis factor
RNA	Ribonucleic acid
RNP	Ribonucleoprotein
RP	Ribosomal protein
rRNA	Ribosomal RNA
S	Svedberg units
snoRNA	Small nucleolar RNA
snRNA	Small nuclear RNA
SSU	Small ribosomal subunit
tRNA	Transfer RNA
UTR	Untranslated region
UV	Ultraviolet
IPTG	Isopropyl- β -D-thiogalactosidase
kDa	Kilodalton
LB	Lysogeny broth
MIF4G	Middle domain of eIF4G
Ni-NTA	Nikel-nitrilotriacetic acid
NT	Non-target
siRNA	Small-interfering RNA
OB-fold	Oligonucleotide binding fold
P _i	Inorganic phosphate
RRM	RNA recognition motif
EJC	Exon junction complex
s.e.m	Standard error of the mean

SDS	Sodium dodecyl sulphate
SF	Superfamily
WH	Winged helix
HCl	Hydrochloric acid
BSA	Bovine serum albumin
DAPI	4' 6-diamidino-2-phenylindole

Acknowledgment

Foremost, I would like to take this opportunity to express my sincere gratitude to my supervisor Prof. Dr. Markus Bohnsack. This work would not have been possible without his support. His encouragement and unwavering motivation, despite his busy schedule, was extremely helpful during my PhD study. He also gave me the opportunity to work on various different projects and tackle novel questions which helped me immensely to expand my scientific outlook.

I would also like to thank the members of my thesis committee, Prof. Dr. Marina Rodnina and Prof. Dr. Jörg Stülke for their invaluable insights and guidance during the course of my PhD study. I would also like to thank my extended committee members: Dr. Alexander Stein, Prof. Dr. Ralf Ficner and Prof. Dr. Michael Meinecke for being a part of my examination board.

I extend my sincere thanks to Dr. Katherine Bohnsack for the constant mentorship, guidance and unending brain storming sessions. Her enthusiasm for science kept me afloat when I faced challenges during my PhD study. I am also greatly thankful to her for her critical evaluation of this dissertation.

I greatly acknowledge the help and support provided by the coordinators of International Max Planck Research School of Molecular Biology, Dr. Steffen Burkhardt and Kerstin Grüniger since the time I stepped into Göttingen.

I would also like to thank all my lab colleagues- Philipp Hackert, Ahmed Warda, Gerald Aquino, Jens Kretschmer, Lukas Brüning, Indira Memet and my lab sister Jimena for maintaining a warm and friendly working environment. I would also like to extend my gratitude to the department of molecular biology which functions as one big happy lab!

I especially thank Jens Kretschmer and Philipp Hackert for their help with the CRAC experiments and bioinformatics analysis of the data.

My stay in Göttingen, this PhD and the last 11 years of my life would not have been so smooth without my sister Ridhima. Thank you, Vedran for being around and writing the thesis at the same time. It was nice sharing the struggle. A special thank you to the first friends I made in Göttingen- Kashish, Arshiya, Prajwal and Ika.

Thank you, Rahul.

Lastly, I would like to thank my family for their support and patience during the course of this study.

Priyanka Choudhury

Personal Born 26.02.1990 in West Bengal, India

Contact priyanka26290@gmail.com

+49-176-68196741

38, Hermann Rein Straße 2B
37075 Göttingen, Germany



Education

- 2015 PhD candidate of Molecular Biology at University of Göttingen
Dissertation titled '*Functional analyses of RNA helicases in human ribosome biogenesis*'
- 2013 Master of Science in Molecular Biology, IMPRS Göttingen
Dissertation titled '*Structural changes in elongation factor-G during translocation*'
- 2011 Master of Science in Biochemistry, University of Delhi, India
Dissertation titled '*Biochemical characterization of a putative UV-B receptor from C.reinhardtii*'
- 2008 Bachelor of Science in Biochemistry, University of Delhi, India

Awards and Scholarships

- 2013 Awarded Stipend of the Excellence Foundation for the promotion of the Max Planck Society
- 2013 Qualified National Eligibility Test for CSIR-UGC
- 2012 Fellowship awarded by the Indian Academy of Sciences
- 2012 UGC-infrastructure grant
- 2011 Monsanto Scholarship (*awarded to top two rankers in University of Delhi*)

List of publications

Choudhury P, Hackert P, Memet I, Sloan KE, Bohnsack MT (2019). The human RNA helicase DHX37 is required for release of the U3 snoRNP from pre-ribosomal particles. *RNA Biol.* ;16(1): 54–68.

Sednev, M. V*, Mykhailiuk, V*, **Choudhury, P.***, Halang, J., Sloan, K. E., Bohnsack, M. T., & Höbartner, C. (2018). N⁶-Methyladenosine-sensitive RNA cleaving Deoxyribozymes. *Angewandte Chemie*; 130 (46): 15337-15341

* These authors contributed equally to this work